B,V Photometry of Variable Stars in the Northeast Arm of the Small Magellanic Cloud

Brian Sharpee, Michele Stark[1], Barton Pritzl [2],

and

Horace Smith[3]

Department of Physics and Astronomy, Michigan State University, East Lansing, MI 48824

smith@pa.msu.edu

Nancy Silbermann[3]

SIRTIF Science Center, California Institute of Technology, MS 220-6, Pasadena, CA 91125

Ronald Wilhelm

Department of Physics, Southwestern University, Georgetown, TX 78627

wilhelmr@southwestern.edu

Alistair Walker

Cerro Tololo Interamerican Observatory, National Optical Astronomy Observatories, P.O. Box 26732, Tucson, AZ 85726

awalker@noao.edu

ABSTRACT

B and V photometry has been obtained for variable stars in the northeast arm of the Small Magellanic Cloud (SMC). Periods and light curves have been

---

[1]Current address: 525 Davey Lab, Department of Astronomy and Astrophysics, Pennsylvania State University, University Park, PA 16802

[2]Current address: National Optical Astronomy Observatories, P.O. Box 26732, Tucson, AZ 85726 pritzl@noao.edu

[3]Visiting Astronomer, Cerro Tololo Inter-American Observatory, National Optical Astronomy Observatories, which is operated by AURA, Inc., under cooperative agreement with the National Science Foundation

determined for 240 periodic variables, including 203 Cepheids. Fundamental mode Cepheids and first overtone mode Cepheids are generally well separated in the B, V color-magnitude diagram, with the latter having bluer mean colors than the former. The Cepheid period-color relationship for this outlying SMC field is indistinguishable from that seen in more centrally located SMC fields, and is bluer than theoretical predictions. The red edge to the populated portion of the instability strip shifts to bluer colors for fainter Cepheids. There is support from our sample for a previously reported steepening in the slope of the period-luminosity relation for fundamental mode Cepheids near a period of 2 days. The Cepheids of the northeast arm may be closer to us than are those of the main body of the SMC, but the difference is smaller than or equal to about 4 kpc, comparable to the tidal radius of the SMC.

Subject headings: Stars:Variables:Cepheids; Galaxies: Magellanic Clouds

1. Introduction

Leavitt (Pickering 1912) discovered the period-luminosity relation using observations of Cepheid variable stars in the Small Magellanic Cloud (SMC). Because the young population of the SMC is now known to be metal-poor relative to that of the solar neighborhood and to that of the Large Magellanic Cloud, SMC Cepheids remain of particular interest in the elucidation of the effects of metallicity upon the properties of Cepheid variable stars. Moreover, it has been proposed that the depth of the SMC along the line of sight is not insignificant compared to its mean distance (Westerlund (1997) and references therein). Cepheids provide a means of measuring the distances to the young populations of different parts of the SMC.

Smith et al. (1992) used photographic photometry in the B band to study the variable star population in an outlying field in the northeast arm of the SMC. Their period-luminosity diagram showed the presence of both fundamental mode and first overtone mode Cepheids, but, because they observed only in the B band, they could not address questions regarding the colors of the variable stars they observed.

We have obtained B and V CCD photometry of variable stars in this field to address several issues. First, the present CCD survey more readily detects low amplitude Cepheids than did the earlier photographic study, providing a more complete picture of the variable star population of the northeast arm. Second, the new data allow us to discover where the fundamental mode and first overtone mode Cepheids fall within the color-magnitude

diagram (CMD). In particular, is there overlap beyond that attributable to observational error in the colors of Cepheids having different pulsation modes, or do fundamental mode and first overtone mode Cepheids occupy distinct and separate regions in the CMD? A substantial overlapping of the fundamental mode and first overtone mode Cepheid domains is visible in the $I_0, (V-I)_0$ CMD based upon data taken in the OGLE survey (Figure 4 of Udalski et al. (1999b)). However, that survey emphasized the crowded central regions of the SMC, and problems with crowding, blended images, and possibly differential reddening may have contributed to the overlap. If that overlapping is real, and not attributable to observational error, then there is no unique dividing line between fundamental mode and first overtone mode SMC Cepheids in the HR diagram. The existence of a hysteresis zone, in which pulsation mode depends upon direction of evolution in the HR diagram, would be one possible way by which such an overlap zone might be produced. Such a hysteresis zone has been proposed for RR Lyrae variables (e.g., Stellingwerf (1975)).

In addition, prior studies have found a break in the slope of the period-luminosity ($P-L$) relation for fundamental mode SMC Cepheids near a period of 2 days (see § 8). This break has not yet been satisfactorily explained, and it is of interest to determine whether the location of the short period Cepheids in the CMD can shed light upon this problem. We also want to compare the period-color relations for Cepheids in the northeast arm with those which have been derived for Cepheids in more central regions of the SMC and with theoretical period-color relations.

Finally, we wish to compare the $P-L$ relations for the northeast arm Cepheids with those derived in the course of microlensing surveys of more central SMC fields. If the slopes of the $P-L$ relations derived for Cepheids in the northeast arm are significantly different from those of Cepheids in the main body of the SMC, that would indicate that the Cepheid population of the SMC is heterogeneous, with properties depending upon location. Alternatively, a difference only in the zero-points of the $P-L$ relations might indicate that the Cepheids of the northeast arm are nearer or more distant than those in other parts of the SMC.

2. Observations and Reductions

Four fields in the northeast arm of the SMC were imaged with the Thomson 1024 × 1024 CCD camera on the CTIO 60-cm Curtis Schmidt telescope. Each field measures 0.5 degrees on a side, together defining a square 1° × 1° area of the SMC centered approximately on RA = 1^h03^m and DEC = $-71°23'$ (J2000), including most of the field studied photographically by Smith et al. (1992). There are small areas of overlap between adjoining fields.

The four fields were observed with Johnson B and V filters during five runs in 1992, 1993, and 1994. A journal of observations for these observing runs is provided in Table 1. During the first runs in September and October, 1992, the usual observing procedure was to obtain three consecutive V and four consecutive B exposures of each field, each 300 s long. These were later combined to constitute one 900 s V and one 1200 s B observation. During runs in September and November, 1993, and October, 1994, the exposure times in B were increased to 420 seconds, so that the total exposure from the combination of four consecutive B images was 1680 s. Because of the poorer blue sensitivity of the Thomson chip, the B images do not reach as faint as the V despite the longer exposure times.

Images were flattened with sky flats, and conventionally reduced with IRAF [4]. Aperture photometry was obtained with the standalone version of DAOPHOT II (Stetson 1987). Because the CCD pixels are $2''$ square, confusion of images can be a significant source of error in the more crowded portions of the fields.

The photometry for the individual frames was first reduced to an adopted instrumental magnitude system. Possible variable stars were then identified from the scatter about the mean value in the instrumental b and v magnitudes. Examination of the images of suspected variables eliminated those stars for which the scatter could be attributed to crowding or other causes not related to true variability. Typically, each variable was observed about 22 times in each filter, although a few variables in the overlap zones between fields were observed more frequently. Cepheid variable stars with periods under 20 days, amplitudes greater than about 0.2 mag, apparent magnitudes brighter than $\langle V \rangle = 18.5$, and which were not subject to severe crowding, should have been detected in this search. However, the identification of SMC RR Lyrae variables, at $\langle V \rangle \sim 19.5$, is very incomplete.

A period search was conducted for the suspected variables using the phase dispersion minimization program (PDM), as implemented in IRAF. The spacing of our observations is well-suited for determining periods for stars which have periods shorter than about 5 days, but is not well suited for longer periods. Determinations of periods longer than 20 days are not possible with any reliability. Hodge & Wright (1977) and Smith et al. (1992) were consulted to identify known variable stars within our fields. Although the periods for most of these previously discovered variables are already known, a new period search was nonetheless carried out for each of them.

Newly discovered variables are identified in Figures 1a-1d. Positions for the new vari-

---

[4]IRAF is distributed by the National Optical Astronomy Observatories, which are operated by the Association of Universities for Research in Astronomy, Inc., under cooperative agreement with the National Science Foundation.

ables were calculated on the system of the Digitized Sky Survey, using routines in IRAF. The resultant positions, good to about 2″, are listed in Table 2. The error was estimated from comparisons of the positions we derived with those listed in the MACS catalog (Tucholke et al. 1996) for stars in common. The numbering scheme for the new variables continues that used by Smith et al. (1992), beginning with number 137.

Local standards were set up in a single $13.6' \times 13.6'$ field, centered on RA = $01^h04^m49^s$, Dec = $-71°23'00''$ (J2000), with the CTIO 0.9-m telescope and CCD imaging system on 8 November 1999. CCD SITe 2048 #3 was used together with the standard 0.9-m $UBVRI$ filter set. Observations of the standard field were made in U, B, V, I filters, of which only B and V are relevant for the calibration purposes required here. Exposure times were 2 × 100s, 500s (V) and 2 × 200s, 1000s (B). Twilight sky flat field exposures successfully reduced systematics to well below one percent.

The night was photometric and observations were made of 105 Landolt (1992) standards in 10 fields at a variety of airmasses. 86 of these stars were retained in the final color equation fits, which confirmed the high quality of the night, with zeropoints constrained to 0.0015 – 0.002 mag.

A set of 21 local standards, selected as being isolated stars covering a wide magnitude and color range ($V : 12-17, B-V : -0.2-+1.5$) were measured using aperture photometry in exactly the same way as the primary standard stars. Stars brighter than magnitude 13.5 were measured on the short exposures only; the remaining stars all have three measurements. Agreement between measurements for any given star is typically 0.01 mag. Photometry and positions for the local standards are listed in Table 3. Results are listed individually for the two shorter and one longer exposures. Values of right ascension and declination were found in the same fashion as for the new variable stars. The local standard stars are identified in Figure 2.

Instrumental b and v magnitudes were transformed to the Johnson B and V systems using the local standard stars. Transformation equations had the form:

$$\mathrm{b} = B + C_B - 0.05(B - V)\,, \tag{1}$$

$$\mathrm{v} = V + C_V - 0.01(B - V)\,. \tag{2}$$

Two existing photometric sequences were used to check the accuracy of the transformation. Our two more northern fields include stars near NGC 362 which were observed photoelectrically and photographically in B and V by Harris (1982). Secondly, one of our fields includes the SMC cluster NGC 411, for which Da Costa & Mould (1986) obtained B, R photometry. Mean differences between our B and V values and those in Harris (1982)

and Da Costa & Mould (1986) are summarized in Table 4. The number of stars compared and the mean differences in the magnitudes, in the sense their values minus ours, are listed in this table. The different photometric systems appear to agree to within about ± 0.02 mag. The photometry for individual variable stars is listed in Table 5. The full table will be given in the electronic version of this paper. The errors listed in column 4 of this table are the formal standard errors returned by the DAOPHOT II code, and may in some cases underestimate the actual uncertainty.

3. Light Curves, Periods, and Mean Colors

Data for the periodic variables are summarized in Table 6. The variable is identified in column (1), by its Harvard Variable number (HV) if one is available, or by its number in Smith et al. (1992) or its number in Table 2 (SMC number) if there is no Harvard number. The variable type is listed in column (2), where F indicates a Cepheid pulsating in the fundamental mode, O indicates a Cepheid pulsating in the first overtone mode, RRab indicates an RR Lyrae star in the fundamental mode, RRc indicates an RR Lyrae star in the first overtone mode, and E indicates an eclipsing variable star. Our derived period, typically good to a few parts in 10^5, is given in column (3). We list luminosity-weighted mean $\langle B \rangle$ and $\langle V \rangle$ magnitudes in columns (4) and (5). Luminosity-weighted $\langle B \rangle - \langle V \rangle$ and magnitude-weighted mean $(B-V)_{mag}$ colors are listed in columns (6) and (7). In column (8) a 1 signifies a variable with a relatively complete and well defined light curve, whereas a 2 indicates that the light curve is noisy or has substantial gaps. In general, only stars with quality "1" light curves were selected for more detailed analysis. For a few variables, a good light curve was obtained in B or V, but not in both bandpasses. These are indicated by a $1(V)$ or $1(B)$ in column (8).

The decision to assign a Cepheid to the first overtone or fundamental mode category was made by inspection of the light curves. Previous studies have indicated that, at a given period, the light curves of first overtone pulsators are characterized by smaller amplitudes and less asymmetry than those of fundamental mode pulsators (e.g. Smith et al. (1992)). Classifications of pulsation mode based on light curves appear to be fully consistent with the locations of the Cepheids in the period-luminosity domain. The number of data points for most of the Cepheids is not large enough to effectively apply Fourier decomposition methods for determining pulsation mode.

B and V light curves for periodic variables are shown in Figure 3, arranged in order of descending period. Phases have been calculated from the formula:

$$\phi = (JD_{\odot}/P)\,, \tag{3}$$

where $JD_{\odot}$ is the heliocentric Julian Date and P is the period in days. Pulsating variables of all types with quality "1" light curves in both B and V are plotted in the $\langle V \rangle$ vs $\log P$ diagram in Figure 4.

4. Reddening

Harris (1982) adopted $E(B-V) = 0.04$ for the globular cluster NGC 362, which is located close to our northeast arm field. Da Costa & Mould (1986) also adopted $E(B-V) = 0.04$ for NGC 411, which is within our field. Caldwell & Coulson (1986) found a mean reddening of $E(B-V) = 0.054$ for all except the central region of the SMC. Grieve & Madore (1986) obtained $E(B-V) = 0.09$ for SMC supergiants, with no trend with location in the SMC. Based upon these results, Smith et al. (1992) adopted a mean reddening of $E(B-V) = 0.06$ for the northeast arm region. More recently, Udalski et al. (1999b) obtained reddening values of $E(B-V) = 0.079$ and 0.084 for their SMC fields SC10 and SC11, the two fields in their survey which were closest to our own. Both SC10 and SC11 lie nearer to the central body of the SMC than does our field. SC10 is centered at RA = $1^h04^m51^s$, DEC = $-72°24'25''$ (J2000), and SC11 is centered at RA = $1^h07^m45^s$ and DEC = $-72°39'30''$ (J2000). Udalski et al. (1999b) assigned $E(B-V) = 0.070$ to their field SC1 which, although on the sky it lies on the other side of the SMC from the northeast arm, may be the OGLE field most similar to our own in terms of stellar density.

We can also estimate the foreground reddening in the direction of the northeast arm using the color data for Galactic RR Lyrae stars within our field. Sturch (1966) and Blanco (1992) determined that the intrinsic colors of ab type RR Lyrae stars were a function only of metallicity and period in the phase interval $0.5 \leq \phi \leq 0.8$ after maximum light. Here we employ the relationship found by Blanco (1992), that the reddening within this phase interval is given by

$$\begin{aligned} E_{B-V} &= (B-V)_{\phi(0.5-0.8)} + 0.0122\Delta S \\ &\quad -0.00045(\Delta S)^2 - 0.185P - 0.356\,, \end{aligned} \tag{4}$$

where P is the period and ΔS is the spectroscopic metallicity index for RR Lyrae stars (Preston 1959). Unfortunately, we have no direct measurement of the metallicity index ΔS

for the foreground RR Lyrae stars. An indirect estimate of ΔS for these variables can be made from the period shift of the star, $\Delta \log P$, as defined in Sandage (1982b):

$$\Delta \log P = -[\log P + 0.129 A_B + 0.088], \quad (5)$$

where A_B is the B amplitude. $\Delta \log P$ is related to [Fe/H] by the relation (Sandage 1982a):

$$\Delta \log P = 0.116[\mathrm{Fe/H}] + 0.173. \quad (6)$$

If we employ the calibration of the ΔS index from Butler (1975),

$$[\mathrm{Fe/H}] = -0.23 - 0.16\Delta S, \quad (7)$$

we can now relate $\Delta \log P$ to ΔS in the Blanco (1992) formula. Values of $E(B-V)$ determined in this fashion for foreground RRab stars are listed in Table 7, along with the inferred values of [Fe/H]. Some uncertainty attaches to this approach, particularly as it is applied to individual stars, since $\Delta \log P$ also may depend upon the evolution of the particular star under consideration. The mean value of $E(B-V)$ derived in this way is 0.05±0.01. The formal error of the mean is undoubtedly an underestimate given the uncertainty which attaches to our determination of the metallicities. If our derived [Fe/H] values were systematically in error by 0.4 dex, the derived mean value of $E(B-V)$ would change by 0.03. Although in principle the same approach can be used to determine reddenings for RRab stars actually belonging to the SMC, our light curves for such stars are too noisy to permit us to use them in that fashion. A foreground reddening of $E(B-V) = 0.05$ is slightly greater than the value of 0.019 ± 0.004 found by McNamara & Feltz (1980) from photometry of foreground stars in the direction of the SMC, but is similar to the 0.04 adopted by Harris (1982) for NGC 362.

For the remainder of this paper we adopt a reddening value $E(B-V) = 0.07$ for the northeast arm field, a value slightly larger than the reddening determined for the foreground RRab stars, and close to the values Udalski et al. (1999b) obtained for outlying parts of the SMC. The adopted value of $E(B-V)$ may be uncertain by ±0.02, an uncertainty which encompasses the most recent determinations of the reddening of the SMC. We follow Udalski et al. (1999b) in adopting the relations:

$$A_B = 4.32\, E_{B-V}, \quad (8)$$

$$A_V = 3.24\, E_{B-V}, \quad (9)$$

giving $A_B = 0.30$ and $A_V = 0.23$.

5. Period-Frequency Relations for Cepheids

Table 8 lists the distribution of the number of fundamental and first overtone mode Cepheids as a function of period for variables in the present survey and in the survey of Smith et al. (1992), which covered a larger $1° \times 1.3°$ area. In this table we include all variables with periods, not just those with first quality light curves. This comparison is shown graphically in Figure 5. Allowing for the larger field size of the Smith et al. photographic study, we see that the present survey identified a modest but significant number of additional fundamental mode Cepheids which were not included in Smith et al. (1992). In contrast, the number of first overtone mode pulsators with periods has been approximately doubled. This can be attributed to the greater ease of identifying low amplitude variables using the CCD images. Somewhat surprisingly, the greatest number of additional first overtone Cepheids occurred in the $0.3 < \log P_1 < 0.4$ bin, among the brighter first overtone Cepheids. Figure 6 compares histograms for all Cepheids with periods and for those with quality "1" light curves. Note that first overtone Cepheids with quality "1" light curves tend to be under-represented at periods close to one day. This reflects the difficulty in obtaining complete phase coverage for variables with one day periods. Likewise, lack of complete phase coverage is responsible for the deficit of quality "1" light curves among the longer period fundamental mode Cepheids.

The maximum number of fundamental mode Cepheids was observed in the $\log P_0 = 0.2 - 0.3$ bin. This is very close to the most common period in the histogram (Fig 6, Udalski et al. (1999b)) over $\log P$ for fundamental mode Cepheids in the more central parts of the SMC studied in the OGLE survey. The period-frequency distribution for fundamental mode Cepheids in the northeast arm is similar in general to that seen in the areas surveyed by OGLE.

In our study, the first overtone mode Cepheids exhibit a broad peak, cutting off sharply at periods longer than $\log P_1 = 0.4$. Udalski et al. (1999b) also found a relatively broad peak in their histogram over $\log P_1$ for first overtone Cepheids in the SMC. However, their cutoff at longer periods is not so sharp as is shown in Table 8, and their histogram is more strongly peaked to periods around $\log P_1 = 0.1$. We note, however, that with the smaller number of first overtone Cepheids in our sample, this difference may not be significant.

6. Color-Magnitude Diagram

In Figure 7, we plot luminosity-weighted, extinction corrected mean V magnitudes, $\langle V \rangle_0$, against magnitude-weighted, reddening corrected mean colors, $(B-V)_{mag,0}$, for those Cepheids in Table 6 which have quality "1" B and V light curves. We choose to plot

magnitude-weighted, rather than luminosity-weighted, colors here since, at least for RR Lyrae stars, it has been argued that magnitude-weighted colors are closely related to the equilibrium temperatures of the stars (De Santis 2001). As is evident from Table 6, the magnitude-weighted and luminosity-weighted colors are in any case similar (though with small differences dependent upon light curve shape). The $(B-V)_{mag}$ colors tend to be about 0.01–0.02 mag redder than $\langle V\rangle - \langle B\rangle$ colors for the variables we observed. For galactic Cepheids, Bono et al. (1999) predict a difference of 0.018 mag at $\log P = 1.0$.

As expected, the Cepheids fall within a well-defined instability strip. The first overtone Cepheids are for the most part well divided from the Cepheids which pulsate in the fundamental mode. There is some overlap at the boundary between first overtone and fundamental mode pulsators, but the overlap is mostly small, and can be accounted for by typical errors of $\pm$ 0.03 mag in $(B-V)_{mag}$. A few stars are, however, significantly bluer or redder than would be expected on the basis of their pulsation mode. Arp (1960) noticed that HV1898 has an unusually blue color compared to other Cepheids of similar light curve shape and period, a result with which we concur. He attributed this to the presence of an unresolved blue companion, a conclusion which seems very plausible. It is quite possible that all of the color overlap between fundamental mode and first overtone mode Cepheids in Figure 7 can be attributed to the combination of observational errors and the existence of a few instances of unresolved companions. There is evidence for a narrowing of the Cepheid instability strip, or at least the populated region of the instability strip, at lower luminosities, with the red edge shifting to bluer colors for fundamental mode Cepheids.

For comparison, Figure 8 shows a color-magnitude diagram in which points for the Cepheids in Udalski et al.'s (1999b) fields SC10 and SC11 are added to those in our field. We note that the OGLE project web page states that the photometry for the SMC Cepheids was revised on April 1, 2000. We have used the revised photometry throughout this paper (Udalski et al. 2000).

The pattern in Figure 8 is similar to that in Figure 7: Fundamental mode pulsators tend to have redder colors than first overtone pulsators of equivalent luminosity. There is more scatter than in Figure 7 and a greater overlap in color between fundamental mode and first overtone mode Cepheids. That can plausibly be attributed to a greater proportion of crowded star images or incomplete light curves in the somewhat more central SC10 and SC11 fields than in the selected data used to make Figure 7. One possibly significant difference between the two color-magnitude diagrams is the existence of a number of faint and relatively red first overtone pulsators at the bottom of the color-magnitude diagram (Figure 8) from the OGLE sample which are not seen in our dataset. The OGLE B and V light curves of some of these redder first overtone stars are noisy, but that is not the case for all of them.

These variables have $\langle V \rangle_0 \sim 18$ and extend to $(B-V)_{mag,0} = 0.4$. It is true that some of our shorter period first overtone Cepheids were excluded from Figure 7 and Figure 8, on the basis that their light curves showed too much scatter (see Table 6). However, we would expect that at least a few of the faint, redder first overtone variables would have been well-observed in our dataset were such stars as common in our field as they seem to be in SC10 and SC11. We also note that there remains evidence for a blueward shift in the colors of the reddest fundamental mode Cepheids as one goes to fainter luminosities. This will be discussed further in § 8.

7. Period-Color Relations

We have determined least squares fits to the period-color relations defined by the fundamental mode and first overtone mode Cepheids within our northeast arm field. For 70 fundamental mode Cepheids with reliable colors we obtain:

$$(B-V)_{mag,0} = 0.27(\pm 0.03) \log P_0 + 0.32(\pm 0.01)\,, \tag{10}$$

with a standard deviation of ± 0.05 mag, whereas for 59 first overtone mode Cepheids we find:

$$(B-V)_{mag,0} = 0.13(\pm 0.03) \log P_1 + 0.29(\pm 0.01)\,, \tag{11}$$

with a standard deviation of ± 0.04 mag. For comparison we include our least squares fits to 1250 fundamental mode Cepheids and 773 first overtone mode Cepheids in Udalski et al. (1999b):

$$(B-V)_{mag,0} = 0.27(\pm 0.01) \log P_0 + 0.32(\pm 0.01)\,, \tag{12}$$

$$(B-V)_{mag,0} = 0.18(\pm 0.02) \log P_1 + 0.301(\pm 0.004)\,. \tag{13}$$

The period-color relations for the fundamental mode and first overtone Cepheids are shown in Figures 9 and 10. Our period-color relations and those defined by stars in the more centrally located OGLE fields are in excellent agreement for the period ranges covered by our data. The agreement is not so good with the theoretical period-color relation for fundamental mode SMC Cepheids (Z = 0.004) taken from Alibert et al. (1999), which is significantly redder than the observed relations. The slope of the period-color relation for fundamental mode Cepheids of Z = 0.004 from Caputo et al. (2000) is closer to that which is observed, but the zero-point is slightly too red. A reduction of 0.04 in the adopted value of $E(B-V)$ would bring the observed period-color relationship into good agreement with that of Caputo

et al. (2000). A change that large is probably unlikely, but an error of 0.02 in the adopted reddening value can certainly not be excluded. The theoretical period-color relationships of Alibert et al. (1999) and Caputo et al. (2000) are plotted in Figure 9.

8. Period-Luminosity Relations

We have fit B and V period-luminosity ($P-L$) relations of the form $M = \alpha \log P + \beta$ to the data for the fundamental mode and first overtone Cepheids, using all the Cepheids from Table 6 with quality "1" photometry in the relevant passbands. Luminosity-weighted $\langle B \rangle_0$ and $\langle V \rangle_0$ magnitudes have been used in these fits and no outliers have been excluded. Coefficients from least squares and least absolute deviation fits are listed in Table 9. The values of σ listed for the least squares fits are the usual mean errors. Those listed for the least absolute deviation fits are a measure of the mean absolute deviation. The period-luminosity relations are plotted in Figures 11, 12, 13, and 14.

The least squares and least absolute deviation fits are almost indistinguishable from one another and return coefficients which are well within the uncertainties of the coefficients in the least squares fits. The scatter about the relationships, as measured by the residuals (σ) from both methods, is similar. Some of the scatter will, of course, be real – reflecting the existence of a finite width to the Cepheid instability strip in the HR diagram. Some of the scatter in the relationships may also be the result of differential reddening across our four fields constituting our northeast arm field. Given the outlying location of our SMC field, and the relatively small range in SMC reddening found by Udalski et al. (1999b), the likelihood of a large range of reddenings for individual stars is probably small. Nonetheless, differential reddening cannot be entirely dismissed as a possible cause of scatter.

To check for the effect of differential reddening, we have calculated the extinction insensitive Wesenheit index W_{BFM} (Madore & Freedman 1991) for each of the Cepheids, where

$$W_{BFM} = V - 3.24 \times (B-V). \tag{14}$$

The coefficients of fits to the W_{BFM} versus $\log P$ diagrams are given in Table 10 and the relations are plotted in Figure 15. The scatter of the $W_{BFM} - \log P$ relation isn't smaller than that for the extinction corrected $\langle V \rangle - \log P$ relations; indeed it is even larger for the first overtone Cepheids, though the difference is not significant. We thus are reassured that the scatter in the $P-L$ relations for B and V is not attributable to differential reddening across our field.

The coefficients of the $P-L$ relations derived from our data can be compared with those derived from the photographic B survey of Smith et al. (1992). The $P-L$ relations

from Smith et al. (1992) are:

$$\langle B\rangle_0 = -2.71(\pm 0.09)\log P_0 + 18.03(\pm 0.14)\,, \tag{15}$$

$$\langle B\rangle_0 = -2.98(\pm 0.17)\log P_1 + 17.35(\pm 0.14)\,, \tag{16}$$

for fundamental mode and first overtone mode Cepheids, respectively. These differ from those in Table 9 in having steeper slopes and fainter zero-points.

At $\log P = 0.8$, near $B = 15.8$, the difference between the CCD and photographic $P-L$ relations for fundamental mode Cepheids is about 0.1 mag.

At $\log P = 0.2$, near $B = 17.3$, the $P - L$ relation derived from the CCD data is about 0.22 mag brighter than that obtained by Smith et al. (1992). Of these differences, 0.04 mag is accounted for by the different adopted reddening values in the two studies. In addition, the mean magnitudes given in Smith et al. (1992) are magnitude averages, rather than the luminosity-weighted magnitudes used here. The effect which this has depends upon the light curve shape of the variable under consideration. For a typical fundamental mode Cepheid, the luminosity-weighted magnitudes will be about 0.08 mag brighter than those obtained from averaging magnitudes. These two differences account for essentially all of the discrepancy in the two $P - L$ relations near $\log P = 0.8$. Together, however, they account for only about half of the discrepancy near $\log P = 0.2$.

As will be discussed below, there may be a break in the slope of the $P-L$ relation near a period of 2 days for fundamental mode Cepheids. This break was not noted in Smith et al. (1992), although there is some evidence for its existence in their $P - L$ relation. There are different numbers of Cepheids with periods longer and shorter than two days in the present study as compared to Smith et al. (1992). The stars of period smaller than the break thus enter with somewhat different weight into the calculation of the photographic and CCD $P - L$ relations. This is responsible for a portion of the remaining discrepancy at fainter magnitudes. Nonetheless, comparison of stars common to the two studies suggests that, at $B \sim 17$ there is a systematic difference of about 0.05 mag between the photographic and CCD magnitude systems, with the latter being the brighter. We note that there is some evidence for a field dependent magnitude error of about 0.1 mag in the photographic photometry (Smith et al. 1992; Graham 1975), so that this zero-point shift may not perfectly apply across the entire photographic field.

The comparison of the B $P - L$ relations for the first overtone Cepheids is more complicated, being influenced by the inclusion in this study of significant numbers of variables not discovered in the earlier photographic survey. Part of the difference between the pho-

tographic and CCD $P - L$ relations appears to be attributable to this. Again, however, comparison of the light curves of individual variables indicates a systematic difference of 0.05 mag at $B \sim 17$, in the sense that the CCD photometry is brighter.

Caputo et al. (2000) predict that, at Z = 0.004, the slope of the B $P-L$ relation will be -2.49, for all fundamental mode Cepheids, and -2.71, if limited to only those Cepheids having $\log P_0 < 1.5$. For V, the corresponding theoretical slopes in Caputo et al. (2000) are -2.60 and -2.94. The Cepheids in this study have periods less than $\log P_0 = 1.5$, but the $P - L$ relation slopes listed in Table 9 are slightly less steep than those predicted for such stars. As shown in Figure 16, a quadratic fit to the V $P - L$ relation describes our data better than a single linear $P - L$ relations. However, because relatively few longer period Cepheids are included in our sample, it is not possible to make a meaningful quantitative comparison with the theoretical second order $P - L$ relationships given in Caputo et al. (2000). The theoretical Wesenheit relation for fundamental mode Cepheids in Table 7 of Caputo et al. (2000) has a slope of -3.65 ± 0.02, which is very close to the observed value of -3.63 ± 0.12 in Table 10.

The EROS group (Bauer et al. 1999) reported the existence of a change in the slope of the $P - L$ relation for fundamental mode Cepheids at periods shorter than 2 days. This steepening of the $P - L$ slope was also noted by the OGLE group (Udalski et al. 1999a). Our sample size is smaller than those of the EROS and OGLE studies, making the recognition of a change in slope difficult. Nevertheless when our population of fundamental mode Cepheids is divided at a period of 2 days, it is evident that the two samples possess distinctly different slopes. This is shown graphically in Figures 17 and 18, and coefficients for the resultant fits are listed in Table 11.

Bauer et al. (1999) note that a similar shift is not clearly seen in the $P - L$ relation of the first overtone Cepheids. To demonstrate this they divide their first overtone population into samples at $P = 1.4$ days, the period of a first overtone Cepheid which would correspond to a 2 day fundamental mode period. Although some steepening of their $P - L$ relationship for first overtone mode Cepheids was present at periods shorter than 1.4 day, the change in slope at that period was not statistically significant.

In Table 11, we list the coefficients we obtain fitting $P-L$ relations to our sample of first overtone mode Cepheids, considering separately those with periods longer and shorter than 1.4 day. The overtone slopes, while they do show a tendency to a steepening below a period of 1.4 days, do not demonstrate as significant a difference as is evident for the fundamental mode pulsators. The difference in the coefficients of the slope for periods above and below 1.4 days falls within the limits expected from the uncertainties of the coefficients. This is consistent with the findings of Bauer et al. (1999).

Bauer et al. (1999) considered four possible explanations for the change in the $P-L$ slope of the fundamental mode Cepheids: superposition of two Cepheid populations of different ages and distances, mixing of classical Cepheids and anomalous Cepheids, non-uniform filling of the instability strip, and a thinning of the instability strip at short periods. Smith et al. (1992) had also noted the possibility that some of the shorter period fundamental mode Cepheids might actually be anomalous Cepheids.

Bauer et al. (1999) found no clear evidence for the superposition hypothesis, particularly since they detected no significant change in the $P-L$ slope for the shortest period first overtone Cepheids. They further argued that the faint Cepheids were unlikely to be anomalous Cepheids of the sort present in dwarf spheroidal systems because a known metallicity dependence of the anomalous Cepheid $P-L$ relation (Nemec et al. 1994) would require metallicities much lower than are thought to be common in the stellar population of the SMC. We note, however, that the dependence of the anomalous Cepheid $P-L$ relation upon metallicity found by Nemec et al. (1994) is tied to an adopted metallicity-luminosity relation for RR Lyrae stars. The slopes of the anomalous Cepheid $P-L$ relations in Nemec et al. (1994) are, however, shallower than those reported in Table 11 for fundamental mode Cepheids with periods smaller than 2 days, which is an argument against the anomalous Cepheid hypothesis.

There is some theoretical support for the idea that the lower end of the Cepheid instability strip might not be completely filled. Cepheids cross into the instability strip during the blue-loop phase of their evolution, with the extent of the loop increasing with mass. Low mass fundamental mode Cepheids are reasoned not to have as broad an excursion into the instability strip, indeed eventually missing portions of the strip, then missing the entire strip as the mass continues to decrease. The result is a truncation of the portion of the instability strip that can be physically occupied by stars pulsating in the fundamental mode. This decreases the "width" of the observed instability strip for fundamental mode Cepheids, with a consequent shift in the $P-L$ relation. The models of Baraffe et al. (1998) and Alibert et al. (1999) show that such an effect can produce a change in the slope of the $P-L$ relation.

This hypothesis suffers from the lack of a similar observed change in the first overtone $P-L$ relation. As noted by Bauer et al. (1999), the region of the instability strip occupied by first overtone pulsators is bluer than that occupied by the fundamental mode pulsators. Stars with blue-loops unable to extend into the fundamental portion of the strip ought not to be able to extend into the overtone portion of the strip either. The result would be a depopulation of the overtone sequence at a period corresponding to the luminosity at which the effect is first noticed in the fundamental sequence. A period of 2 days for the fundamental mode Cepheids would translate to the aforementioned 1.4 days for overtone mode Cepheids.

Thus, were this explanation correct, we would expect the first overtone sequences to be depopulated at periods shorter than 1.4 days. While the EROS photometry (Bauer et al. 1999), our photometry, and the OGLE photometry (Udalski et al. 1999b) all indicate that there may be some steepening of the $P-L$ slope for short period first overtone Cepheids, in each case the effect is of doubtful statistical significance. Moreover, relatively large numbers of first overtone mode Cepheids are present at periods shorter than 1.4 day. Alibert et al. (1999) notes that their models suggest that the change in slope of the first overtone $P-L$ relation might be less pronounced, due to a narrowing of the portion of the instability strip occupied by first overtone mode pulsators with respect to that in which fundamental mode pulsators reside. However, Alibert et al. (1999) further noted, though, that their models require that first overtone Cepheids in the SMC with periods shorter than one day should be in the first crossing of the instability strip. Because first crossing stars evolve quickly through the instability strip, they cannot explain the relatively large number of short period first overtone Cepheids which are actually observed, unless stars immersed in this phase of their evolution somehow preferentially pulsate in the first overtone mode.

Our color-magnitude data for SMC Cepheids, and those from Udalski et al. (1999b), do indicate that there may be some change either in the boundaries of the instability strip, or in the occupied region of the instability strip, at lower luminosities. Figures 7 and 8 show that the redward limit of the region occupied by fundamental mode pulsators shifts to bluer colors at $\langle V\rangle_0 \geq 17$. This shift is also noticeable as a slight bend at the very faint end of the period-color relation for fundamental mode Cepheids. The situation for the first overtone pulsators is less clear, particularly because of the redder first overtone pulsators seen in SC10 and SC11 but not within our field. If all else were equal, a blueward shift in the red boundary of the instability strip would tend to remove the longer period Cepheids from the sample at a given luminosity. By itself, this would not produce a shift in the right direction to explain the observed change in $P-L$ slope.

The EROS study (Bauer et al. 1999) employed photometric bandpasses different from the Johnson B and V, preventing a direct comparison of their $P-L$ relations with our own. The coefficients of the $P-L$ relations determined in our study are more readily compared to those determined from the OGLE group's analysis of their SMC sample (Udalski et al. 1999a). As of this writing, this sample is the largest available for the SMC with photometry reduced to the standard BVI system. The OGLE group concentrated primarily on fundamental mode Cepheids, due to their usefulness as distance calibrators.

Udalski et al. (1999a) applied an iterative least squares fitting routine to fundamental mode Cepheids with periods above $\log P = 0.4$, a cutoff they selected to avoid the possible change in slope among the short period Cepheids. Their initial fit in V yielded a shallower

slope (-2.57) for the V $P-L$ relation in the SMC compared to that derived from their LMC sample (-2.76). On the basis of the more numerous population of longer period ($\log P \geq 0.4$) fundamental mode Cepheids in the LMC, and the smaller scatter about the LMC V $P-L$ relation, Udalski et al. (1999a) decided to adopt the steeper LMC slope as the effective SMC slope, and consequently re-fitted the SMC data. In Table 12 we list both their original SMC fits, as well as the V fit obtained with the adopted, steeper LMC slope. The $P-L$ relations listed in Table 12 are those from the OGLE website, and so include the revisions made in 2000 (Udalski et al. 2000).

The $P-L$ relations in Table 12 may be compared with those obtained for the fundamental mode Cepheids in our sample having periods longer than 2 days (Table 11). The least squares fit to our sample gives a slope consistent with the Udalski et al. (1999a) original fit to their V data. However, the uncertainty is large enough to encompass the steeper slope of their adopted fit. The zero-points of the $P-L$ relations of our sample are, however, slightly smaller than those found by Udalski et al. That is particularly so for their "adopted" fit, but is true to a lesser extent for their "original" fit.

9. Relative distance and depth of the northeast arm Cepheids

There has been some debate regarding the depth of the SMC along the line of sight and whether different regions of the SMC lie at different mean distances. Caldwell & Coulson (1986) used $BVRI$ observations of 63 Cepheids to conclude that we see the central bar of the SMC about edge on, and that it has a depth of about 10 kpc. They found the northeast arm to be nearer to us than the central bar, and the southwest region to be more distant, though with a superimposed nearer component. Mathewson et al. (1986) argued for a distance spread of some 30 kpc among SMC Cepheids, while Mathewson et al. (1988) used observations of 61 Cepheids to argue that the SMC as a whole has a depth of some 20 kpc. They interpreted their data as showing that the northeastern arm Cepheids were some 10-15 kpc closer than those in the southern section. However, they found the Cepheids in the northeastern arm to be only slightly nearer than those of the central bar. In contrast, Welch et al. (1987) concluded from infrared observations of SMC Cepheids that the depth of the SMC was smaller, and that the Cepheids generally fell within the circa 4 kpc tidal radius of the SMC.

Hatzidimitriou & Hawkins (1989) investigated the distribution of a different stellar population, using photometry of horizontal branch/red clump stars in outlying northeastern and southwestern regions to conclude that the older SMC population shows a relatively large line of sight depth. In their northeastern region, which is further from the central part of the

SMC than our field, they found a line of sight depth of 17 kpc on average.

To provide further insight into this issue, we can compare the $P-L$ relations for our northeast arm field with those Udalski et al. (1999a) obtained for the main body of the SMC, and with those which may be derived from the Udalski et al. data for the more northeasterly of the fields covered in their survey.

We have constructed $P-L$ relations for Cepheids in OGLE fields SC10 and SC11 (Udalski et al. (1999b) using updated photometry in Udalski et al. (2000)) which, as we have noted earlier, are the OGLE fields closest on the sky to our own. These $P-L$ relations are listed in Table 13 and depicted in Figures 19 through 22. For the fits to the fundamental mode Cepheids, the slopes of the SC10–11 $P-L$ relations are steeper than those obtained for our northeast arm field and the zero points are about 0.08 or 0.09 magnitudes fainter than those which we obtained (Table 9), but the differences are significant only at the one sigma level. At $\log P = 0.4$, the $P-L$ relations for our fundamental mode Cepheids predict B and V magnitudes which are brighter by 0.04 mag or less than those predicted by the $P-L$ relations derived for the Cepheids in SC10 and SC11. The $P-L$ relations for the first overtone mode Cepheids are somewhat more discrepant, but this is mainly attributable to the faint, redder first overtone Cepheids which, as we have noted, seem to be present in SC10 and SC11, but not within our field. We conclude that our northeast arm Cepheids can be at most only slightly closer than those in SC10 and SC11; i.e. there is no steep gradient in mean distance in going along the northeast arm from the SC10 and SC11 fields to our more outlying field.

The scatter about the mean $P-L$ relation for each field is contributed by at least three separate effects: observational uncertainty (including blending of images and differential reddening), the finite color width of the $P-L$ relation, and the geometric depth of the SMC in the region under consideration. The scatter of the individual Cepheids about the mean $P-L$ relation is smaller for our dataset ($\sigma = 0.20$ in V) than for the SC10 and SC11 dataset ($\sigma = 0.24$). However, it is unclear whether this signifies a genuine difference between these fields. The northeast arm field is less crowded than SC10 and SC11, on average, and in deriving its $P-L$ relation we included only Cepheids with good light curves.

Correcting for the observed width of the Cepheid domain in the color-magnitude diagram (see Figure 7), the residual scatter of the northeast arm Cepheids about the $P-L$ relations is about $\sigma = 0.15$, when results from both fundamental mode and first overtone mode Cepheids are combined. Taken at face value, this corresponds to a depth along the line of sight of $\pm$ 4 kpc. There are, of course, outliers for which a distance greater than 4 kpc from the mean would be determined, but it is also true that some of the deduced range in distance is actually attributable to observational error rather than a true distance spread. It is difficult

to decide therefore the extremes in distance of the Cepheids in the northeast arm field. It is clear, however, that most Cepheids within this field are located within ± 4 kpc of the mean distance, and that a very large proportion are located within ± 6 kpc.

The differences between our $P-L$ relations for the northeast arm field and those derived by Udalski et al. (1999a) from their entire SMC Cepheid dataset are somewhat greater. The least squares fit to the V data for our longer period fundamental mode Cepheids (Table 11), predicts $\langle V\rangle_0 = 16.33 \pm 0.07$ at $\log P = 0.4$, whereas Udalski et al.'s (1999a, 2000) original fit to the full OGLE dataset (Table 12) predicts $\langle V\rangle_0 = 16.46 \pm 0.02$, and their adopted fit gives $\langle V\rangle_0 = 16.53$. The corresponding predictions in the B passband are $\langle B\rangle_0 = 16.78 \pm 0.09$ for our fit, and 16.84 ± 0.03 for the original fit of Udalski et al. (1999a). The differences for the first overtone $P-L$ relations are larger, but, as noted earlier, they are more difficult to interpret because of the apparent presence of some types of first overtone Cepheids in the OGLE fields not found within our northeast arm field.

Considering the respective uncertainties, these differences must be regarded as of marginal significance. Nonetheless, they are consistent with the northeast arm being closer than the main body of the SMC by about 4 kpc. The smaller scatter of the observations about the mean $P-L$ relation for our northeast arm Cepheids compared to the entire OGLE dataset is consistent with the existence of a greater dispersion in distances among the entire OGLE Cepheid population than among the Cepheids of the northeast arm. However, because the entire OGLE sample also includes some Cepheids which suffer significant problems with crowding, photometric errors may also contribute to that increased scatter.

10. RR Lyrae Stars

Two groups of RR Lyrae variables are apparent in Figure 4. Foreground field RR Lyrae stars have the periods and light curve shapes typical of RR Lyrae stars, but their mean magnitudes scatter between 15 and 18. Then there are the actual SMC RR Lyrae stars, clustered at $V \geq 19$. The survey of SMC RR Lyrae stars within our field is very incomplete, and their light curves are fairly noisy. Even those SMC RR Lyrae labeled as having quality "1" light curves in Table 6 have poorer quality light curves than quality "1" SMC Cepheids (but better light curves than the SMC RR Lyrae labeled quality "2"). The seven RRab stars in the SMC with quality "1" V light curves have $\langle V\rangle = 19.39 \pm 0.06$. The five RRab stars with relatively good B light curves have $\langle B\rangle = 19.74 \pm 0.07$. These values are likely to be biased because the RR Lyrae with the better light curves also tend to be among the brighter SMC RR Lyrae in the sample. The mean value of the luminosity-weighted $\langle V\rangle$ values for 11 probable SMC RR Lyrae stars (including some with poorer light curves) is 19.43 ± 0.05.

The luminosity-weighted mean magnitude for the 9 SMC RR Lyrae with usable values of $\langle B \rangle$ is 19.78 ± 0.05. Smith et al. (1992) found a range in $\langle B \rangle$ among the RR Lyrae stars of the northeast arm of the SMC, with a mean magnitude weighted B of 19.88 ± 0.04. The corresponding magnitude weighted mean B magnitude for the present study is 19.83 ± 0.05, in good agreement considering the uncertainties, even though the search for RR Lyrae stars in the present study is more incomplete than in the earlier photographic survey.

Our mean magnitudes for the RR Lyrae stars in the northeast arm field are slightly brighter than the intensity weighted averages Walker & Mack (1988) found for RR Lyrae stars in the SMC cluster NGC 121, $\langle V \rangle = 19.58$ and $\langle B \rangle = 19.91$, or Graham's (1975) values for RR Lyrae stars in the field around NGC 121, $\langle V \rangle = 19.57$ and $\langle B \rangle = 19.95$. It is difficult to state to what degree the incompleteness of the RR Lyrae sample in the present survey is responsible for the difference. However, because of the possibility that our survey is biased toward the brighter RR Lyrae stars, the differences with the Graham and Walker & Mack studies cannot be regarded as evidence that the RR Lyrae population in our northeast arm field is nearer than that around NGC 121.

11. Conclusions

We observe a Cepheid population in the northeast arm which is in most respects indistinguishable from that seen in prior studies of other regions of the SMC. The absence of the faint, redder first overtone Cepheids found in SC10 and SC11 is a possible exception to that conclusion. To within the uncertainties, the slopes of the period-luminosity relations we derive for the northeast arm field are identical to those which have been obtained for more central regions of the SMC. The northeast arm Cepheids may be slightly nearer on average than the Cepheids in the main body of the SMC, but the difference is no greater than about 4 kpc. The Cepheids in the northeast arm region covered by our observations are, at most, only slightly nearer than those in OGLE fields SC10 and SC11, which lie between our field and the central area of the SMC.

Although the number of faint fundamental mode Cepheids within our sample is relatively small, our data support the existence of a break in the slope of the $P - L$ relation for fundamental mode Cepheids at periods shorter than 2 days. There is evidence for a similar break in the $P - L$ relation for the first overtone mode Cepheids near a period of 1.4 days, but in this case the evidence for the break is not statistically significant. The independent EROS and OGLE studies also found marginal evidence for such a break in the slope of the first overtone $P - L$ relation, which strengthens the case for its reality, but is still not conclusive.

The first overtone mode and fundamental mode Cepheids occupy distinct regions of the $V, (B-V)$ CMD. There is some overlap between the fundamental mode and first overtone mode Cepheid regions in the CMD, but this overlap can in most cases be attributed to the observational uncertainty of the photometry. In the few cases in which the overlap in color is too large to be explained in this fashion, the existence of a few instances of unresolved red or blue companions to the Cepheids provides a satisfactory alternative. Below $\langle V \rangle = 17$, the red edge of the region of the CMD occupied by fundamental mode pulsators shifts to bluer colors. This shift does not, by itself, provide an explanation for the break in the slope of the $P-L$ relation at $P = 2$ days.

The period-color relations we obtain are in excellent agreement with those found in analyses of Cepheids in the OGLE survey. However, the observed period-color relation for fundamental mode Cepheids is significantly bluer than the theoretical period-color relation of Alibert et al. (1999) and is slightly bluer than that of Caputo et al. (2000).

We acknowledge use of the Digitized Sky Survey, which was produced at STScI based on photographic data obtained using the UK Schmidt Telescope, operated by the Royal Observatory Edinburgh. The research described in this paper was partially carried out by the Jet Propulsion Laboratory, California Institute of Technology, under a contract with NASA. We thank Jason Lisle for his assistance in early stages of the data reduction. This work has been supported in part by the National Science Foundation under grants AST-9317403 and AST-9986943.

REFERENCES

Alibert, Y., Baraffe, I., Hauschildt, P., & Allard, F. 1999, A&A, 344, 551

Arp, H. 1960, AJ, 65, 404

Baraffe, I., Alibert, Y., M'era, D., Chabrier, G., Beaulieu, J.-P., 1998, ApJ, 499, L205

Bauer, F. et al. 1999, A&A, 348, 175

Blanco, V. M. 1992, AJ, 104, 734

Bono, G., Caputo, F., Castellani, V., & Marconi, M. 1999, ApJ, 512, 711

Butler, D. 1975, ApJ, 200, 68

Caldwell, J.A.R. & Coulson, I.M. 1986, MNRAS, 218, 223

Caputo, F., Marconi, M., & Musella, I. 2000, A&A, 354, 610

Da Costa, G.S. & Mould, J.R. 1986, ApJ, 305, 214

De Santis, R. 2001, MNRAS, 326, 397

Graham, J.A. 1975, PASP, 87, 641

Grieve, G.R. & Madore, B.F. 1986, ApJS, 62, 427

Harris, W.E. 1982, ApJS, 50, 573

Hatzidimitriou, D., & Hawkins, M.R.S. 1989, MNRAS, 241, 667

Hodge, P.W. & Wright, F.W. 1977, The Small Magellanic Cloud (University of Washington Press, Seattle)

Landolt, A. 1992, AJ, 104, 340

Madore, B.F. & Freedman, W.L. 1991, PASP, 103, 933

Mathewson, D.S., Ford, V.L., & Visvanathan, N. 1986, ApJ, 301, 664

Mathewson, D.S., Ford, V.L., & Visvanathan, N. 1988, ApJ, 333, 617

McNamara,D.H., & Feltz, K.A., 1980, PASP, 92, 587

Nemec, J.M., Nemec, Amanda F.L., Lutz, T., 1994, AJ, 108, 222

Payne-Gaposchkin, C. & Gaposchkin, S. 1966, Variable Stars in the Small Magellanic Cloud, Smithsonian Contributions to Astrophysics, vol. 9

Pickering, E.C. 1912, HCO Circ. No. 173, 3

Preston, G.W. 1959, ApJ, 130, 507

Sandage, A., 1982a, ApJ, 252, 553

Sandage, A., 1982b, ApJ, 252, 574

Smith, H.A., Silbermann, N.A., Barid, S.R., & Graham, J.A. 1992, AJ, 104, 1430

Stellingwerf, R. F. 1975, ApJ, 195, 441

Stetson, P. B. 1987, PASP, 99, 191

Sturch, C. 1966, ApJ, 143, 774

Tucholke, H.-J., de Boer, K. S., & Seitter, W. C, 1996, A&AS, 119, 91

Udalski, A., Szymonski, M., Kubiak, M., Pietrzynski, G., Soszynski, I., Wozniak, P., & Zebrun, K. 1999a, Acta Astron. 49, 201

Udalski, A., Soszynski, I., Szymanski, M, A., Kubiak, M., Pietrzynski, G., Wozniak, P., & Zebrun,K., 1999b, Acta Astron. 49, 437

Udalski, A., Szymonski, M., Kubiak, M., Pietrzynski, G., Soszynski, I., Wozniak, P., & Zebrun, K. 2000, ftp://bulge.princeton.edu/ogle/ogle2/var_stars/smc/cep/catalog/

Welch, D.L., McLaren, R.A., Madore, B.F., & McAlary, C.W. 1987, ApJ, 321, 162

Westerlund, B. E. 1997, The Magellanic Clouds (Cambridge University Press, Cambridge)

Walker, A.R. & Mack, P. 1988, AJ, 96, 872

Fig. 1a.— Finding chart for newly discovered variable stars in the northwest quadrant (field 1). East is at the bottom and north is at the left.

Fig. 1b.— Finding chart for newly discovered variable stars in the northeast quadrant (field 2). East is at the bottom and north is at the left.

Fig. 1c.— Finding chart for newly discovered variable stars in the southeast quadrant (field 3). East is at the bottom and north is at the left.

Fig. 1d.— Finding chart for newly discovered variable stars in the southwest quadrant (field 4). East is at the bottom and north is at the left.

Fig. 2.— Finding chart for the local photometric standards. North is at the bottom and east is at the left.

Fig. 3.— B and V light curves for variable stars within the northeast arm field. Variables observed in both B and V are shown first. Variables observed in only a single color are included at the end of the figure.

Fig. 4.— Pulsating variable stars with quality "1" (see Table 6) light curves in both B and V in the $\langle V \rangle$ versus $\log P$ diagram. Fundamental mode Cepheids, first overtone mode Cepheids, and RR Lyrae stars are identified.

Fig. 5.— Histograms over period for fundamental mode and first overtone mode Cepheids reported in this paper and in Smith et al. (1992)

Fig. 6.— Histograms over period for quality "1" Cepheids and for all Cepheids reported in this paper.

Fig. 7.— $\langle V \rangle_o - (B-V)_{mag,o}$ Color-magnitude diagram for fundamental mode (filled triangles) and first overtone mode (open circles) Cepheids in the northeast arm. Only those stars with quality "1" light curves in both B and V are included.

Fig. 8.— Same as Figure 7, but including fundamental mode (filled squares) and first overtone mode (open squares) Cepheids from fields SC10 and SC11 of Udalski et al. (1999b).

Fig. 9.— Period-color relation for fundamental mode Cepheids. Included are the theoretical period-color relations of Alibert et al. (1999) and Caputo et al. (2000).

Fig. 10.— Period-color relation for first overtone mode Cepheids. Least squares fits to our data and to the OGLE dataset (Udalski et al. 1999b) are shown.

Fig. 11.— B period-luminosity relation for fundamental mode Cepheids in the northeast arm field. Least squares and least absolute deviation fits are shown.

Fig. 12.— B period-luminosity relation for first overtone mode Cepheids in the northeast arm field. The overlapping least squares and least absolute deviation fits are shown.

Fig. 13.— V period-luminosity relation for fundamental mode Cepheids in the northeast arm field. The overlapping least squares and least absolute deviation fits are shown.

Fig. 14.— V period-luminosity relation for first overtone mode Cepheids in the northeast arm field. The overlapping least squares and least absolute deviation fits are shown.

Fig. 15.— Reddening insensitive W_{BFM} versus $\log P$ relations for northeast arm Cepheids. Least square fit shown.

Fig. 16.— Second order fit to the V period-luminosity relation for fundamental mode Cepheids.

Fig. 17.— Change in slope of the B period-luminosity relation for fundamental mode Cepheids at $P = 2$ days.

Fig. 18.— Change in slope of the V period-luminosity relation for fundamental mode Cepheids at $P = 2$ days.

Fig. 19.— B period-luminosity relation for fundamental mode Cepheids in OGLE fields SC10 and SC11 (Udalski et al. 1999b). Our linear least squares and least absolute deviation fits to the SC10 and SC11 data are shown, as is the least squares fit to our northeast arm sample.

Fig. 20.— V period-luminosity relation for fundamental mode Cepheids in OGLE fields SC10 and SC11.

Fig. 21.— B period-luminosity relation for first overtone mode Cepheids in OGLE fields SC10 and SC11.

Fig. 22.— V period-luminosity relation for first overtone mode Cepheids in OGLE fields SC10 and SC11.

Table 1. Journal of Observations

Heliocentric Julian Dates	Year	Months
2448888 - 2448890	1992	September
2448924 - 2448926	1992	October
2449250 - 2449253	1993	September
2449301 - 2449304	1993	November
2449652 - 2449656	1994	October

Table 2. Coordinates of New Variables

SMC	RA (J2000)	DEC (J2000)
137	0:57:08.6	-71:40:06
138	0:57:15.1	-71:49:26
139	0:57:15.9	-71:50:33
140	0:57:27.5	-71:40:57
141	0:57:54.7	-71:40:52
142	0:57:58.7	-71:36:37
143	0:58:02.5	-71:24:57
144	0:58:02.5	-71:24:57
145	0:58:13.4	-71:26:54
146	0:58:13.4	-71:26:55
147	0:58:17.2	-71:51:54
148	0:58:24.7	-71:42:38
149	0:58:33.5	-71:34:46
150	0:58:43.3	-71:42:38
151	0:58:53.7	-71:49:28
152	0:58:55.1	-71:39:03
153	0:59:12.9	-71:48:13
154	0:59:13.4	-71:34:46
155	0:59:16.4	-71:43:30
156	0:59:31.5	-71:51:40
157	0:59:35.4	-71:17:44
158	1:00:02.3	-71:42:08
159	1:00:36.1	-71:47:30
160	1:00:54.3	-71:44:44
161	1:00:56.4	-71:01:42
162	1:00:59.8	-71:12:59
163	1:01:10.1	-71:28:12
164	1:01:16.8	-71:48:41
165	1:01:43.4	-71:25:34
166	1:01:56.7	-71:16:31
167	1:01:56.8	-71:09:60

Table 2—Continued

SMC	RA (J2000)	DEC (J2000)
168	1:02:03.2	-71:43:11
169	1:02:21.6	-71:29:49
170	1:02:32.1	-71:44:00
171	1:02:42.6	-71:08:22
172	1:02:46.1	-71:32:19
173	1:02:50.8	-71:43:45
174	1:03:04.4	-71:34:38
175	1:03:04.4	-71:34:39
176	1:03:14.9	-71:44:53
177	1:03:19.5	-70:56:03
178	1:03:23.2	-71:11:42
179	1:03:32.7	-70:53:19
180	1:03:33.7	-71:36:39
181	1:03:48.3	-71:22:12
182	1:03:49.9	-71:24:40
183	1:03:51.1	-71:42:02
184	1:04:09.9	-71:23:51
185	1:04:20.5	-71:40:38
186	1:04:21.8	-71:46:03
187	1:04:28.7	-71:04:19
188	1:04:32.9	-71:41:24
189	1:04:38.2	-71:40:08
190	1:04:39.6	-71:47:16
191	1:04:45.1	-71:53:41
192	1:04:52.2	-71:25:20
193	1:05:01.2	-71:43:34
194	1:05:07.6	-71:44:33
195	1:05:28.1	-71:40:11
196	1:05:39.4	-71:29:13
197	1:05:49.7	-71:46:56
198	1:06:02.2	-71:41:02

Table 2—Continued

SMC	RA (J2000)	DEC (J2000)
199	1:06:08.5	-71:49:18
200	1:06:18.4	-71:41:43
201	1:06:30.0	-71:08:04
202	1:06:44.3	-71:42:12
203	1:06:49.0	-71:29:22
204	1:06:51.3	-71:53:29
205	1:06:53.3	-71:37:05
206	1:06:59.1	-71:41:06
207	1:07:03.5	-71:39:15
208	1:07:22.8	-70:53:14
209	1:07:42.2	-71:42:56
210	1:07:43.4	-71:13:21
211	1:07:50.6	-71:33:03
212	1:07:52.7	-71:14:13
213	1:07:53.9	-71:50:18
214	1:08:07.4	-71:11:42
215	1:08:08.7	-71:17:24
216	1:08:27.7	-70:53:06
217	1:08:32.9	-71:29:13
218	1:08:50.3	-71:22:33
219	1:08:59.8	-71:34:14
220	1:09:00.0	-71:52:14
221	1:09:02.8	-70:55:13
222	1:09:09.3	-71:19:34
223	1:09:10.2	-71:30:28
224	1:09:13.7	-70:53:33
225	1:09:15.6	-70:55:28
226	1:09:22.6	-71:14:39
227	1:09:25.0	-71:18:11

Table 3. Photometry of Local Standard Stars

ID	RA (J2000)	DEC (J2000)	V	$B-V$	$U-B$	$V-I$
A	1:05:59.9	-71:26:11	13.173	0.628	···	0.714
			13.176	0.627	0.098	0.716
B	1:04:43.2	-71:25:56	12.706	0.770	···	0.819
			12.706	0.774	0.386	0.817
C	1:05:53.4	-71:22:39	14.074	0.760	···	0.869
			14.073	0.755	0.199	0.865
			14.082	0.744	0.188	0.874
D	1:05:57.8	-71:19:14	12.456	0.040	···	0.114
			12.457	0.040	-0.121	0.116
E	1:06:08.9	-71:17:08	13.817	0.746	0.394	0.773
			13.821	0.742	···	0.771
			13.825	0.740	0.377	0.778
F	1:05:06.6	-71:18:06	13.422	0.643	0.180	0.698
			13.435	0.651	···	0.691
G	1:04:41.6	-71:16:46	12.880	0.426	···	0.540
			12.879	0.422	-0.096	0.539
H	1:04:10.0	-71:17:13	14.833	0.688	0.178	0.727
			14.852	0.675	···	0.755
			14.846	0.679	0.171	0.742
I	1:03:53.8	-71:18:54	15.076	-0.240	-0.931	-0.247
			15.070	-0.237	···	-0.263
			15.066	-0.233	-0.947	-0.266
J	1:04:44.3	-71:20:29	15.939	0.599	···	0.734
			15.934	0.613	0.071	0.710
			15.951	0.606	0.051	0.745
K	1:04:53.3	-71:19:59	15.331	0.757	0.318	0.828
			15.335	0.760	···	0.835
			15.330	0.763	0.325	0.826
L	1:05:51.7	-71:18:16	14.807	0.711	0.203	0.822
			14.800	0.719	0.214	0.821
			14.805	0.714	···	0.818

Table 3—Continued

ID	RA (J2000)	DEC (J2000)	V	$B-V$	$U-B$	$V-I$
M	1:04:13.5	-71:25:16	15.092	0.836	0.386	0.986
			15.087	0.824	···	0.962
			15.077	0.830	0.360	0.951
N	1:04:42.3	-71:25:08	15.754	-0.225	-0.894	-0.255
			15.744	-0.218	-0.871	-0.256
			15.754	-0.220	···	-0.238
O	1:05:56.2	-71:20:25	16.829	1.486	0.621	1.443
			16.830	1.522	···	1.421
			16.852	1.509	2.516	1.462
P	1:05:10.5	-71:19:04	16.497	1.230	···	1.300
			16.483	1.244	0.898	1.298
			16.483	1.219	0.949	1.282
Q	1:05:16.1	-71:19:22	16.722	0.969	0.545	1.027
			16.749	0.967	···	1.052
			16.747	0.933	0.430	1.029
R	1:04:52.0	-71:25:39	16.909	0.967	···	1.062
			16.885	0.943	0.690	1.045
			16.891	0.959	0.480	1.071
S	1:04:04.7	-71:28:23	16.853	0.557	···	0.824
			16.846	0.551	-0.011	0.716
			16.825	0.555	0.127	0.774
T	1:04:05.3	-71:27:37	15.641	0.689	0.237	0.727
			15.646	0.686	···	0.758
			15.640	0.686	0.211	0.751
U	1:05:31.4	-71:21:32	15.688	0.026	···	0.022
			15.690	0.033	-0.065	0.025
			15.689	0.027	-0.038	0.026

Table 4. Comparison of Photometry

Reference	n	ΔV	ΔB
Harris	12	0.021 ± 0.010	0.013 ± 0.014
Da Costa et al.	4	···	-0.003 ± 0.021

Table 5. Photometry of Individual Variable Stars

Star ID	Field	Bandpass	HJD	Mag	Error
HV214	2	B	2448889.646	16.342	0.007
HV214	2	B	2448889.779	16.351	0.007
HV214	2	B	2448890.656	16.551	0.008
HV214	2	B	2448890.798	16.565	0.007
HV214	2	B	2448924.587	16.602	0.009
HV214	2	B	2448924.824	16.544	0.009
HV214	2	B	2448925.584	15.205	0.004
HV214	2	B	2448925.734	15.289	0.004
HV214	2	B	2448926.596	15.910	0.006
HV214	2	B	2448926.748	15.996	0.006
HV214	2	B	2449252.722	16.810	0.008
HV214	2	B	2449253.618	15.059	0.003
HV214	2	B	2449253.771	15.292	0.003
HV214	2	B	2449301.596	16.307	0.005
HV214	2	B	2449301.749	16.314	0.006
HV214	2	B	2449302.662	16.552	0.007
HV214	2	B	2449303.660	15.723	0.004
HV214	2	B	2449304.648	15.644	0.004
HV214	2	B	2449304.815	15.747	0.004
HV214	2	B	2449653.556	15.600	0.004
HV214	2	B	2449653.761	15.714	0.005
HV214	2	B	2449656.603	16.593	0.008
HV214	2	V	2448888.628	15.202	0.005
HV214	2	V	2448888.749	15.126	0.005
HV214	2	V	2448888.841	15.216	0.005
HV214	2	V	2448889.663	15.438	0.004
HV214	2	V	2448889.797	15.473	0.005
HV214	2	V	2448890.671	15.589	0.005
HV214	2	V	2448924.652	15.647	0.005
HV214	2	V	2448924.843	15.736	0.008
HV214	2	V	2448925.598	14.589	0.003
HV214	2	V	2448925.753	14.701	0.003
HV214	2	V	2448926.572	15.281	0.005
HV214	2	V	2448926.722	15.226	0.004
HV214	2	V	2449253.601	14.420	0.003
HV214	2	V	2449253.789	14.655	0.003
HV214	2	V	2449301.612	15.400	0.004
HV214	2	V	2449302.645	15.636	0.006

Table 5—Continued

Star ID	Field	Bandpass	HJD	Mag	Error
HV214	2	V	2449302.793	15.634	0.005
HV214	2	V	2449303.643	15.087	0.004
HV214	2	V	2449303.786	14.780	0.003
HV214	2	V	2449304.798	15.020	0.004
HV214	2	V	2449652.721	14.968	0.005
HV214	2	V	2449653.574	14.886	0.004
HV214	2	V	2449653.744	14.968	0.004
HV214	2	V	2449656.621	15.573	0.005

Note. — The complete version of this table is in the electronic edition of the Journal. The printed edition contains only a sample.

Table 6. Attributes of Observed Variables

Num	Type	P (days)	$\langle B \rangle$	$\langle V \rangle$	$\langle B \rangle - \langle V \rangle$	$(B-V)_{mag}$	Qual	Notes
HV								
214	F	4.20494	16.232	15.775	0.457	0.498	2	
841	F	1.90951	17.010	16.696	0.314	0.347	1	
856	F	6.07682	15.936	15.139	0.798	0.810	2	
1717	F	1.87023	17.117	16.766	0.351	0.394	1	
1718	F	4.04534	16.439	15.954	0.485	0.497	2	
1727	F	2.22099	16.636	16.362	0.275	0.300	1(V)	
1732	F	1.75459	17.158	16.844	0.314	0.323	1(V)	
1755	O	1.50575	16.837	16.525	0.311	0.322	1	
1759	F	1.73444	17.156	16.758	0.399	0.404	1	
1779	O	1.78335	16.532	16.144	0.388	0.398	1	
1788	O	3.47885	15.762	15.338	0.424	0.428	1	
1793	F	4.18158	16.549	16.021	0.528	0.558	2	
1807	F	4.08858	16.569	16.067	0.502	0.523	2	
1855	F	6.83922	15.922	15.361	0.561	0.579	1	
1860	O	1.98478	16.345	16.001	0.344	0.349	1	
1863	RRab	0.51327	18.162	17.733	0.430	0.430	2	(a)
1869	F	2.46485	17.381	16.849	0.532	0.541	1	
1871	F	1.30090	17.515	17.175	0.339	0.380	1	
1883	O	2.01315	16.536	16.102	0.434	0.444	1	
1890	F	1.77851	17.215	16.825	0.390	0.428	1	
1892	F	5.65497	16.292	15.700	0.592	0.601	2	
1897	O	1.24131	17.089	16.738	0.351	0.360	1(V)	
1898	F	3.01818	16.434	16.141	0.293	0.296	2	(b)
1901	F	3.57357	16.900	16.323	0.577	0.591	1	
1906	F	3.06560	16.759	16.230	0.529	0.551	2	
1907	F	1.64318	17.243	16.873	0.370	0.420	1(B)	
1919	F	1.71874	17.501	17.071	0.430	0.478	1	
1929	F	5.58692	15.958	15.520	0.438	0.442	1	
1934	F	4.87545	16.294	15.758	0.536	0.560	1	
1945	F	6.47378	15.936	15.382	0.554	0.579	1	

Table 6—Continued

Num	Type	P (days)	$\langle B \rangle$	$\langle V \rangle$	$\langle B \rangle - \langle V \rangle$	$(B-V)_{mag}$	Qual	Notes
HV								
1950	F	7.98574	15.752	15.108	0.644	0.655	1(B)	
1958	F	1.33443	17.653	17.256	0.397	0.460	1	
1970	F	3.33609	16.630	16.195	0.435	0.484	1(V)	
1976	F	1.90304	17.386	17.018	0.367	0.425	1(B)	
1982	F	5.22421	16.259	15.659	0.601	0.618	2	
1983	F	3.43840	16.255	15.824	0.431	0.459	1	
1987	F	3.13062	16.671	16.167	0.504	0.522	1	
1989	O	1.08200	17.014	16.627	0.387	0.398	1	
1999	F	1.96777	17.351	16.905	0.446	0.468	1	
2002	F	2.34646	16.966	16.543	0.423	0.477	1	
2003	F	5.05307	16.571	15.932	0.638	0.646	1	
2013	F	2.85747	16.756	16.321	0.435	0.486	1	
2014	F	2.20378	16.803	16.412	0.391	0.445	1	
2015	F	2.87409	17.091	16.549	0.543	0.565	1	
2017	F	11.40440	15.457	14.749	0.709	0.718	2	
2043	RRab	0.60337	15.593	15.220	0.373	0.389	1	
2045	F	2.84686	16.827	16.284	0.543	0.574	1	
2053	F	3.21897	16.805	16.332	0.473	0.499	1	
2054	F	7.16373	15.799	15.212	0.587	0.597	2	
2055	F	3.54469	16.974	16.363	0.611	0.615	2	
2057	F	1.90899	17.202	16.809	0.393	0.447	1	
2059	F	2.85985	16.739	16.328	0.411	0.422	1(V)	
2063	F	11.17360	15.425	14.777	0.649	0.672	2	
2068	O	1.80701	16.863	16.438	0.425	0.436	1	
2074	O	2.19972	16.487	16.120	0.367	0.378	1	
2076	F	2.49908	16.706	16.269	0.437	0.487	1	
2078	F	4.70610	16.330	15.801	0.528	0.559	1	
2085	F	3.71630	16.837	16.287	0.549	0.568	1	
2088	F	14.57880	15.533	14.754	0.779	0.807	2	
2102	RRab	0.51404	16.162	15.863	0.299	0.339	1	

Table 6—Continued

Num	Type	P (days)	$\langle B \rangle$	$\langle V \rangle$	$\langle B \rangle - \langle V \rangle$	$(B-V)_{mag}$	Qual	Notes
HV								
2107	F	2.41154	16.885	16.439	0.446	0.482	1	
10364	F	1.50304	17.870	17.238	0.632	0.683	1(V)	
10365	O	1.25811	17.202	16.840	0.362	0.377	1	
10367-1	F	1.54812	17.488	17.109	0.379	0.427	1	
10367-2	F	2.76831	17.194	16.680	0.514	0.531	1	
10373	F	3.07538	16.940	16.362	0.579	0.627	2	
10375	F	5.94034	16.402	15.783	0.618	0.625	1	
11190	O	1.36617	17.030	16.670	0.360	0.370	1(B)	
11191	F	1.96643	16.904	16.497	0.407	0.445	1	
11192	F	2.35403	16.964	16.570	0.394	0.423	2	
11197	F?	1.07507	17.109	16.713	0.396	0.409	2	
11199	F	2.09523	17.266	16.874	0.392	0.408	1	
11206	F	3.39809	16.691	16.195	0.496	0.507	1	
11209	O	1.92843	16.641	16.238	0.403	0.413	1	
11375	O	1.11490	17.134	...	...	...	1	
11395	F	1.29710	18.081	17.621	0.460	0.478	1	
11449	O	1.31566	17.057	16.686	0.371	0.377	1	
11457	O	2.27465	16.619	16.234	0.385	0.391	1	
11463	F	1.75536	17.625	17.176	0.450	0.473	1	
11485	F	1.20924	17.829	17.449	0.381	0.421	1	
11500	O	1.78969	16.620	16.244	0.375	0.385	1	
11501	F	3.57905	16.914	16.306	0.608	0.614	2	
11502	?	3.27030	16.410	15.941	0.469	0.473	2	(c)
12942	F	3.89314	16.426	15.890	0.536	0.554	2	
12943	F	3.71538	16.643	16.090	0.553	0.572	1	
12949	RRab	0.47498	17.592	17.286	0.306	0.353	1	
13020	O	0.98915	17.424	17.111	0.312	0.326	2	
13021	O	1.81468	16.734	16.320	0.414	0.420	1	

Table 6—Continued

Num	Type	P (days)	$\langle B \rangle$	$\langle V \rangle$	$\langle B \rangle - \langle V \rangle$	$(B-V)_{mag}$	Qual	Notes
SMC								
4	O	1.59263	17.114	16.649	0.464	0.478	1	
5	F	2.50085	17.144	16.657	0.487	0.509	1	
6	RRab	0.60537	19.689	19.240	0.450	0.474	2	
7	F	1.02203	18.130	17.751	0.379	0.394	2	
9	RRab	0.58500	···	18.833	···	···	2	
10	RRab	0.59463	19.939	19.535	0.405	0.417	2	
11	F	1.07980	18.182	17.781	0.401	0.414	2	
12	F	1.33366	17.474	17.157	0.317	0.365	1	
14	F	1.72298	17.736	17.233	0.503	0.521	1	
18	E	0.31872	18.528	···	···	···	2	(d)
19	E	0.43382	18.422	18.343	0.079	0.078	2	
20	F	1.49082	17.616	17.192	0.425	0.452	1	
24	F	1.43056	···	17.320	···	···	2	
25	RRab?	0.52774	···	19.531	···	···	2	
26	RRab	0.44636	17.538	17.188	0.351	0.401	1	
27	F	1.50863	17.604	17.020	0.584	0.608	1	
29	RRab	0.47084	18.135	17.856	0.279	0.335	1	
31	O	0.58038	18.137	17.774	0.363	0.371	1	
32	F	2.26841	17.123	16.742	0.381	0.427	1	
34	O	1.93682	16.663	16.233	0.430	0.439	1	
36	F	2.11420	17.505	16.989	0.516	0.548	1	
37	RRab	0.59659	19.884	19.507	0.377	0.393	1	
38	F	1.63004	17.576	17.234	0.342	0.393	2	
42	F	1.33152	17.814	17.449	0.364	0.405	1(B)	
45	RRab	0.52640	19.702	19.451	0.251	0.266	1(V)	
46	F?	2.55475	17.206	16.671	0.535	0.545	2	
48	F	2.29939	17.395	···	···	···	1	
50	F	0.88530	18.653	18.380	0.273	0.308	1	
53	O	0.82857	17.639	17.335	0.304	0.311	1	
55	E	1.35994	18.666	18.673	-0.006	-0.000	1	

Table 6—Continued

Num	Type	P (days)	$\langle B \rangle$	$\langle V \rangle$	$\langle B \rangle - \langle V \rangle$	$(B-V)_{mag}$	Qual	Notes
SMC								
57	O	0.72152	17.821	17.494	0.328	0.341	1	
59	O	0.86133	17.737	17.392	0.345	0.359	1	
61	?	0.51718	18.757	18.122	0.636	0.635	2	(e)
62	O	0.78903	17.837	17.341	0.496	0.502	1(V)	
65	F	2.00666	17.520	17.015	0.504	0.534	1	
66	O	1.19755	17.244	16.891	0.354	0.363	1	
68	F	2.04065	17.221	16.772	0.449	0.483	1(V)	
72	O	0.91060	17.761	17.413	0.348	0.361	1	
73	O	1.26752	17.108	16.742	0.366	0.377	1	
74	F	1.52872	17.394	17.044	0.350	0.383	1	
75	F	1.52205	17.595	17.116	0.478	0.493	2	
77	O	1.35339	17.026	16.672	0.354	0.365	1	
80	F	1.28913	17.588	17.194	0.394	0.396	1	
84	O	0.76310	17.672	17.392	0.280	0.295	1	
87	O	0.88342	17.438	17.071	0.367	0.384	1	
88	O	0.81100	17.744	17.380	0.363	0.379	1	
89	RRab	0.45418	17.128	16.880	0.248	0.290	1	
90	O	2.71711	16.377	15.901	0.475	0.481	1	
92	O	0.84835	17.760	17.405	0.355	0.368	1	
95	F	2.61612	17.317	16.735	0.583	0.594	1	
96	F	1.34841	17.990	17.540	0.450	0.473	1(V)	
103	F	1.54345	17.514	17.156	0.358	0.378	2	
107	F	6.49091	15.833	15.286	0.547	0.571	1	
110	O	2.06922	16.808	16.395	0.413	0.420	1	
111	F	1.83433	17.089	16.740	0.349	0.376	2	
113	F	1.08116	18.290	17.945	0.345	0.390	1	
114	O	0.97918	17.192	16.918	0.275	0.285	2	
117	F	3.09329	16.987	16.452	0.535	0.547	1	
124	O	0.86375	17.041	16.925	0.116	0.116	2	(f)
128	O	0.76036	18.099	17.735	0.365	0.377	1	

Table 6—Continued

Num	Type	P (days)	$\langle B \rangle$	$\langle V \rangle$	$\langle B \rangle - \langle V \rangle$	$(B-V)_{mag}$	Qual	Notes
SMC								
133	F	1.04962	18.048	17.710	0.338	0.368	1	
137	F	1.87056	17.074	16.746	0.328	0.379	1	
138	F	2.23245	17.431	16.825	0.605	0.595	2	
139	O	1.17628	17.155	16.840	0.315	0.325	1	
140	E	2.30000	17.408	17.390	0.018	0.024	2	
141	O	1.16093	17.350	16.992	0.358	0.368	2	
142	O	1.29270	16.975	16.660	0.315	0.325	1	
143	O	0.93092	17.457	17.130	0.326	0.334	2	
144	O	0.93102	17.492	17.105	0.388	0.395	1	
145	O	2.07337	16.265	15.924	0.341	0.344	1	
146	O	2.07366	16.315	15.945	0.370	0.373	1	
147	O	2.29499	16.439	16.044	0.395	0.401	1	
148	F?	1.70068	17.285	16.851	0.434	0.451	2	(g)
149	F	1.64127	17.579	17.149	0.430	0.442	1	
150	RRc?	0.30425	16.806	16.916	-0.110	-0.110	1	
151	F	2.73870	16.707	16.186	0.521	0.526	1	
152	O	1.72946	16.930	16.525	0.404	0.410	1	
153	F	4.18143	16.546	16.019	0.528	0.557	1	
154	O	1.29851	16.821	16.505	0.316	0.321	1	
155	E	3.07225	16.469	16.543	-0.075	-0.075	1	
156	O	1.58453	16.709	16.316	0.394	0.402	1	
157	O	1.20883	16.844	16.504	0.339	0.349	1	
158	E	2.56280	15.322	15.500	-0.178	-0.179	1	
159	O?	1.06209	17.185	16.870	0.315	0.324	2	
160	F?	3.93866	16.808	16.513	0.295	0.298	2	(h)
161	F	1.16736	18.462	18.024	0.438	0.453	2	
162	O?	0.86912	17.501	17.175	0.326	0.337	2	
163	E	1.47070	15.522	15.580	-0.058	-0.058	2	
164	O	2.41914	15.950	15.651	0.299	0.303	1	
165	O?	0.89960	17.908	17.438	0.470	0.476	2	

Table 6—Continued

Num	Type	P (days)	$\langle B \rangle$	$\langle V \rangle$	$\langle B \rangle - \langle V \rangle$	$(B-V)_{mag}$	Qual	Notes
SMC								
166	O	1.25427	17.041	16.688	0.353	0.362	1	
167	RRab	0.57382	19.860	19.498	0.362	0.391	1	
168	F	5.65365	16.284	15.702	0.583	0.593	1	
169	F	3.57270	16.925	16.331	0.594	0.611	1	
170	F	1.87530	17.838	17.292	0.547	0.549	1	
171	O	1.13510	17.227	16.884	0.343	0.349	2	
172	F	2.73273	17.348	16.801	0.546	0.551	1	
173	F	1.51413	17.892	17.435	0.457	0.469	2	
174	E	0.95080	17.865	18.002	-0.137	-0.138	2	(i)
175	E	0.48735	17.994	18.026	-0.032	-0.030	2	
176	F	4.87578	16.304	15.729	0.575	0.602	1	
177	F	3.86046	16.355	15.896	0.460	0.514	1(B)	
178	E	1.78000	18.213	16.739	1.474	1.472	2	
179	RRab	0.47324	15.836	15.533	0.303	0.356	1	
180	RRab	0.59722	19.465	19.202	0.263	0.295	1	
181	F	1.30524	18.691	18.243	0.448	0.452	2	
182	F	1.87157	17.463	16.999	0.465	0.479	1	
183	F	1.87780	17.316	16.846	0.470	0.473	1	
184	O	1.05237	17.407	17.067	0.340	0.355	2	
185	O	0.97429	16.613	16.461	0.152	0.154	2	(j)
186	O	1.92178	16.508	16.093	0.415	0.417	1	
187	RRab	0.62042	19.705	19.347	0.358	0.382	1	
188	O	1.13099	17.064	16.770	0.294	0.306	1	
189	O	2.44532	16.324	15.908	0.416	0.421	1	
190	O	1.18244	17.165	16.875	0.290	0.303	1	
191	E	1.25565	17.018	17.119	-0.101	-0.102	2	
192	RRab	0.53193	19.791	19.183	0.608	0.632	1	
193	O	2.31180	16.410	...	...	...	1	
194	O	1.76335	16.537	16.133	0.404	0.415	1	
195	O	1.02323	16.948	16.764	0.184	0.182	2	(k)

Table 6—Continued

Num	Type	P (days)	$\langle B \rangle$	$\langle V \rangle$	$\langle B \rangle - \langle V \rangle$	$(B-V)_{mag}$	Qual	Notes
SMC								
196	F	1.32225	17.962	17.416	0.546	0.554	2	
197	O	1.38819	16.690	16.390	0.300	0.304	1	
198	O	1.05222	17.200	16.884	0.316	0.326	2	
199	O	1.71675	16.630	16.281	0.348	0.354	1	
200	O	2.45760	16.208	15.809	0.399	0.403	1	
201	O	3.15021	15.944	15.557	0.387	0.389	1	
202	O	2.31693	16.358	15.959	0.400	0.406	1	
203	F	1.55752	17.783	17.280	0.502	0.522	1	
204	E	1.07459	17.522	17.584	-0.062	-0.064	2	
205	F	3.37341	17.028	16.409	0.619	0.623	1	
206	F	3.16083	16.882	16.403	0.479	0.484	2	
207	O	2.00913	16.482	16.072	0.410	0.412	1	
208	F	4.59607	16.720	16.058	0.662	0.687	2	
209	O	1.52643	17.139	16.731	0.407	0.412	1	
210	F	2.64359	16.667	16.192	0.475	0.481	1	
211	O	2.42039	16.381	15.964	0.417	0.423	2	
212	O	0.95101	18.082	17.625	0.457	0.463	2	(1)
213	F	1.36882	17.924	17.522	0.403	0.410	1	
214	F	5.48753	16.518	15.909	0.609	0.612	1	
215	O	1.35233	17.116	16.756	0.359	0.367	1	
216	E	0.79765	...	18.489	...	...	2	
217	O	2.24879	16.613	16.143	0.470	0.476	1	
218	O	3.07698	15.964	15.578	0.387	0.389	2	
219	O	0.83412	17.613	17.282	0.331	0.336	1	
220	F	3.16419	16.802	16.345	0.457	0.490	2	
221	RRab	0.56426	19.992	19.697	0.295	0.317	2	
222	O	2.40705	16.401	16.009	0.392	0.398	2	
223	O	1.17509	17.142	17.203	-0.060	-0.053	1(B)	
224	RRab	0.49061	...	19.571	...	...	1	
225	E	1.52010	17.547	17.069	0.479	0.506	2	

Table 6—Continued

Num	Type	P (days)	$\langle B \rangle$	$\langle V \rangle$	$\langle B \rangle - \langle V \rangle$	$(B-V)_{mag}$	Qual	Notes
SMC								
226	O	2.11747	16.681	16.186	0.494	0.497	1	
227	F	6.06841	16.347	15.718	0.629	0.637	2	

[a]Payne-Gaposchkin & Gaposchkin (1966) give P (days)=0.527340 and classify as possible RRab

[b]Probable blue companion (Arp 1960)

[c]Payne-Gaposchkin & Gaposchkin (1966) classify as possible irregular, typing here indeterminate

[d]Much brighter here ($\langle B \rangle = 18.528$) than in Smith et al. (1992) ($\langle B \rangle = 20.1$)

[e]Non-periodic?

[f]Possible blue companion?

[g]Noisy light curve makes typing uncertain

[h]Noise in curves mimicking periodicity?

[i]Blue companion?

[j]Blue companion?

[k]Blue companion?

[l]Extremely low amplitude in V, curve morphology in B more indicative of fundamental mode

Table 7. Reddenings of RR Lyrae Stars

Star	[Fe/H]	ΔS	E_{B-V}
HV12949	-1.15	5.76	0.04
HV2043	-1.50	7.96	0.07
HV2102	-1.18	5.97	0.06
SSBG26	-0.84	3.79	0.09
SSBG29	-1.03	4.97	0.05
SSBG89	-0.93	4.37	0.01

Table 8. Frequency Distribution of Samples: (a) Present Sample, (b) Smith et al. (1992)

Period Range ($\log_{10}$ days)	N(fundamental) (a)	(b)	N(first overtone) (a)	(b)
-0.3 -0.2	0	0	1	0
-0.2 -0.1	0	0	4	6
-0.1 0.0	1	1	16	8
0.0 0.1	7	5	17	6
0.1 0.2	20	15	11	6
0.2 0.3	21	18	12	8
0.3 0.4	15	9	17	4
0.4 0.5	16	13	3	0
0.5 0.6	15	8	1	1
0.6 0.7	9	5	0	0
0.7 0.8	9	6	0	1
0.8 0.9	4	3	0	0
0.9 1.0	1	2	0	0
1.0 1.1	2	4	0	0

Table 9: Coefficients of $P - L$ relations.

Fundamental Mode				
76 Stars in B, 77 Stars in V		α	β	
$\langle B \rangle_o$	least squares	-2.50($\pm$0.12)	17.76($\pm$0.05)	$\sigma = 0.23$
	least abs. deviation	-2.58	17.78	$\sigma = 0.19$
$\langle V \rangle_o$	least squares	-2.79($\pm$0.11)	17.47($\pm$0.05)	$\sigma = 0.20$
	least abs. deviation	-2.79	17.45	$\sigma = 0.16$
First Overtone Mode (1-OT)				
63 Stars in B, 61 Stars in V				
$\langle B \rangle_o$	least squares	-2.88($\pm$0.12)	17.10($\pm$0.03)	$\sigma = 0.16$
	least abs. deviation	-2.88	17.10	$\sigma = 0.12$
$\langle V \rangle_o$	least squares	-3.04($\pm$0.10)	16.83($\pm$0.03)	$\sigma = 0.14$
	least abs. deviation	-3.02	16.83	$\sigma = 0.11$

Table 10: W_{BFM} vs. $\log P$

Fundamental Mode				
77 Stars in V		α	β	
W_{BFM}	least squares	-3.63($\pm$0.12)	16.42($\pm$0.05)	$\sigma = 0.21$
	least abs. deviation	-3.55	16.39	$\sigma = 0.14$
First Overtone Mode				
61 Stars in V				
W_{BFM}	least squares	-3.41($\pm$0.12)	15.88($\pm$0.03)	$\sigma = 0.16$
	least abs. deviation	-3.55	15.91	$\sigma = 0.12$

Table 11: $P - L$ Relations for Different Ranges of Period

Fundamental Mode		α	β	
Period > 2 days (43 stars in B, 44 stars in V)				
$\langle B \rangle_o$	least squares	-2.51($\pm$0.21)	17.78($\pm$0.12)	$\sigma = 0.23$
	least absolute deviation	-2.70	17.87	$\sigma = 0.18$
$\langle V \rangle_o$	least squares	-2.60($\pm$0.19)	17.37($\pm$0.10)	$\sigma = 0.19$
	least absolute deviation	-2.75	17.43	$\sigma = 0.15$
Period < 2 days (33 stars in B, 33 stars in V)				
$\langle B \rangle_o$	least squares	-3.47($\pm$0.44)	17.92($\pm$0.09)	$\sigma = 0.22$
	least absolute deviation	-3.86	17.98	$\sigma = 0.18$
$\langle V \rangle_o$	least squares	-3.86($\pm$0.37)	17.67($\pm$0.08)	$\sigma = 0.19$
	least absolute deviation	-3.56	17.58	$\sigma = 0.15$
First Overtone Mode				
Period > 1.4 days (33 stars in B, 32 stars in V)				
$\langle B \rangle_o$	least squares	-3.05($\pm$0.36)	17.18($\pm$0.12)	$\sigma = 0.17$
	least absolute deviation	-3.09	17.19	$\sigma = 0.14$
$\langle V \rangle_o$	least squares	-3.13($\pm$0.31)	16.88($\pm$0.10)	$\sigma = 0.14$
	least absolute deviation	-3.02	16.84	$\sigma = 0.12$
Period < 1.4 days (30 stars in B, 29 stars in V)				
$\langle B \rangle_o$	least squares	-3.50($\pm$0.26)	17.09($\pm$0.03)	$\sigma = 0.14$
	least absolute deviation	-3.20	17.08	$\sigma = 0.11$
$\langle V \rangle_o$	least squares	-3.49($\pm$0.24)	16.82($\pm$0.03)	$\sigma = 0.14$
	least absolute deviation	-3.10	16.83	$\sigma = 0.10$

Table 12: Coefficients of SMC $P - L$ Relations for Udalski et al. (1999a, as revised 2000)

Fundamental Mode		α	β		N
$\langle V \rangle_o$	*adopted*	-2.78	17.64	$\sigma = 0.26$	464
	original	-2.57($\pm$0.04)	17.49($\pm$0.03)	$\sigma = 0.25$	464
$\langle B \rangle_o$	*original*	-2.21($\pm$0.05)	17.72($\pm$0.04)	$\sigma = 0.32$	465
First Overtone Mode					
$\langle V \rangle_o$	*original*	-3.09($\pm$0.08)	17.14($\pm$0.01)	$\sigma = 0.26$	725
$\langle B \rangle_o$	*original*	-2.93($\pm$0.06)	17.44($\pm$0.02)	$\sigma = 0.32$	729

Table 13: Coefficients of $P - L$ relations: Udalski et al. (1999b) Fields SC10 and SC11

Fundamental Mode		α	β	
107 Stars in B, 107 Stars in V				
$\langle B \rangle_o$	least squares	-2.67($\pm$0.10)	17.85($\pm$0.06)	$\sigma = 0.30$
	least abs. deviation	-2.76	17.91	$\sigma = 0.25$
$\langle V \rangle_o$	least squares	-2.91($\pm$0.08)	17.56($\pm$0.05)	$\sigma = 0.24$
	least abs. deviation	-2.91	17.58	$\sigma = 0.20$
First Overtone Mode (1-OT)				
95 Stars in B, 95 Stars in V				
$\langle B \rangle_o$	least squares	-3.04($\pm$0.18)	17.27($\pm$0.05)	$\sigma = 0.35$
	least abs. deviation	-3.07	17.28	$\sigma = 0.28$
$\langle V \rangle_o$	least squares	-3.20($\pm$0.15)	17.01($\pm$0.04)	$\sigma = 0.30$
	least abs. deviation	-3.28	17.03	$\sigma = 0.24$

SMC Paper
Draft 28 Sept 2001
All Figures.

Fig 1a

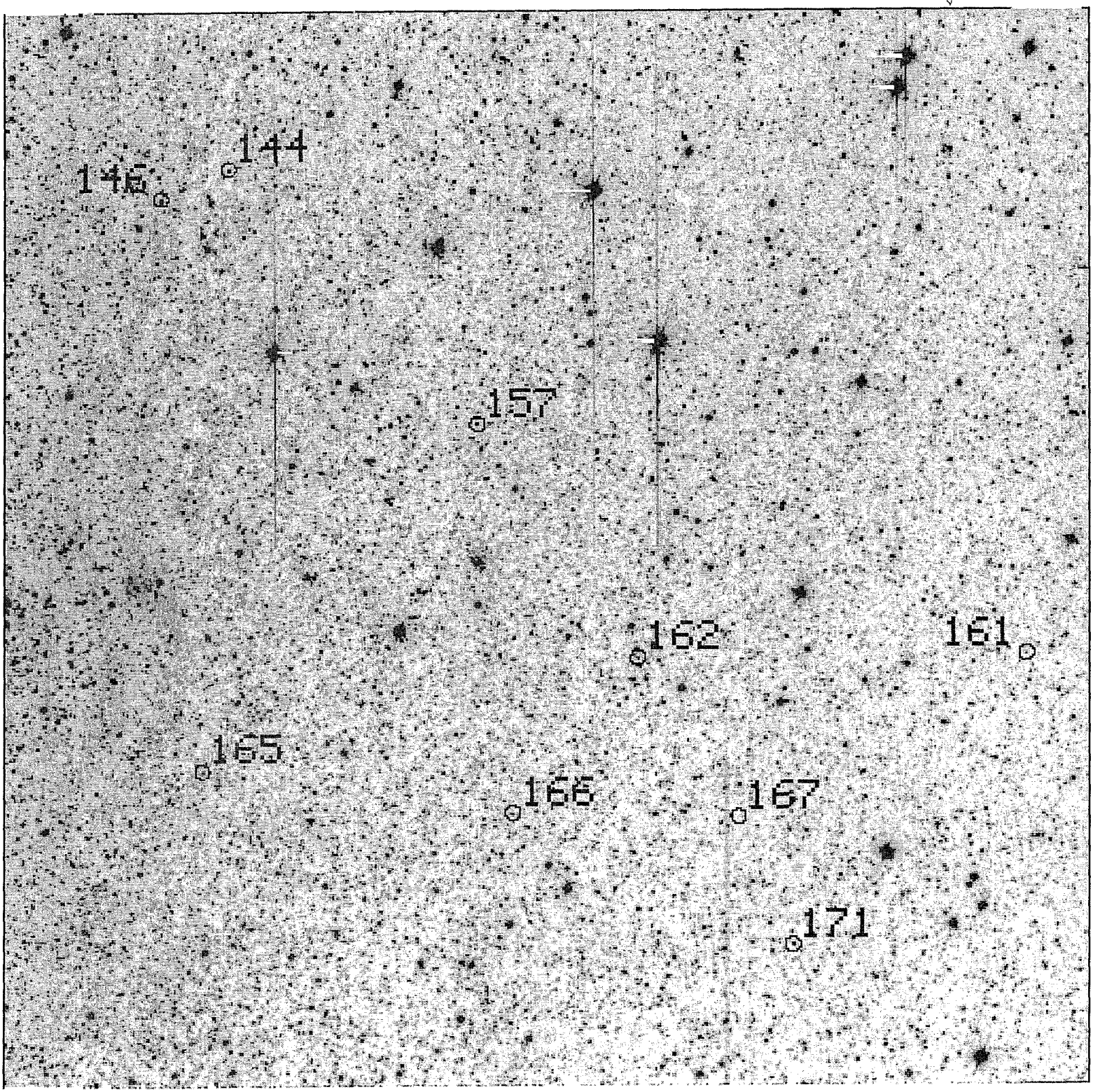

Fig 1b

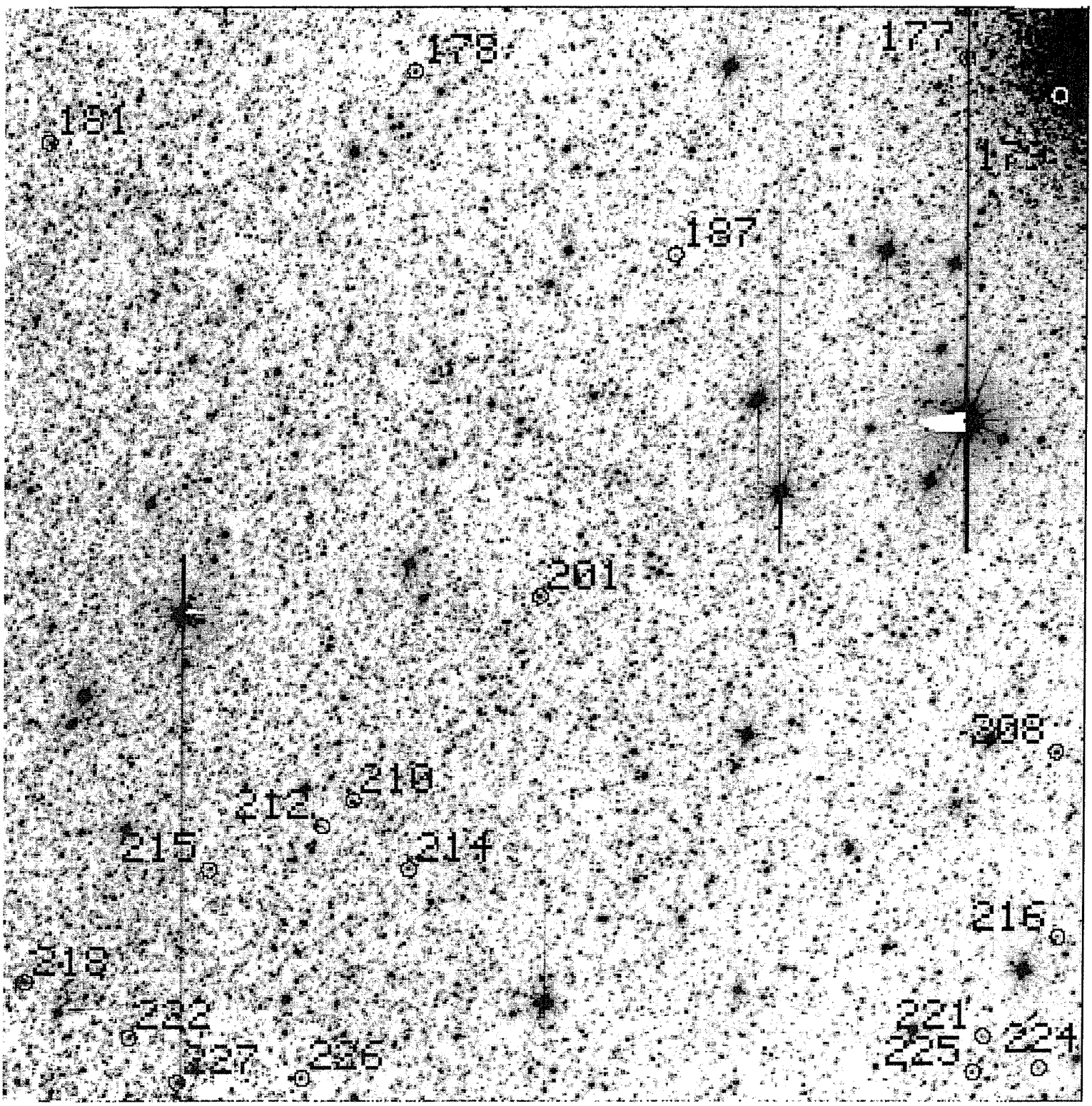
178
177
181
187
201
208
210
212
215
214
216
218
232
227
226
221
225
224

Fig 1c

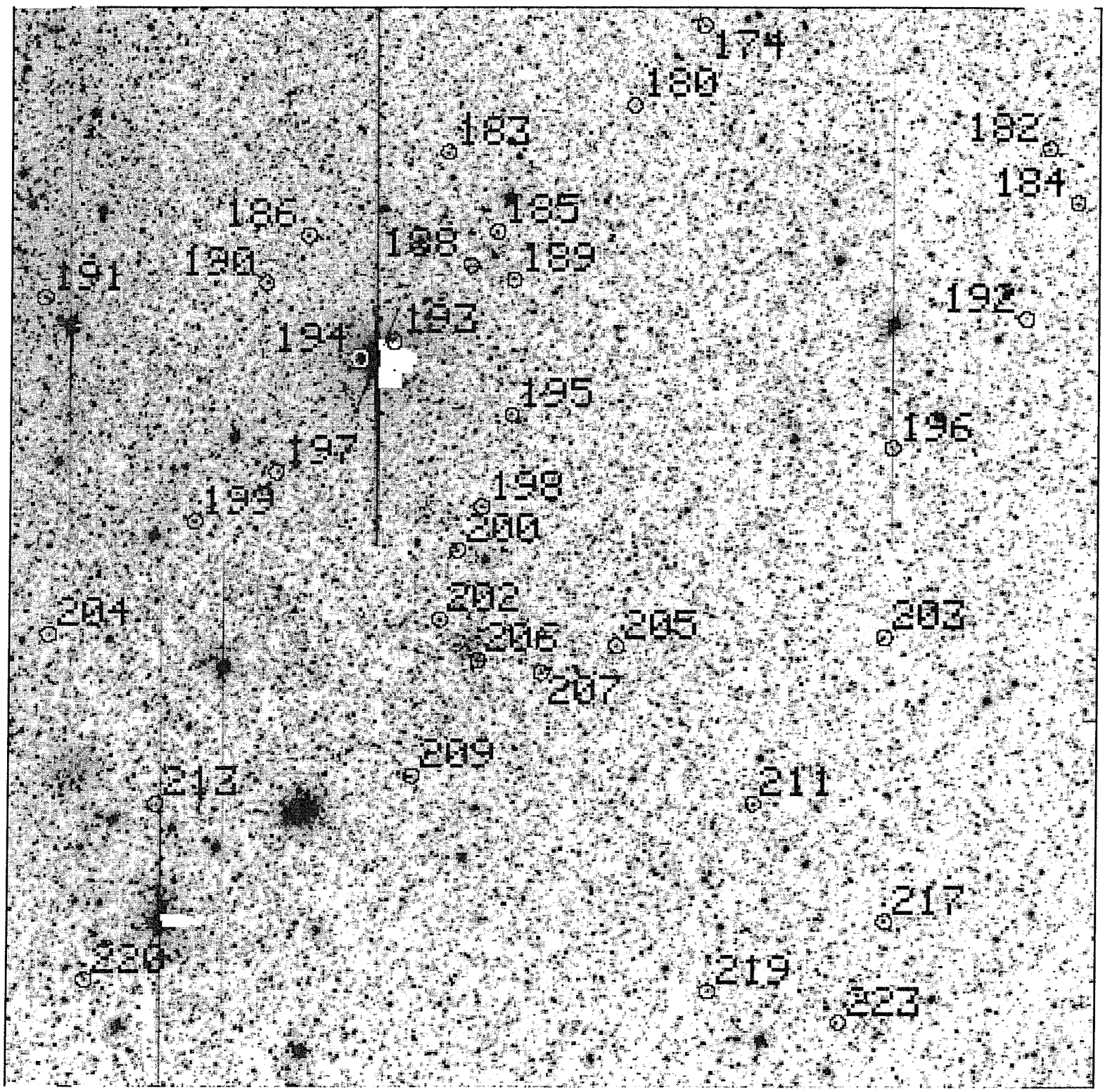
174
180
183
182
184
186
185
188
189
191
190
192
193
194
195
196
197
198
199
200
202
204
206
205
203
207
209
211
213
217
219
223

Fig 1d

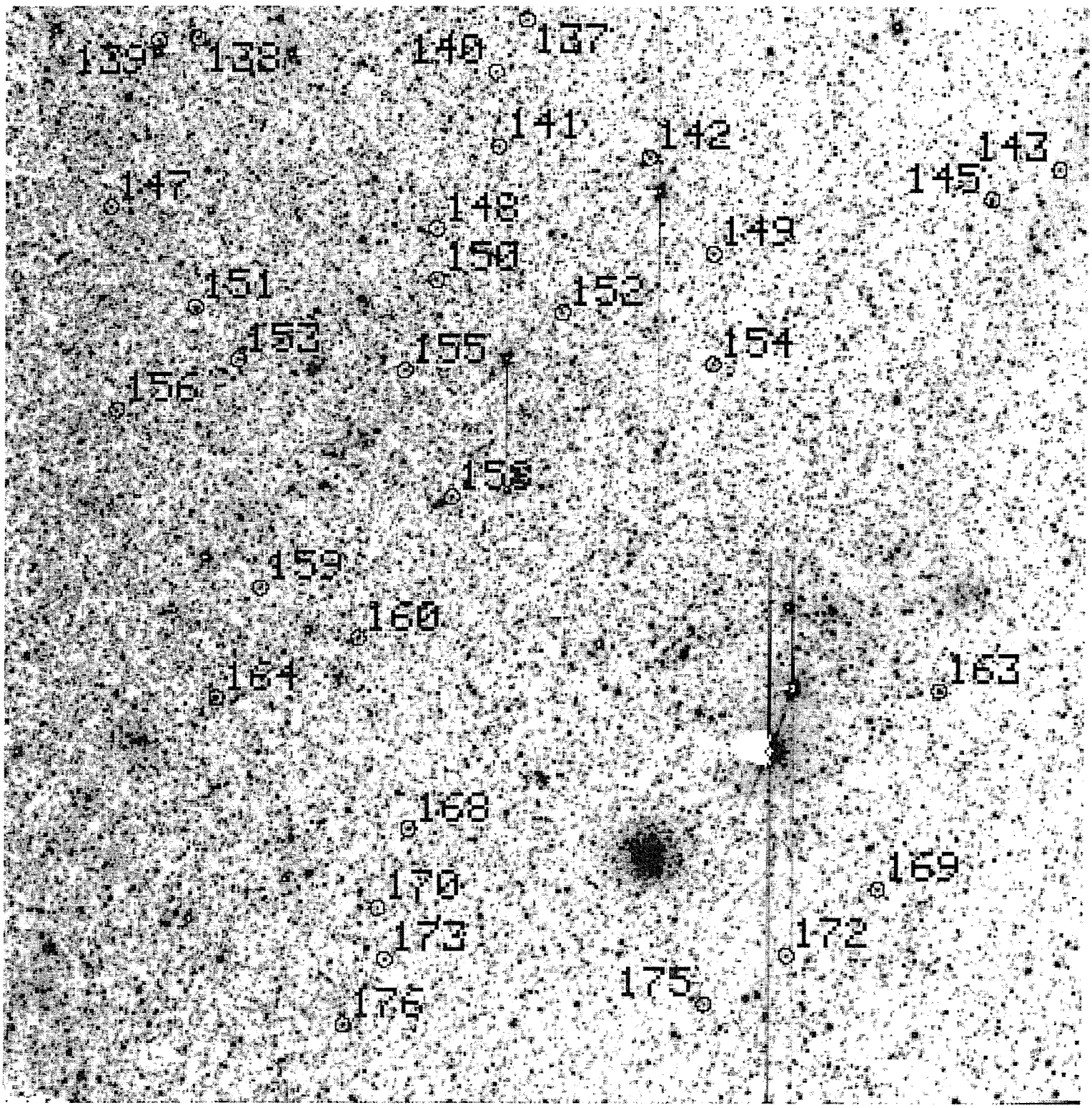
139
138
140
137
141
142
143
147
145
148
149
150
151
152
153
154
155
156
158
159
160
163
164
168
169
170
172
173
175
176

Fig 1e

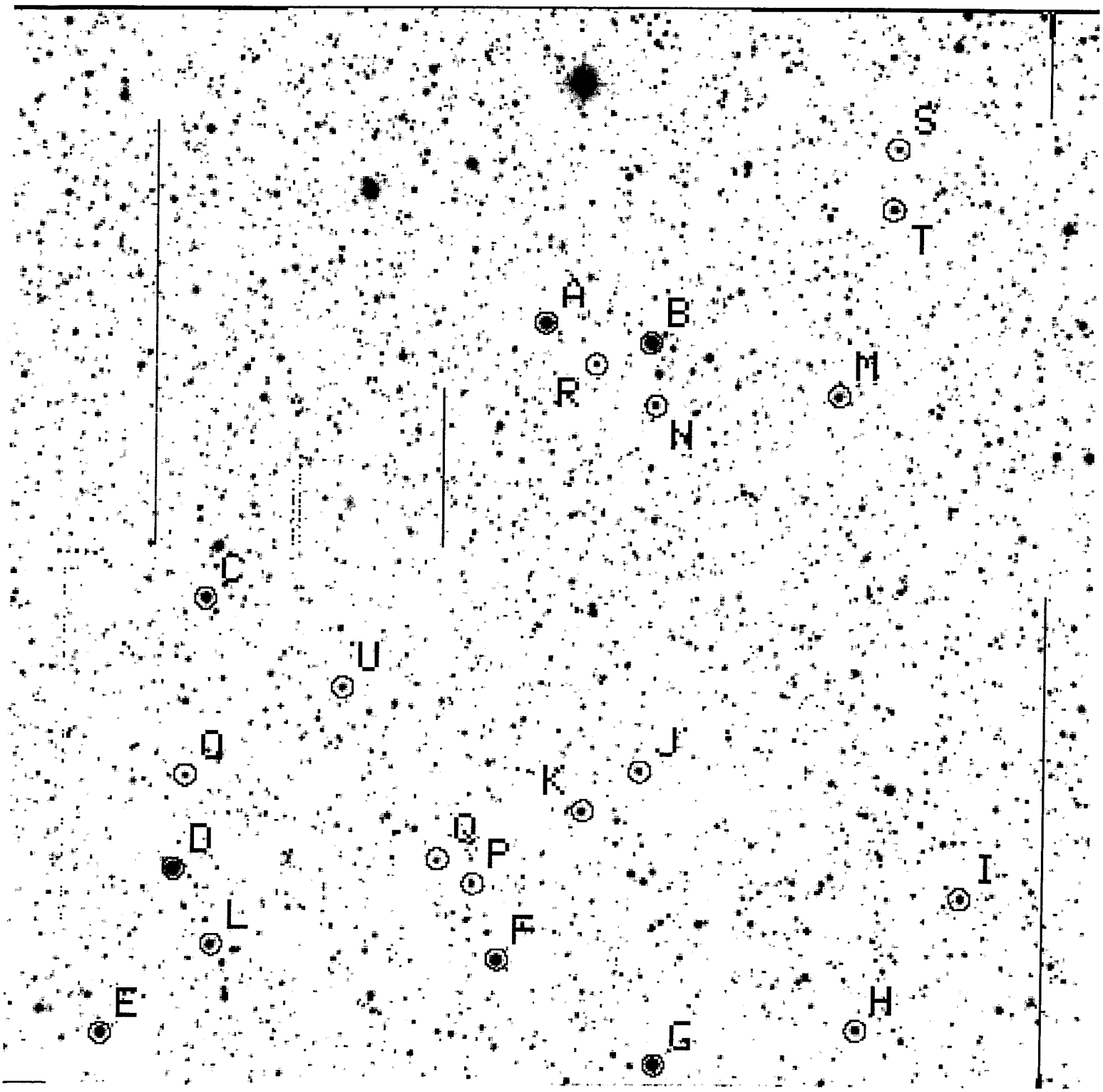

Fig 2

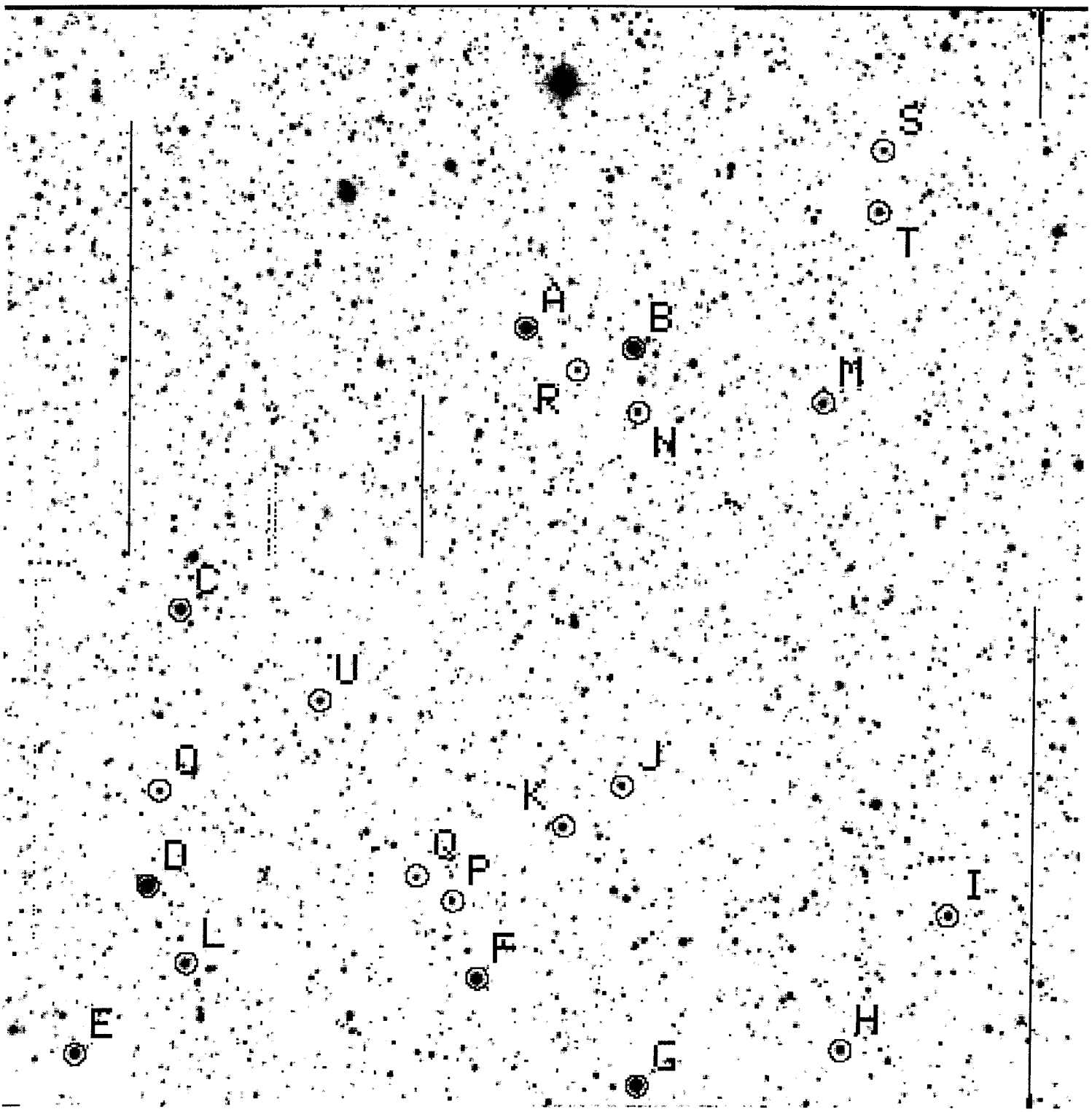

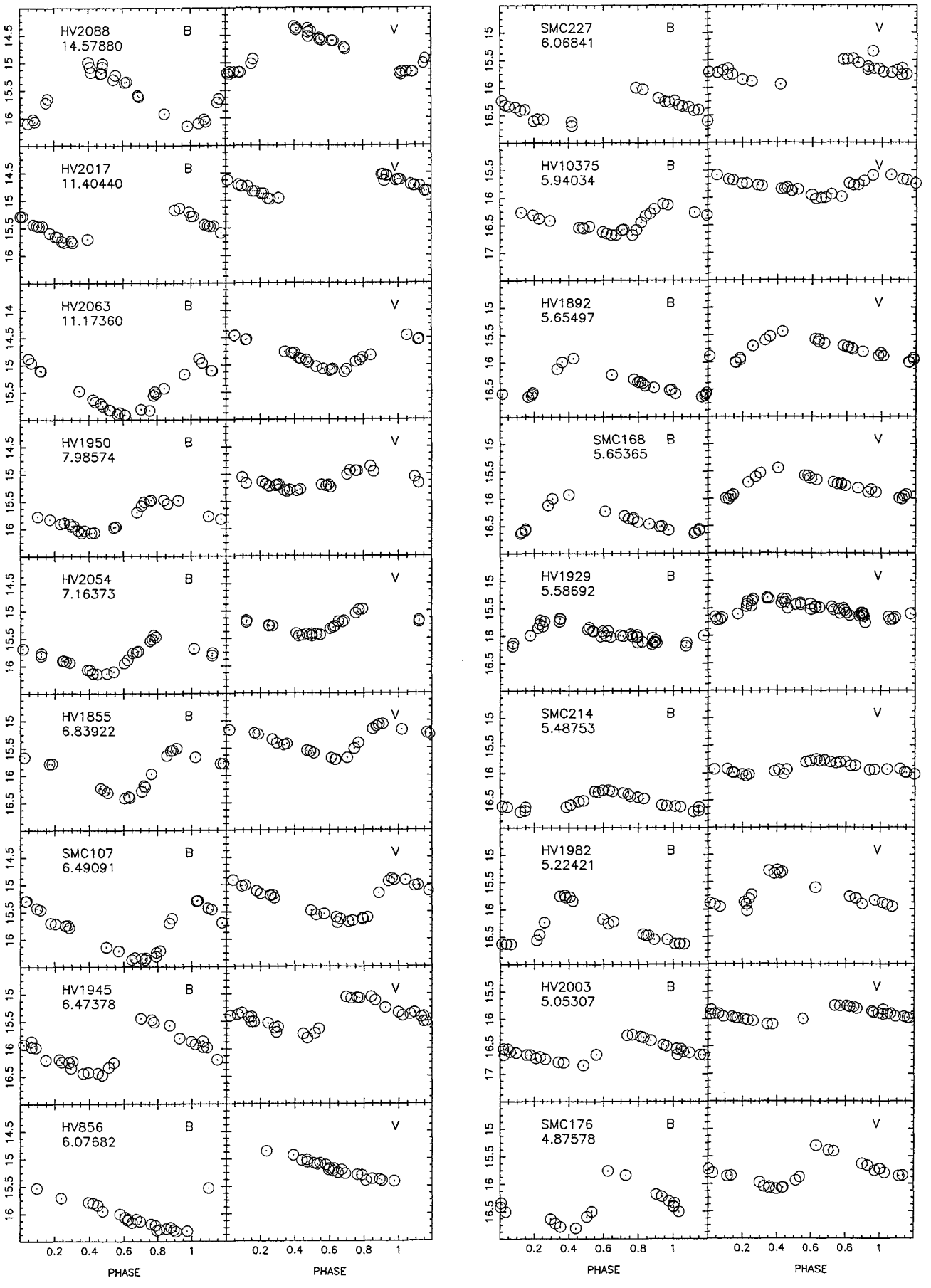
HV2088
14.57880
B
V
HV2017
11.40440
HV2063
11.17360
HV1950
7.98574
HV2054
7.16373
HV1855
6.83922
SMC107
6.49091
HV1945
6.47378
HV856
6.07682
SMC227
6.06841
HV10375
5.94034
HV1892
5.65497
SMC168
5.65365
HV1929
5.58692
SMC214
5.48753
HV1982
5.22421
HV2003
5.05307
SMC176
4.87578
PHASE

Fig 3

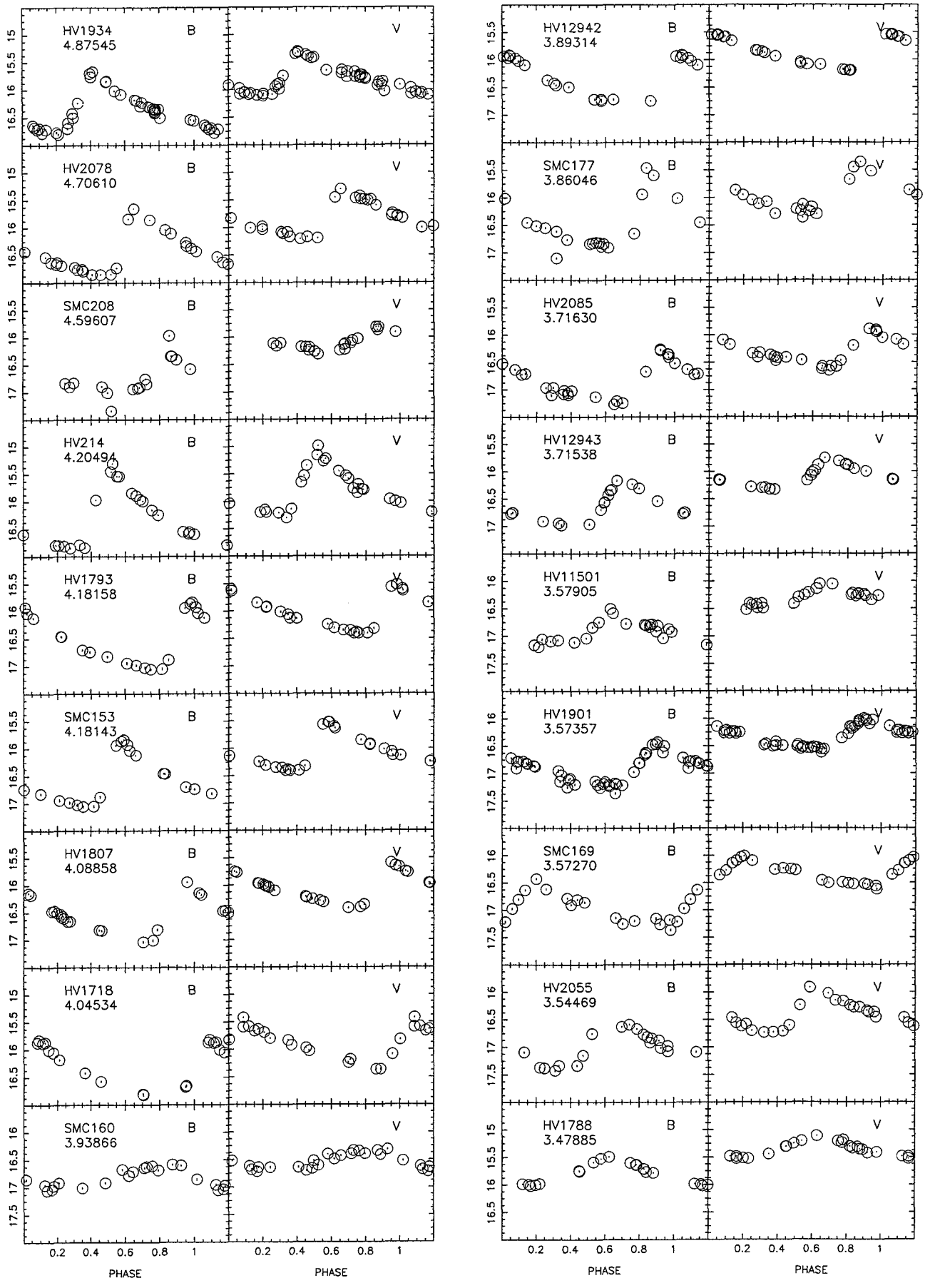
HV1934
4.87545
B
V
HV2078
4.70610
SMC208
4.59607
HV214
4.20494
HV1793
4.18158
SMC153
4.18143
HV1807
4.08858
HV1718
4.04534
SMC160
3.93866
HV12942
3.89314
SMC177
3.86046
HV2085
3.71630
HV12943
3.71538
HV11501
3.57905
HV1901
3.57357
SMC169
3.57270
HV2055
3.54469
HV1788
3.47885
PHASE
PHASE

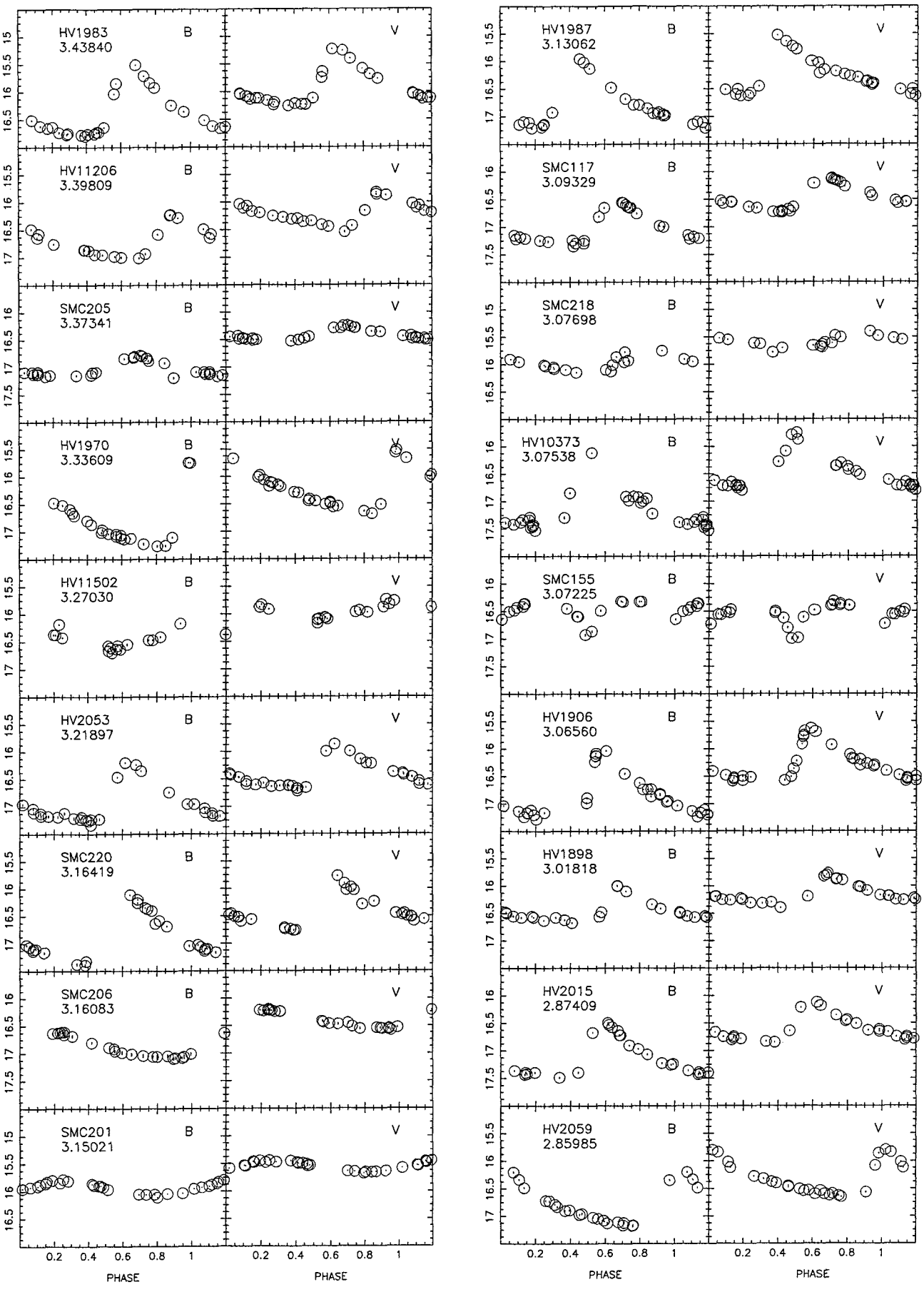
HV1983
3.43840
B
V
HV11206
3.39809
SMC205
3.37341
HV1970
3.33609
HV11502
3.27030
HV2053
3.21897
SMC220
3.16419
SMC206
3.16083
SMC201
3.15021
HV1987
3.13062
SMC117
3.09329
SMC218
3.07698
HV10373
3.07538
SMC155
3.07225
HV1906
3.06560
HV1898
3.01818
HV2015
2.87409
HV2059
2.85985
PHASE

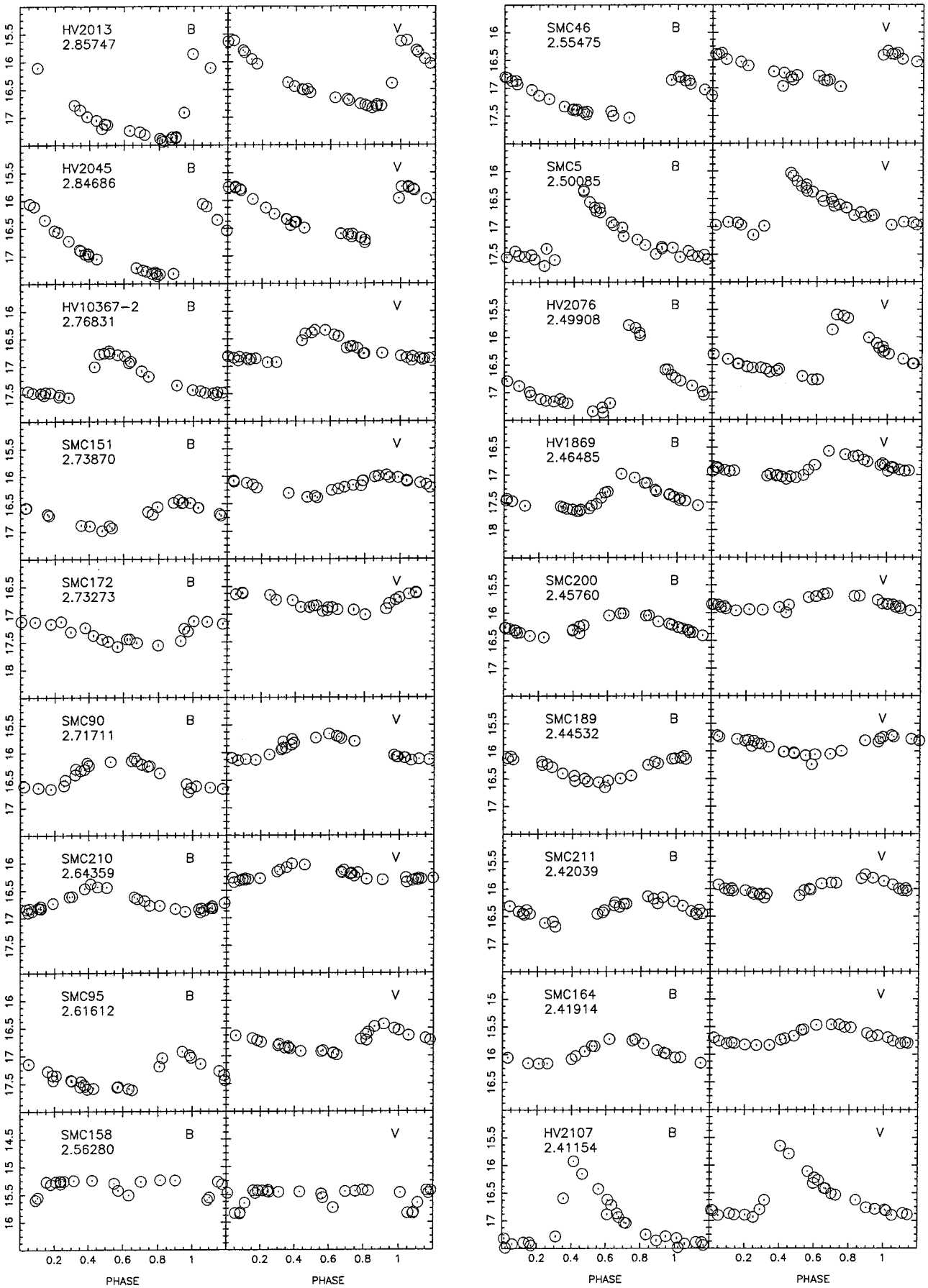
HV2013
2.85747
B
V
HV2045
2.84686
HV10367−2
2.76831
SMC151
2.73870
SMC172
2.73273
SMC90
2.71711
SMC210
2.64359
SMC95
2.61612
SMC158
2.56280
SMC46
2.55475
SMC5
2.50085
HV2076
2.49908
HV1869
2.46485
SMC200
2.45760
SMC189
2.44532
SMC211
2.42039
SMC164
2.41914
HV2107
2.41154
PHASE
PHASE

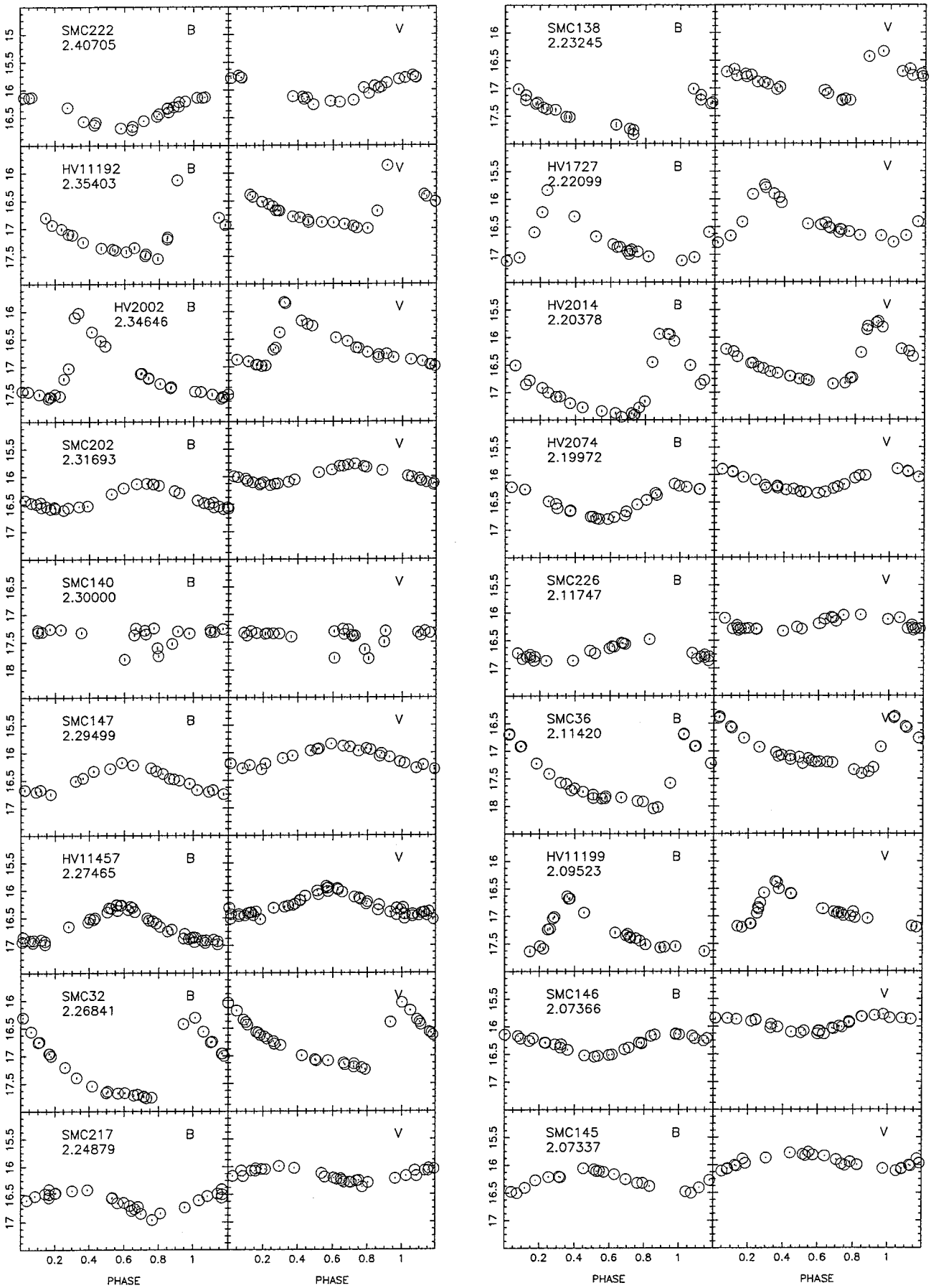
SMC222
2.40705
B
V
HV11192
2.35403
HV2002
2.34646
SMC202
2.31693
SMC140
2.30000
SMC147
2.29499
HV11457
2.27465
SMC32
2.26841
SMC217
2.24879
SMC138
2.23245
HV1727
2.22099
HV2014
2.20378
HV2074
2.19972
SMC226
2.11747
SMC36
2.11420
HV11199
2.09523
SMC146
2.07366
SMC145
2.07337
PHASE

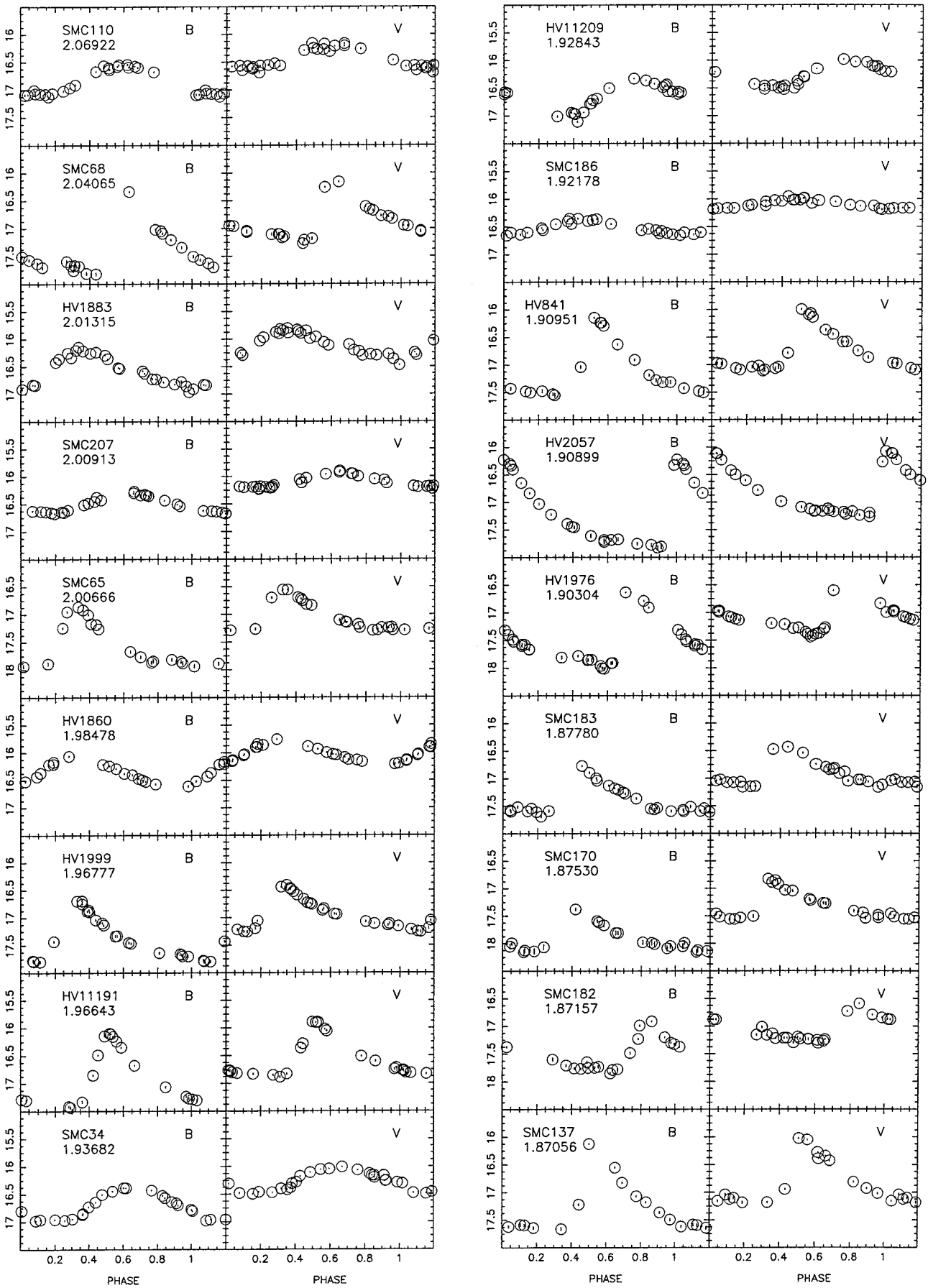
SMC110
2.06922
B
V
SMC68
2.04065
HV1883
2.01315
SMC207
2.00913
SMC65
2.00666
HV1860
1.98478
HV1999
1.96777
HV11191
1.96643
SMC34
1.93682
HV11209
1.92843
SMC186
1.92178
HV841
1.90951
HV2057
1.90899
HV1976
1.90304
SMC183
1.87780
SMC170
1.87530
SMC182
1.87157
SMC137
1.87056
PHASE

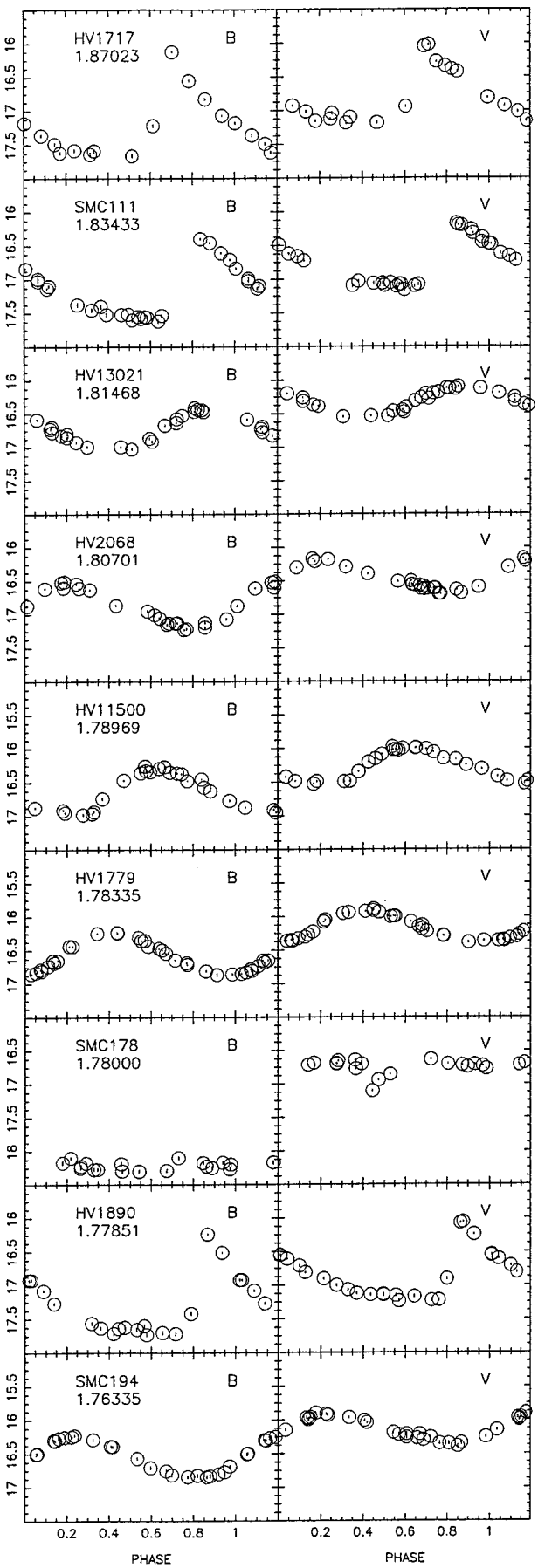
HV1717
1.87023
B
V
SMC111
1.83433
HV13021
1.81468
HV2068
1.80701
HV11500
1.78969
HV1779
1.78335
SMC178
1.78000
HV1890
1.77851
SMC194
1.76335
PHASE
PHASE

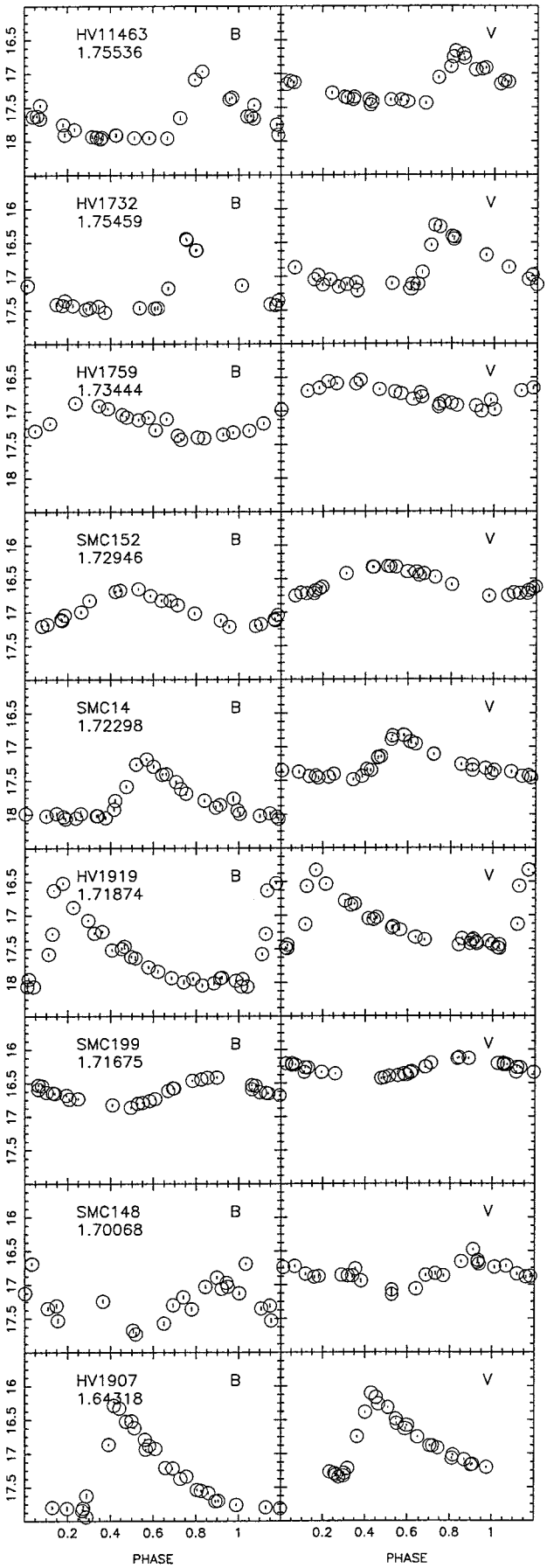
HV11463
1.75536
B
V
HV1732
1.75459
HV1759
1.73444
SMC152
1.72946
SMC14
1.72298
HV1919
1.71874
SMC199
1.71675
SMC148
1.70068
HV1907
1.64318
PHASE
PHASE

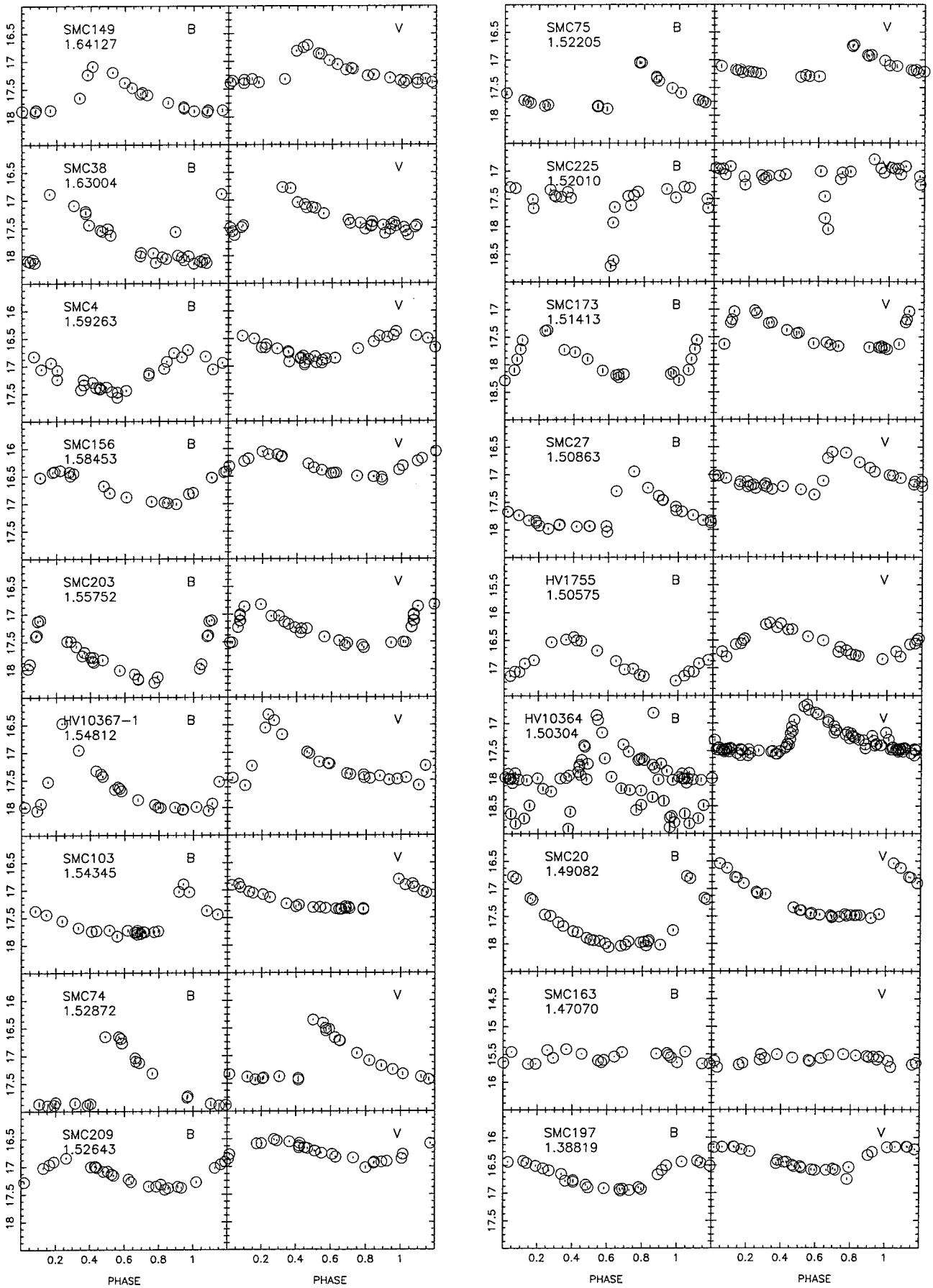
SMC149
1.64127
B
V
SMC38
1.63004
SMC4
1.59263
SMC156
1.58453
SMC203
1.55752
HV10367−1
1.54812
SMC103
1.54345
SMC74
1.52872
SMC209
1.52643
SMC75
1.52205
SMC225
1.52010
SMC173
1.51413
SMC27
1.50863
HV1755
1.50575
HV10364
1.50304
SMC20
1.49082
SMC163
1.47070
SMC197
1.38819
PHASE
PHASE

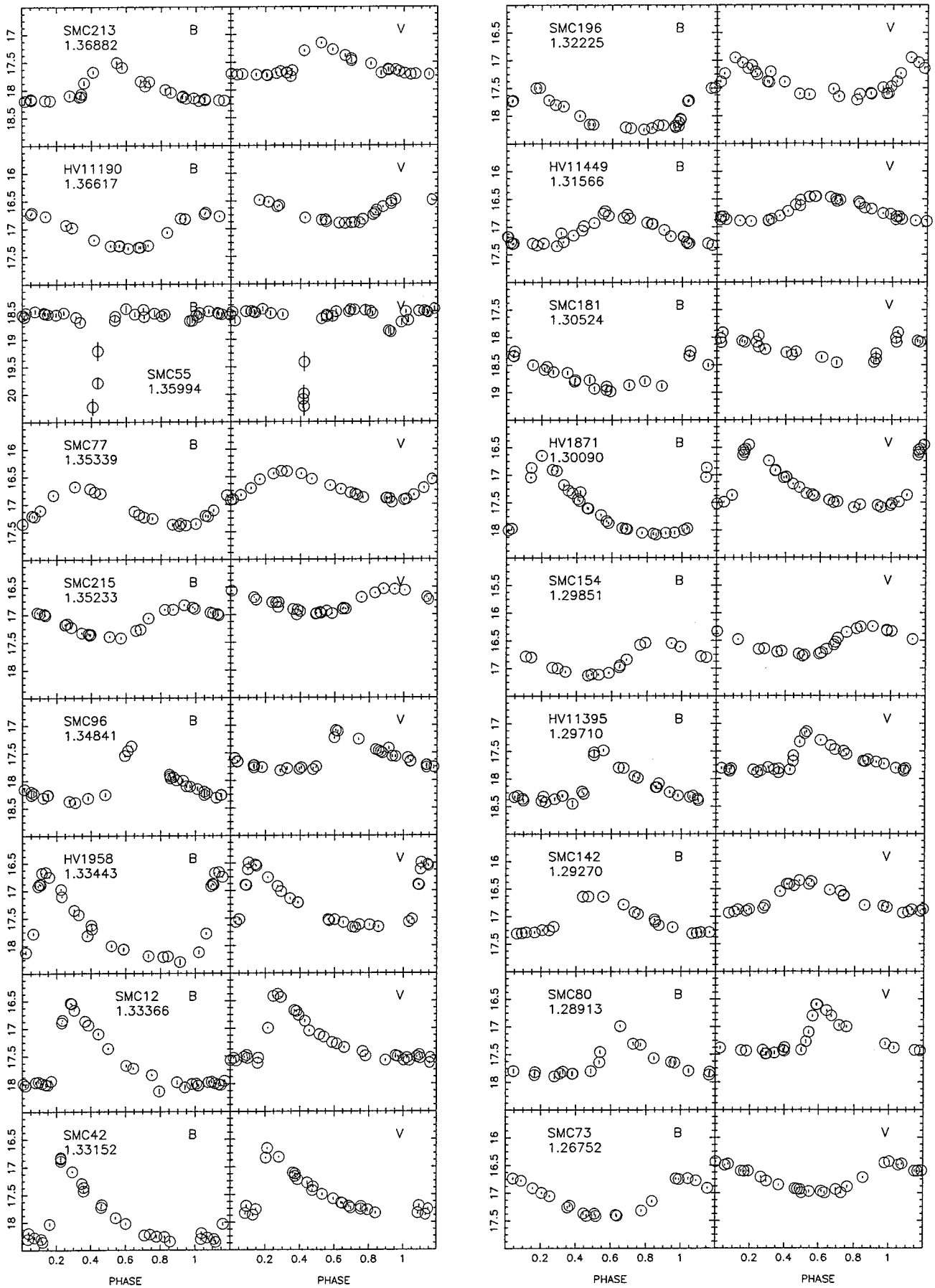
SMC213
1.36882
B
V
HV11190
1.36617
SMC55
1.35994
SMC77
1.35339
SMC215
1.35233
SMC96
1.34841
HV1958
1.33443
SMC12
1.33366
SMC42
1.33152
SMC196
1.32225
HV11449
1.31566
SMC181
1.30524
HV1871
1.30090
SMC154
1.29851
HV11395
1.29710
SMC142
1.29270
SMC80
1.28913
SMC73
1.26752
PHASE

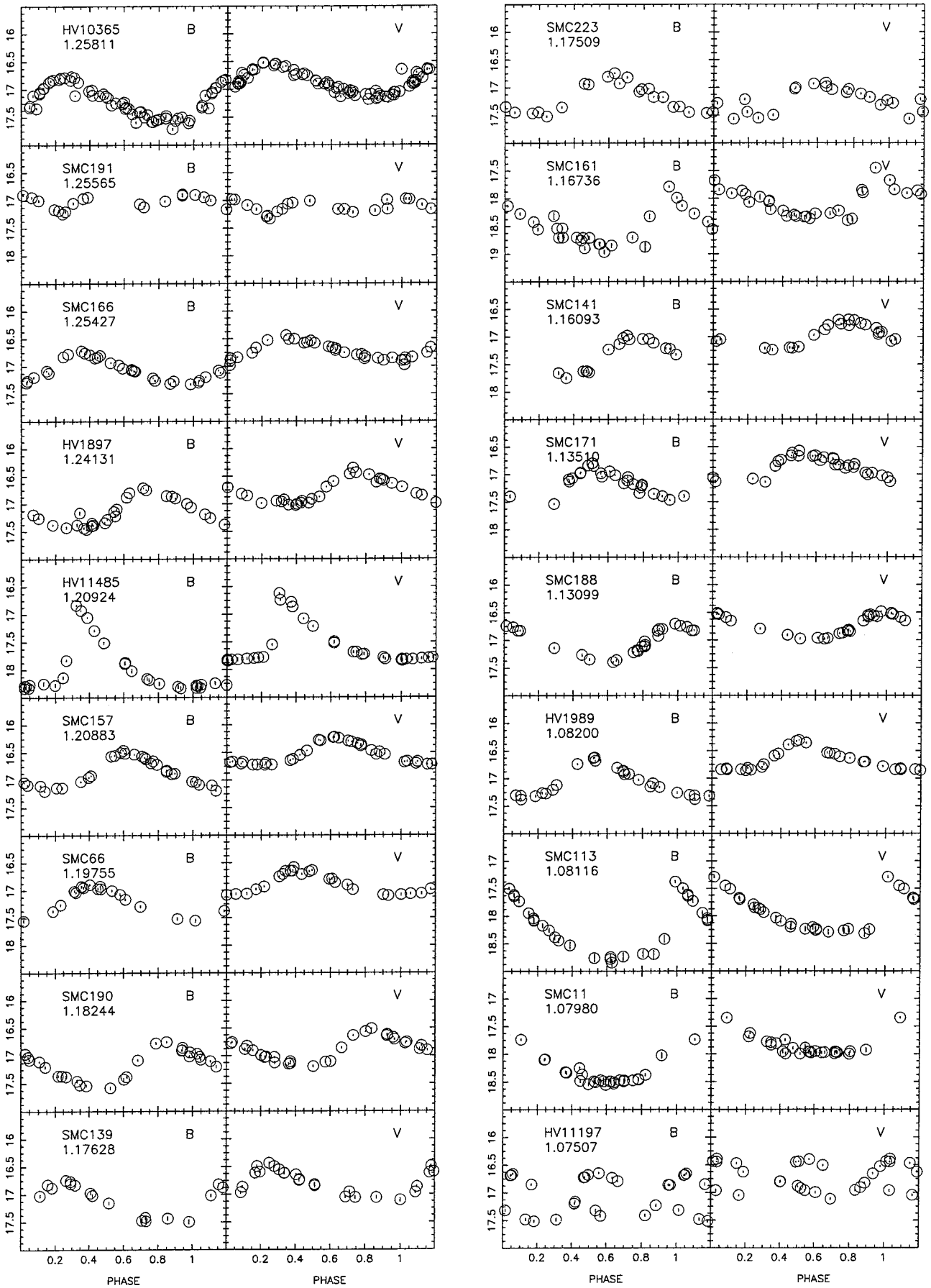
HV10365
1.25811
B
V
SMC191
1.25565
SMC166
1.25427
HV1897
1.24131
HV11485
1.20924
SMC157
1.20883
SMC66
1.19755
SMC190
1.18244
SMC139
1.17628
SMC223
1.17509
SMC161
1.16736
SMC141
1.16093
SMC171
1.13510
SMC188
1.13099
HV1989
1.08200
SMC113
1.08116
SMC11
1.07980
HV11197
1.07507
PHASE

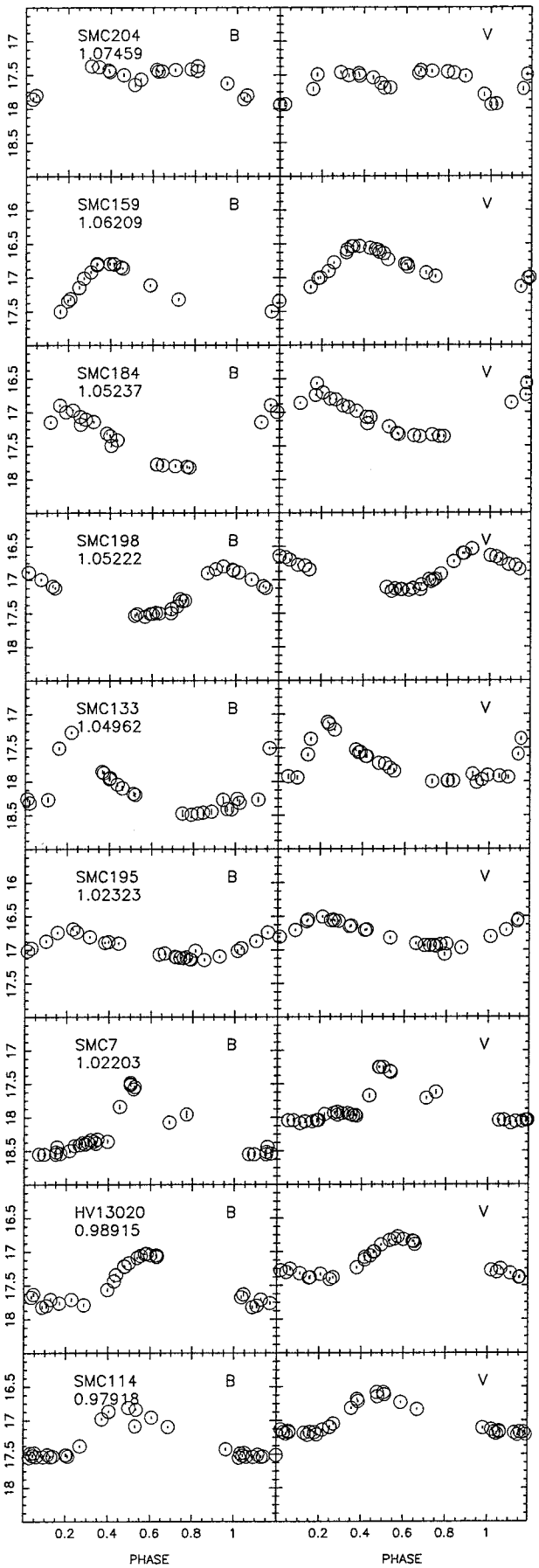
SMC204
1.07459
B
V
SMC159
1.06209
SMC184
1.05237
SMC198
1.05222
SMC133
1.04962
SMC195
1.02323
SMC7
1.02203
HV13020
0.98915
SMC114
0.97918
PHASE
PHASE

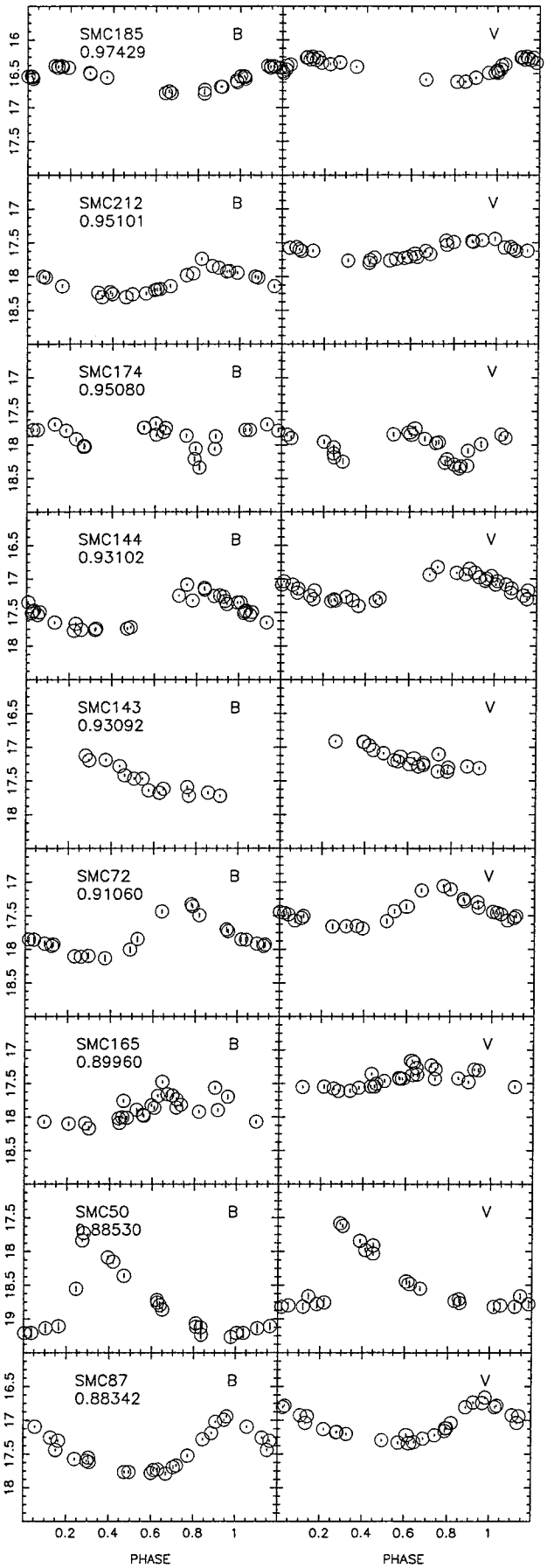
SMC185
0.97429
B
V
SMC212
0.95101
SMC174
0.95080
SMC144
0.93102
SMC143
0.93092
SMC72
0.91060
SMC165
0.89960
SMC50
0.88530
SMC87
0.88342
PHASE
PHASE

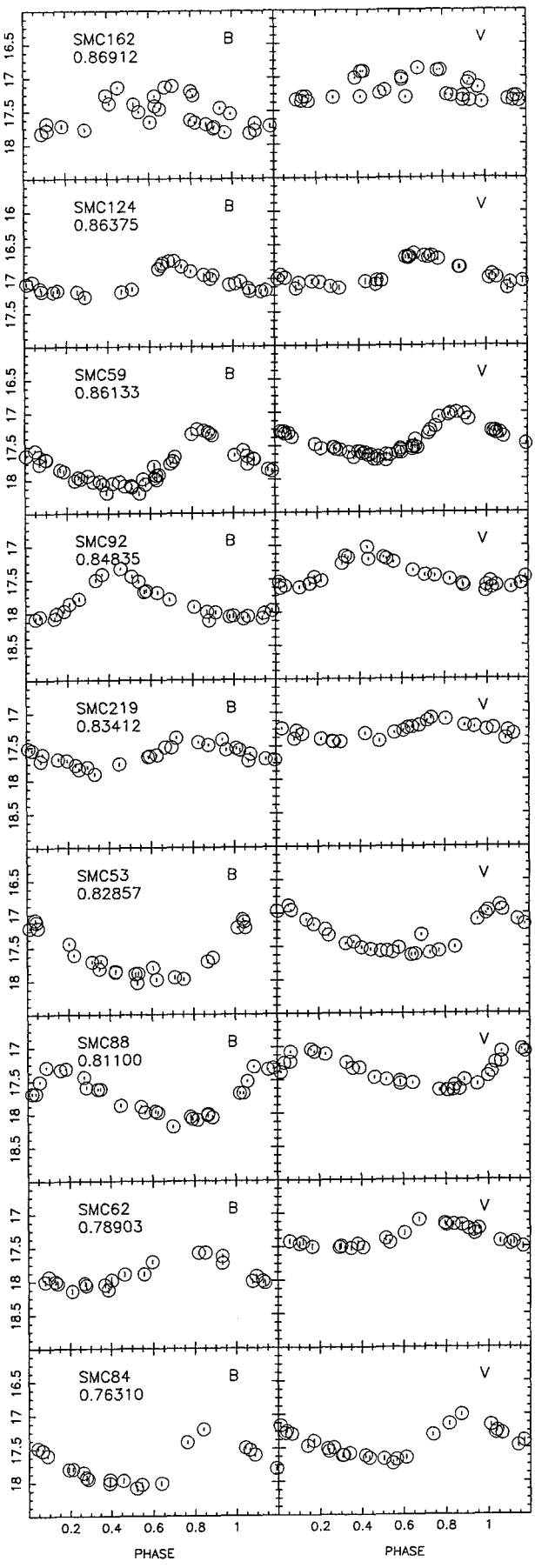
SMC162
0.86912
B
V
SMC124
0.86375
SMC59
0.86133
SMC92
0.84835
SMC219
0.83412
SMC53
0.82857
SMC88
0.81100
SMC62
0.78903
SMC84
0.76310
PHASE
PHASE

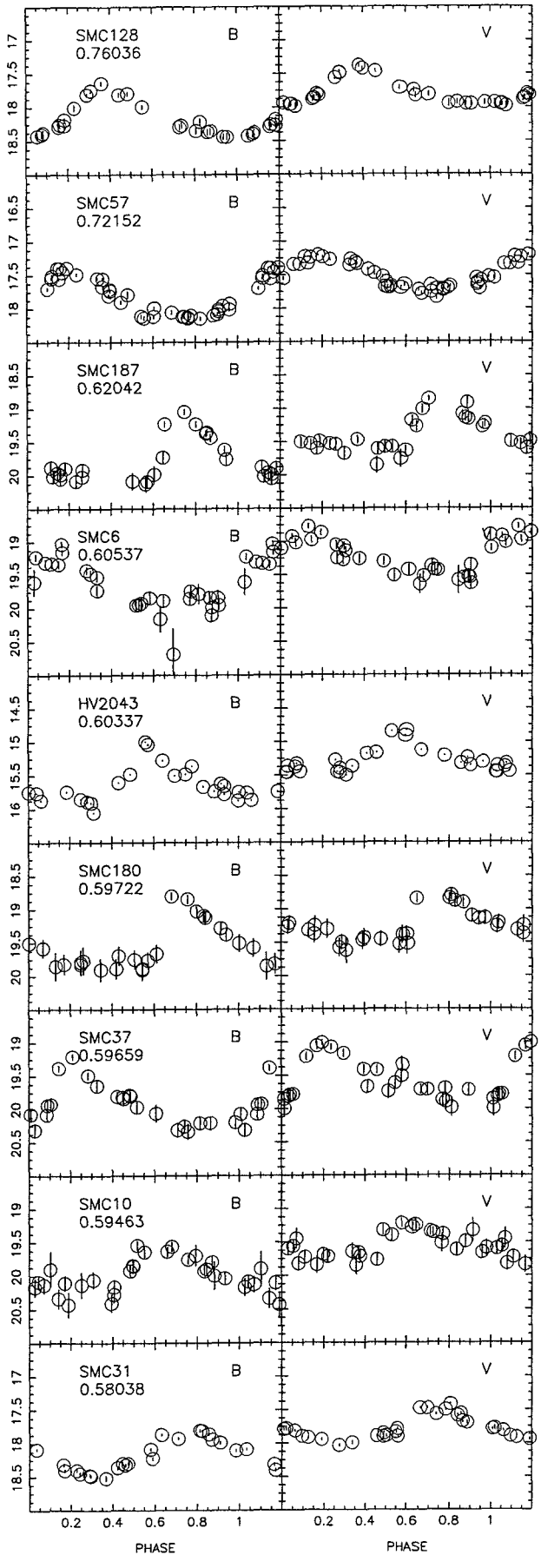
SMC128
0.76036
B
V
SMC57
0.72152
SMC187
0.62042
SMC6
0.60537
HV2043
0.60337
SMC180
0.59722
SMC37
0.59659
SMC10
0.59463
SMC31
0.58038
PHASE
PHASE

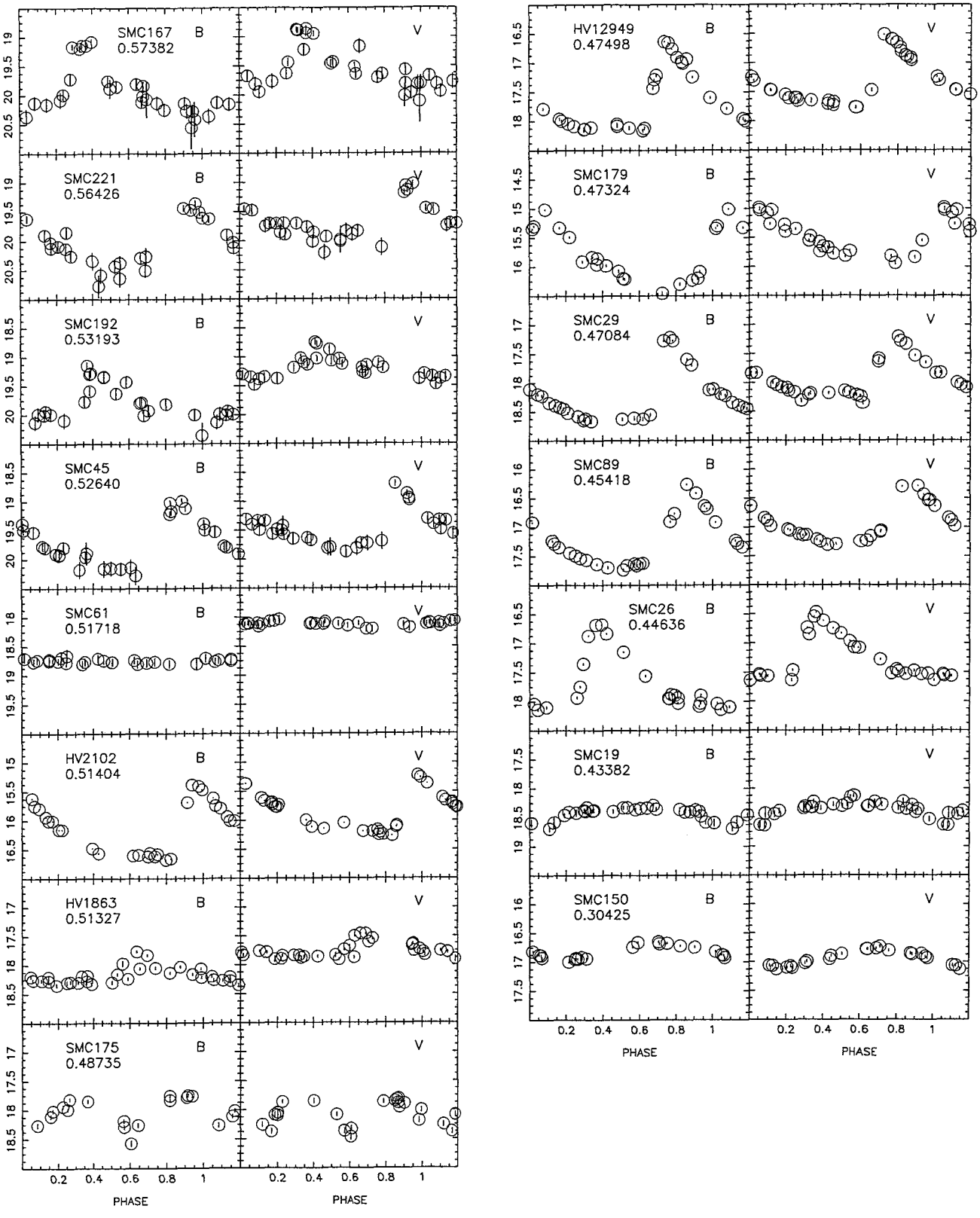
SMC167 B
0.57382
V
SMC221 B
0.56426
V
SMC192 B
0.53193
V
SMC45 B
0.52640
V
SMC61 B
0.51718
V
HV2102 B
0.51404
V
HV1863 B
0.51327
V
SMC175 B
0.48735
V
HV12949 B
0.47498
V
SMC179 B
0.47324
V
SMC29 B
0.47084
V
SMC89 B
0.45418
V
SMC26 B
0.44636
V
SMC19 B
0.43382
V
SMC150 B
0.30425
V
PHASE
PHASE

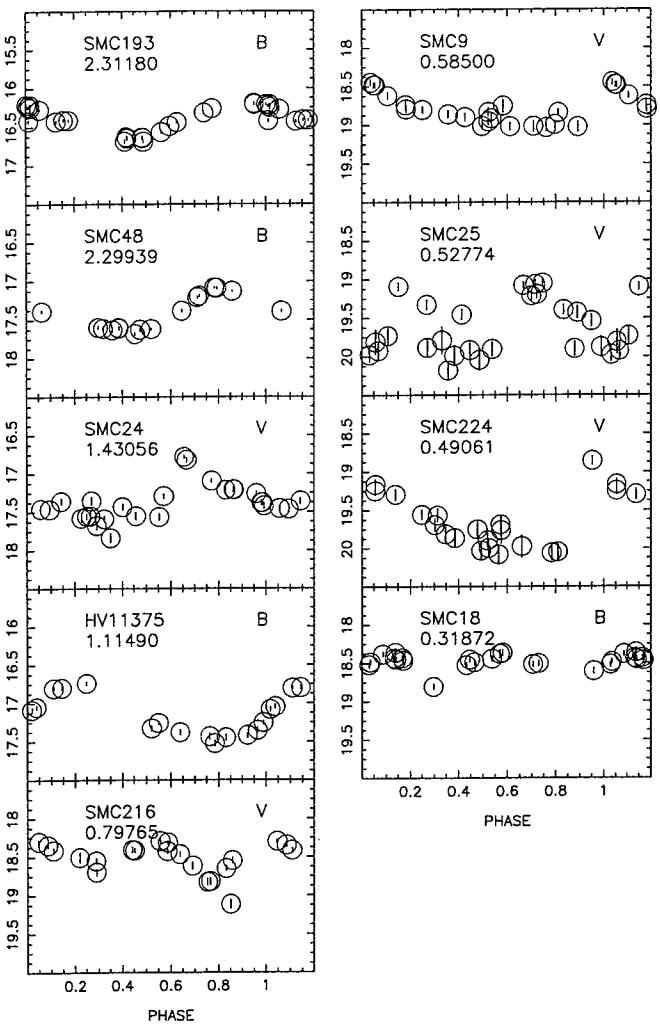
SMC193
2.31180
B
SMC48
2.29939
B
SMC24
1.43056
V
HV11375
1.11490
B
SMC216
0.79765
V
SMC9
0.58500
V
SMC25
0.52774
V
SMC224
0.49061
V
SMC18
0.31872
B
PHASE
PHASE

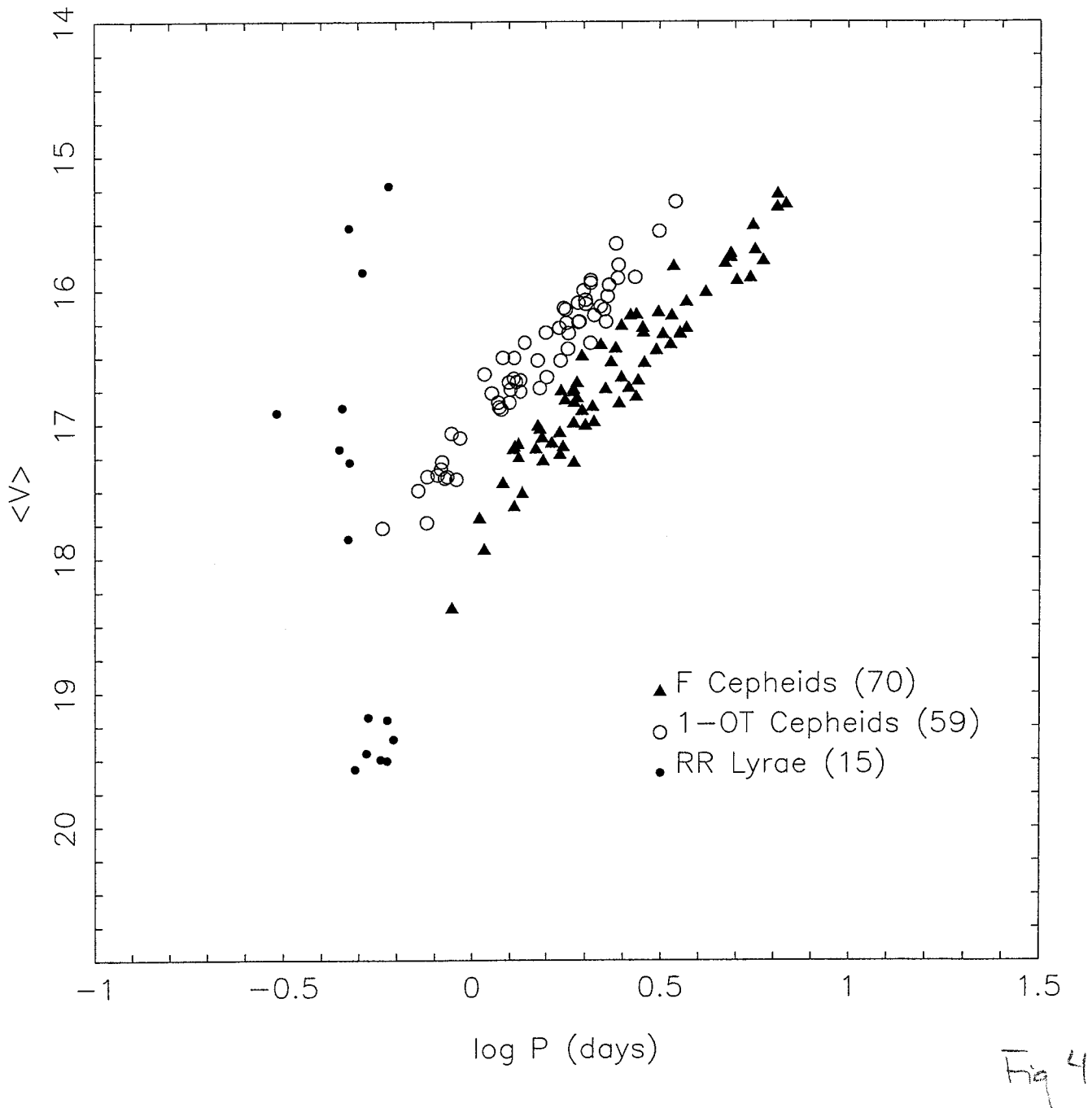
14
15
16
17
18
19
20
<V>
−1
−0.5
0
0.5
1
1.5
log P (days)
F Cepheids (70)
1−OT Cepheids (59)
RR Lyrae (15)

Fig 4

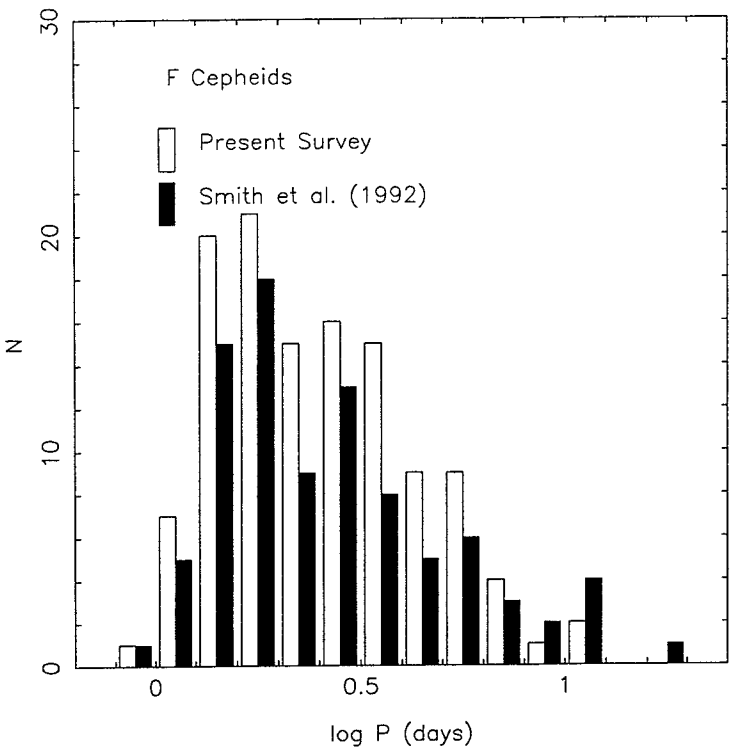
F Cepheids
Present Survey
Smith et al. (1992)
N
0
10
20
30
0
0.5
1
log P (days)

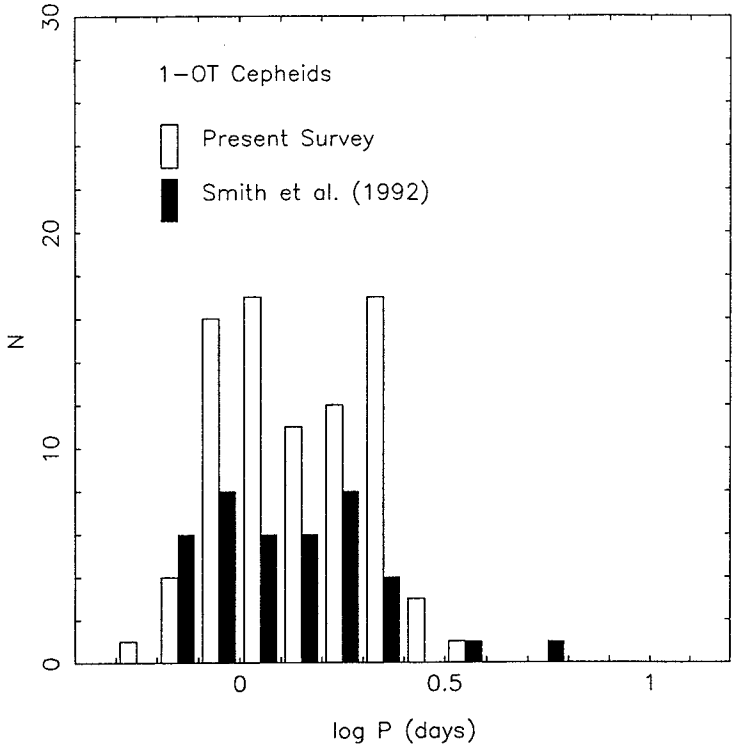
1−OT Cepheids
Present Survey
Smith et al. (1992)
N
0
10
20
30
0
0.5
1
log P (days)

Fig 5

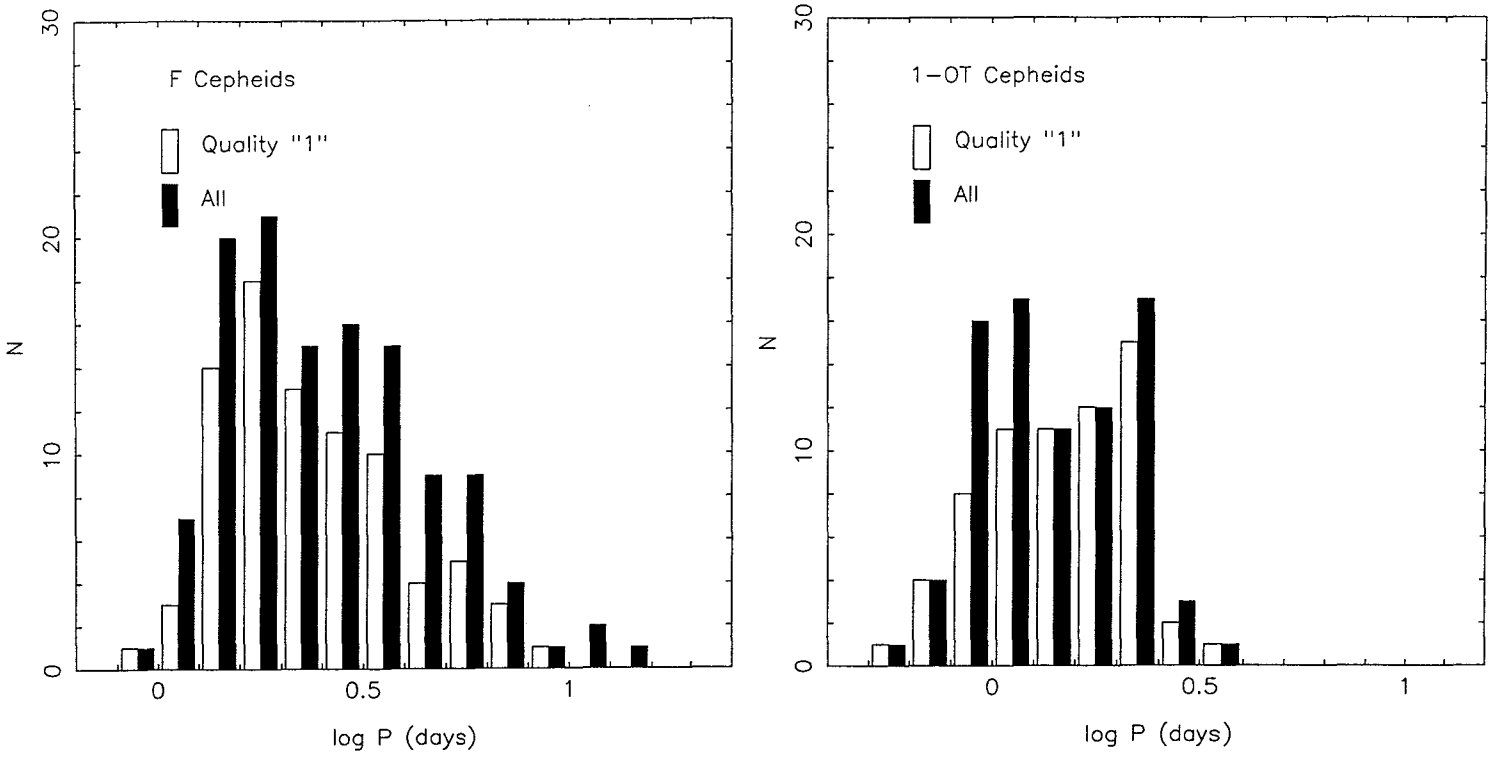
F Cepheids
Quality "1"
All
N
log P (days)
1−OT Cepheids
Quality "1"
All
N
log P (days)

Fig 6

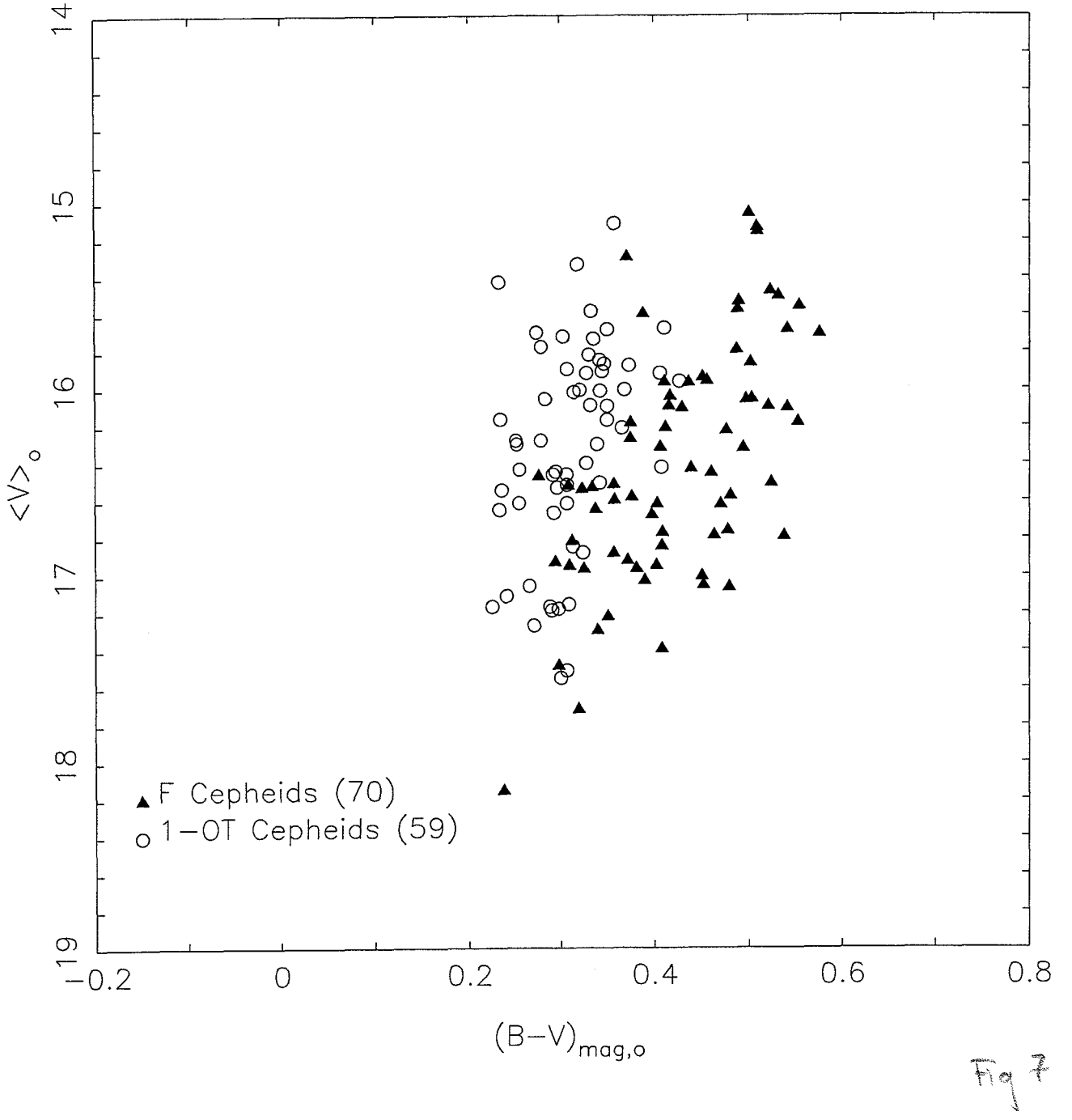
14
15
16
17
18
19
−0.2
0
0.2
0.4
0.6
0.8
<V>o
(B−V)mag,o
F Cepheids (70)
1−OT Cepheids (59)

Fig 7

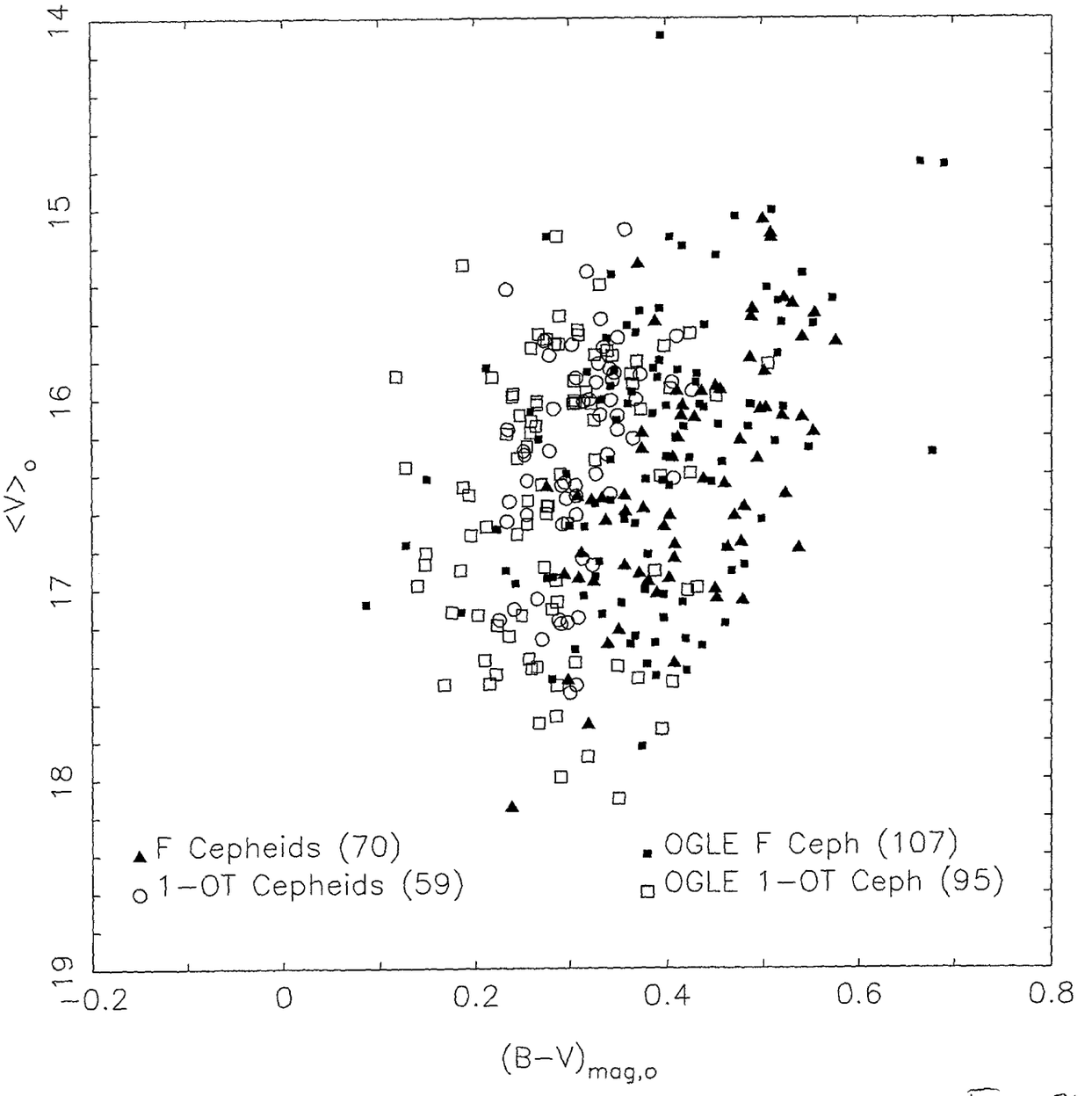
14
15
16
17
18
19
<V>o
-0.2
0
0.2
0.4
0.6
0.8
(B-V)mag,o
F Cepheids (70)
1-OT Cepheids (59)
OGLE F Ceph (107)
OGLE 1-OT Ceph (95)

Fig 8

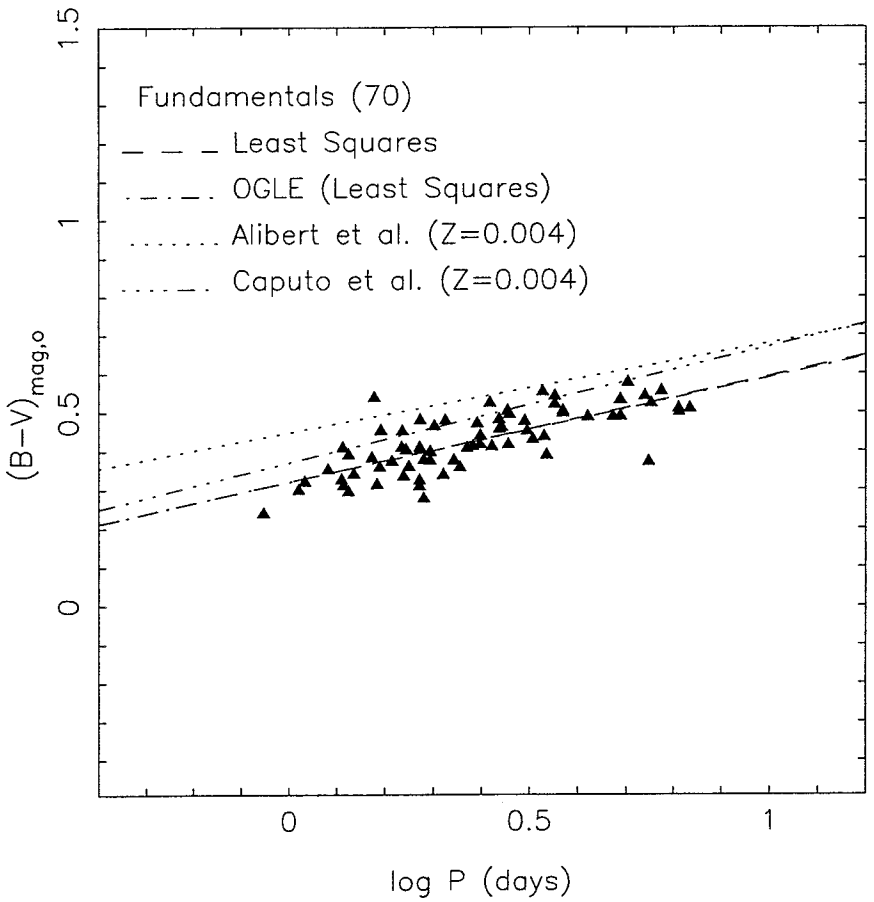
Fundamentals (70)
Least Squares
OGLE (Least Squares)
Alibert et al. (Z=0.004)
Caputo et al. (Z=0.004)
$(B-V)_{mag,o}$
log P (days)
0
0.5
1
1.5

Fig 9

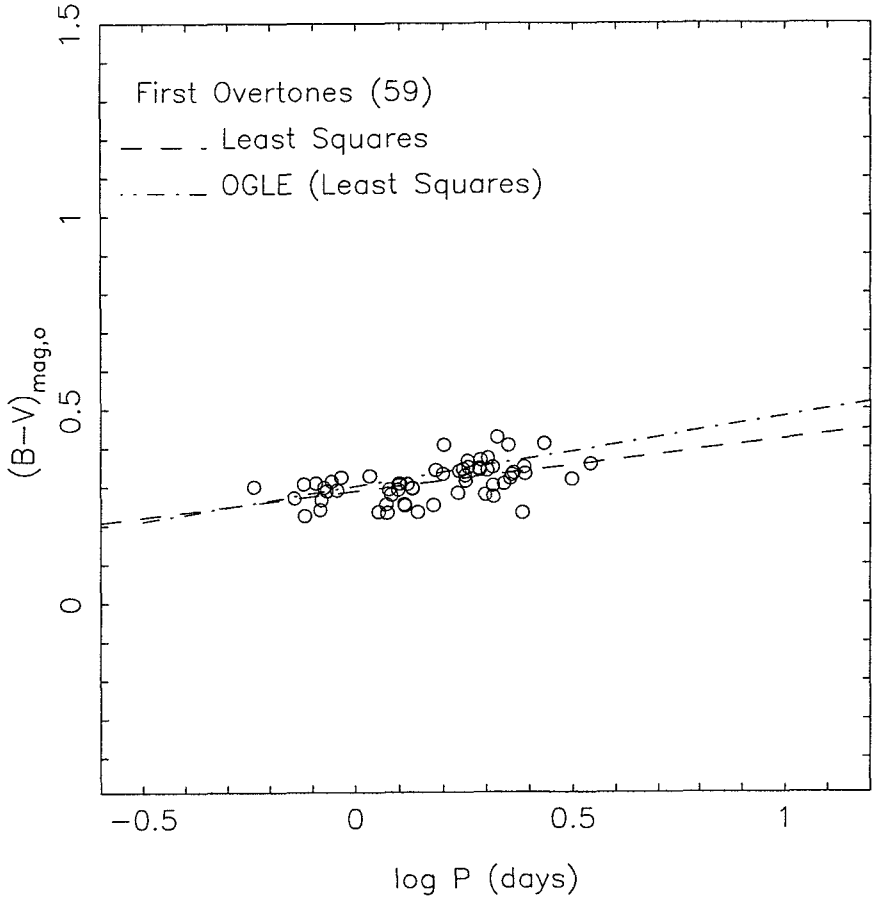
First Overtones (59)
Least Squares
OGLE (Least Squares)
$(B-V)_{mag,o}$
1.5
1
0.5
0
−0.5
0
0.5
1
log P (days)

Fig 10.

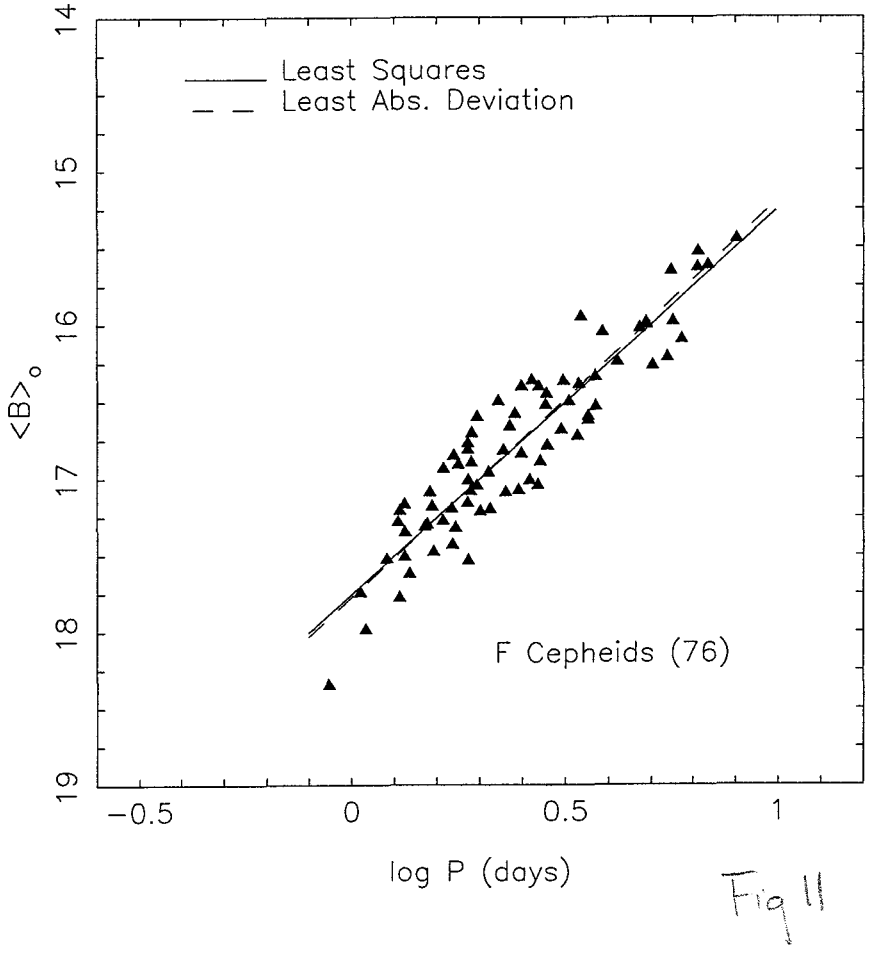
Least Squares
Least Abs. Deviation
F Cepheids (76)
<B>o
14
15
16
17
18
19
−0.5
0
0.5
1
log P (days)

Fig 11

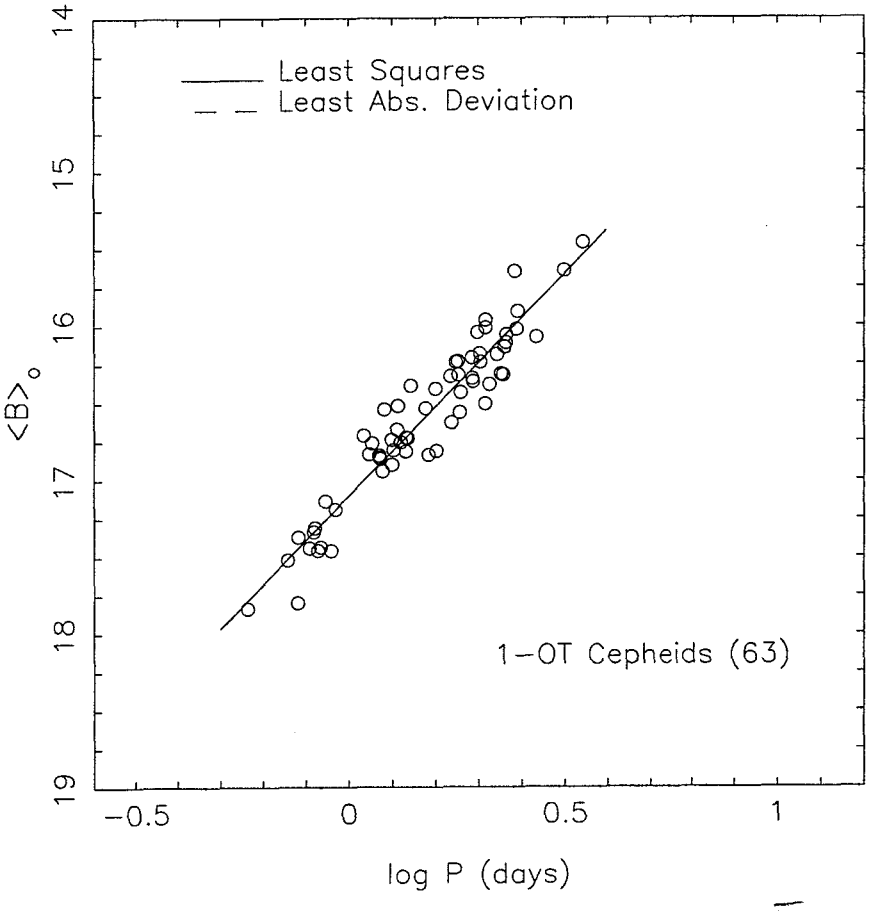
Least Squares
Least Abs. Deviation
1-OT Cepheids (63)
<B>o
14
15
16
17
18
19
-0.5
0
0.5
1
log P (days)

Fig 12

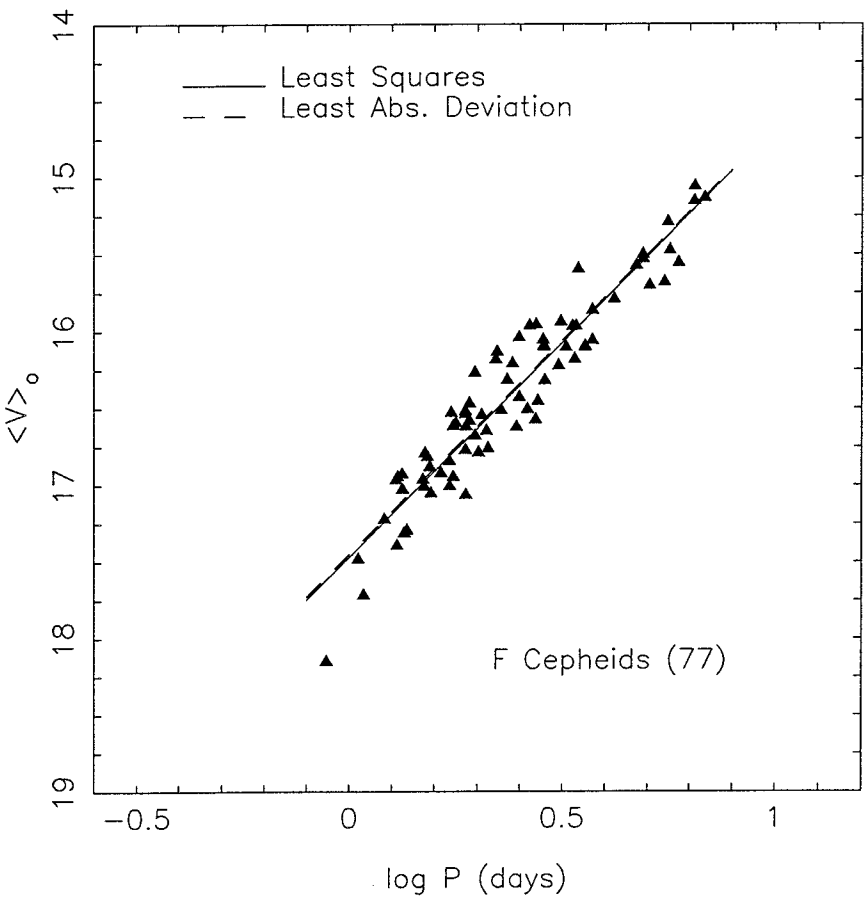
Least Squares
Least Abs. Deviation
F Cepheids (77)
<V>o
log P (days)
14
15
16
17
18
19
−0.5
0
0.5
1

Fig 13

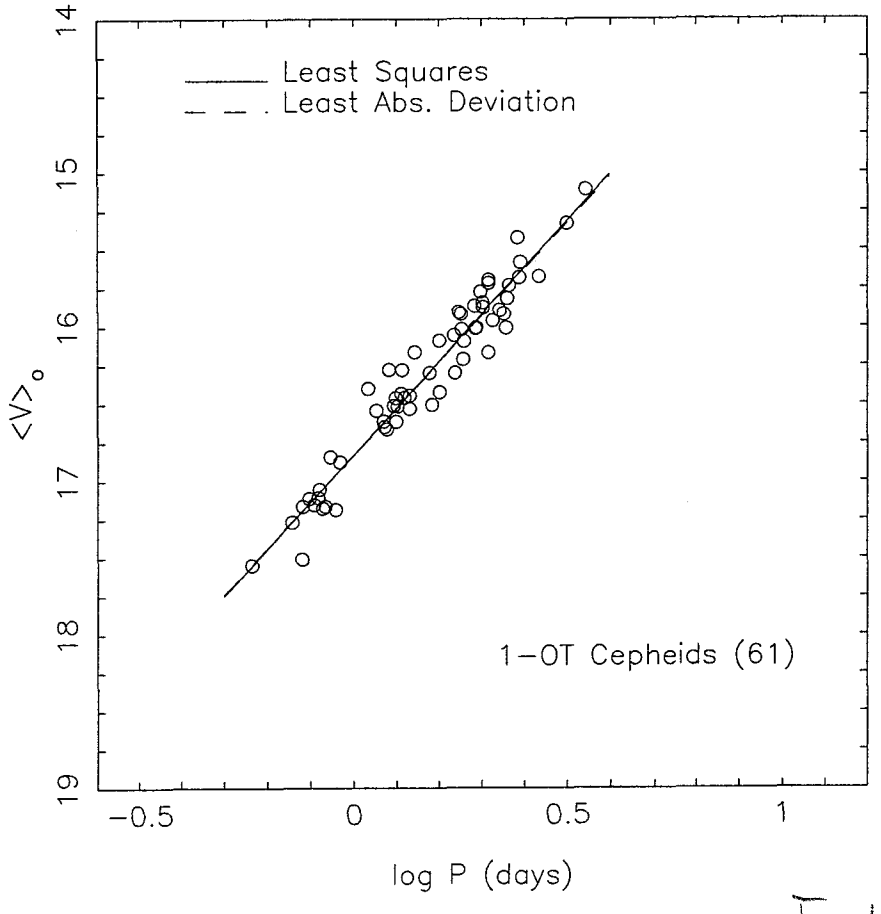
Least Squares
Least Abs. Deviation
1−OT Cepheids (61)
<V>o
log P (days)
14
15
16
17
18
19
−0.5
0
0.5
1

Fig 14

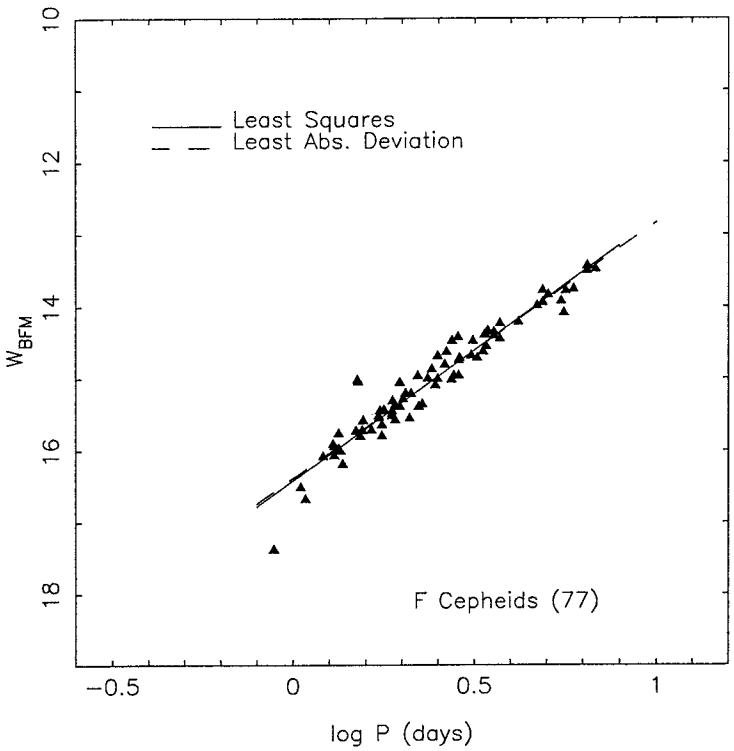
Least Squares
Least Abs. Deviation
F Cepheids (77)
W_{BFM}
log P (days)
10
12
14
16
18
−0.5
0
0.5
1

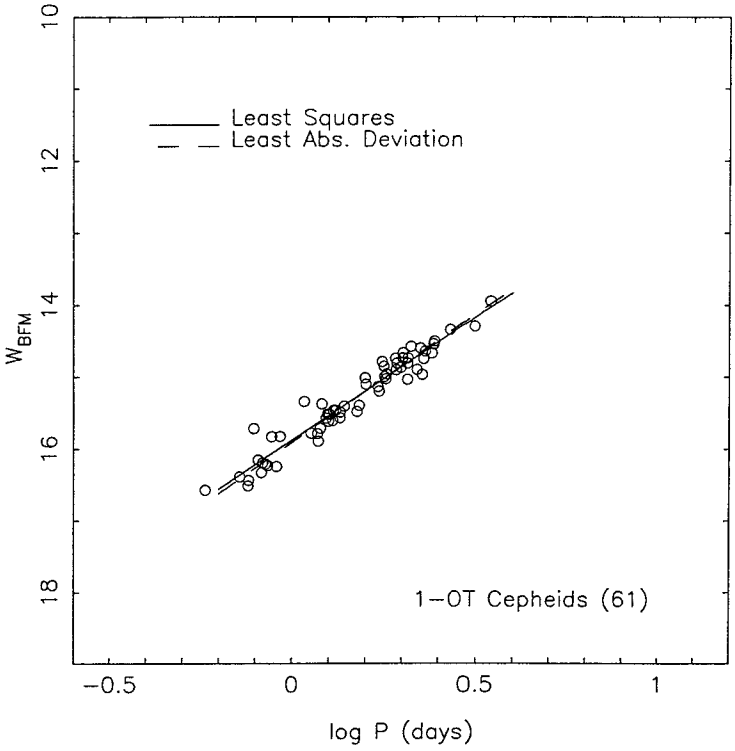
Least Squares
Least Abs. Deviation
1−OT Cepheids (61)
W_{BFM}
log P (days)
10
12
14
16
18
−0.5
0
0.5
1

Fig 15

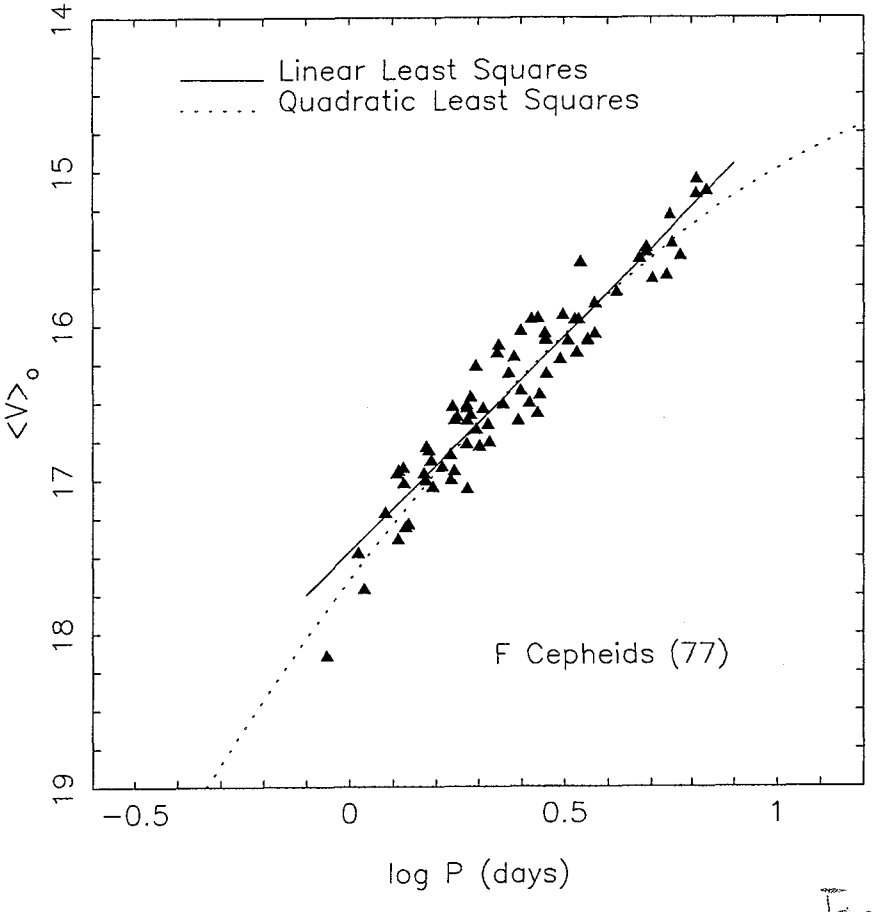
Linear Least Squares
Quadratic Least Squares
F Cepheids (77)
<V>o
14
15
16
17
18
19
−0.5
0
0.5
1
log P (days)

Fig 16

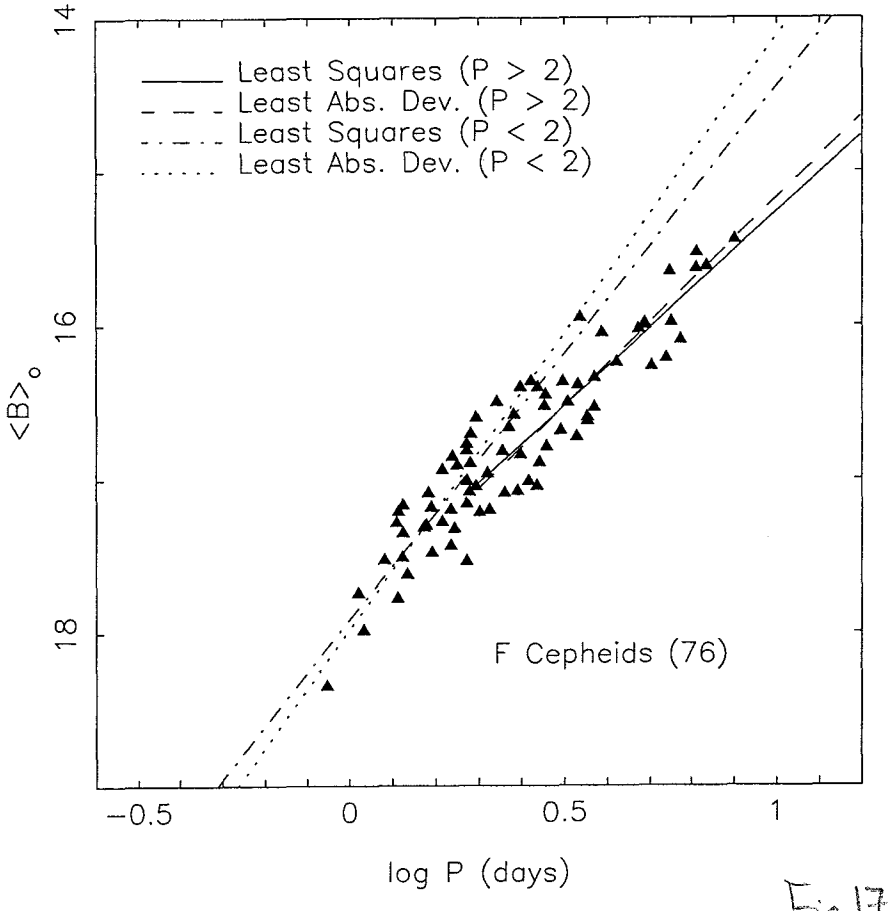
Least Squares (P > 2)
Least Abs. Dev. (P > 2)
Least Squares (P < 2)
Least Abs. Dev. (P < 2)
F Cepheids (76)
<B>o
14
16
18
−0.5
0
0.5
1
log P (days)

Fig 17

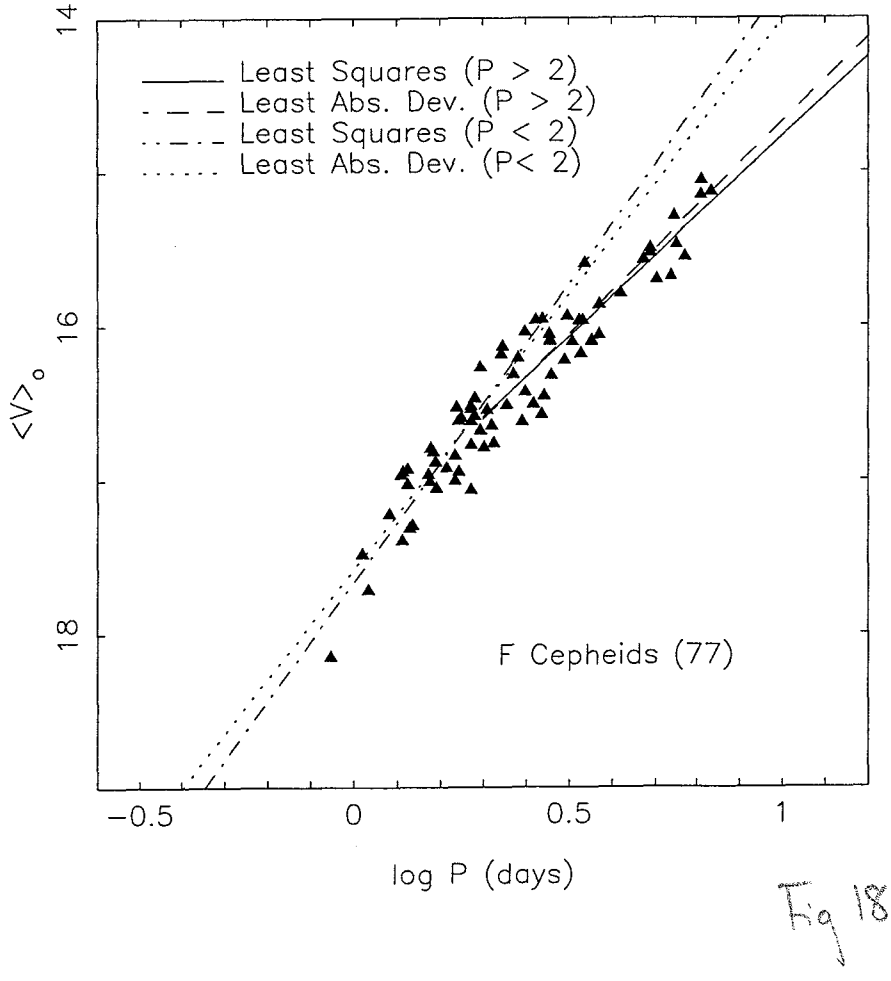
Least Squares (P > 2)
Least Abs. Dev. (P > 2)
Least Squares (P < 2)
Least Abs. Dev. (P< 2)
F Cepheids (77)
<V>o
14
16
18
−0.5
0
0.5
1
log P (days)

Fig 18

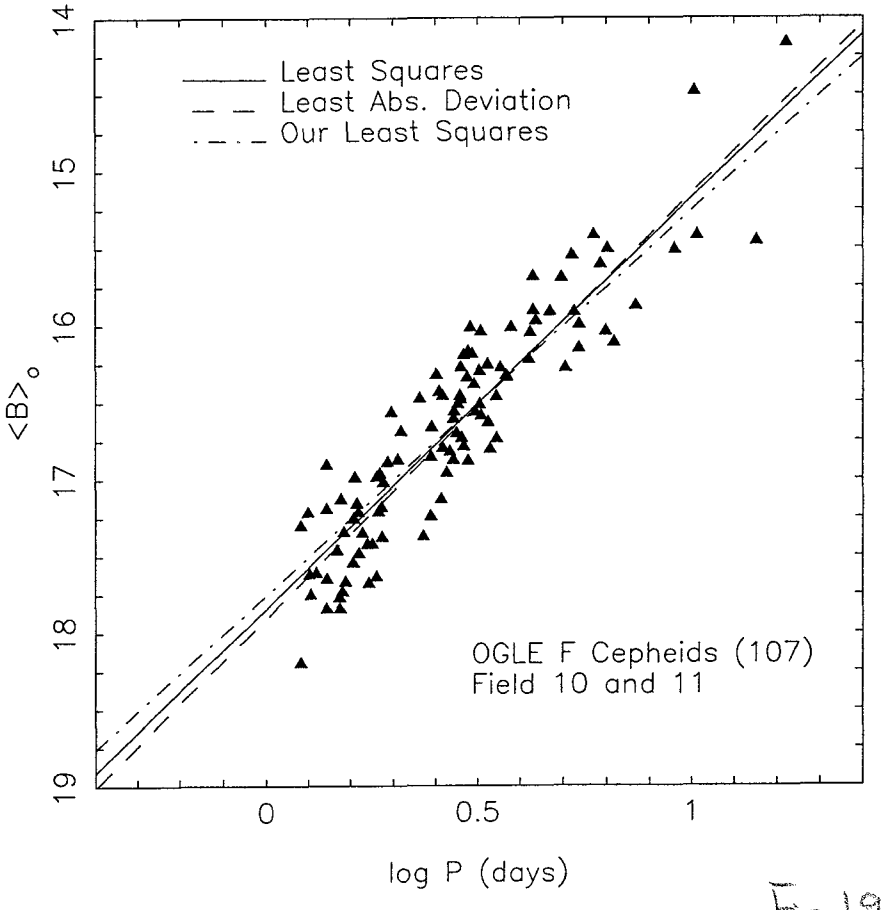
Least Squares
Least Abs. Deviation
Our Least Squares
OGLE F Cepheids (107)
Field 10 and 11
<B>o
log P (days)
14
15
16
17
18
19
0
0.5
1

Fig 19

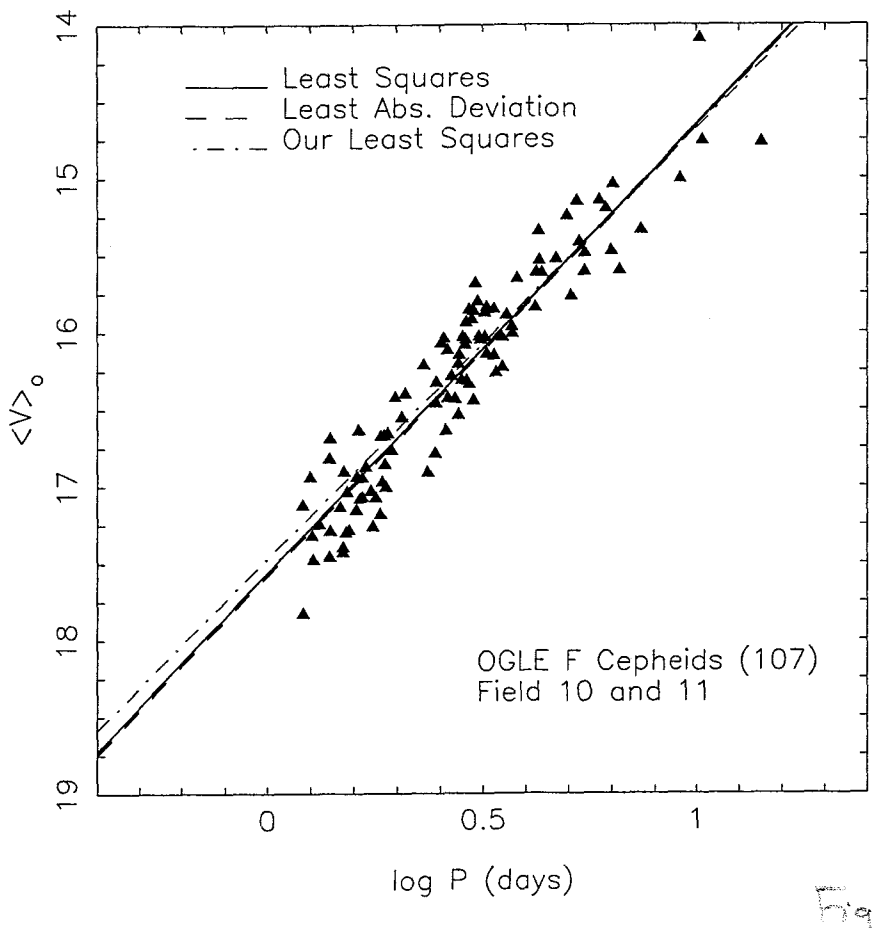
Least Squares
Least Abs. Deviation
Our Least Squares
OGLE F Cepheids (107)
Field 10 and 11
<V>o
log P (days)
14
15
16
17
18
19
0
0.5
1

Fig 20

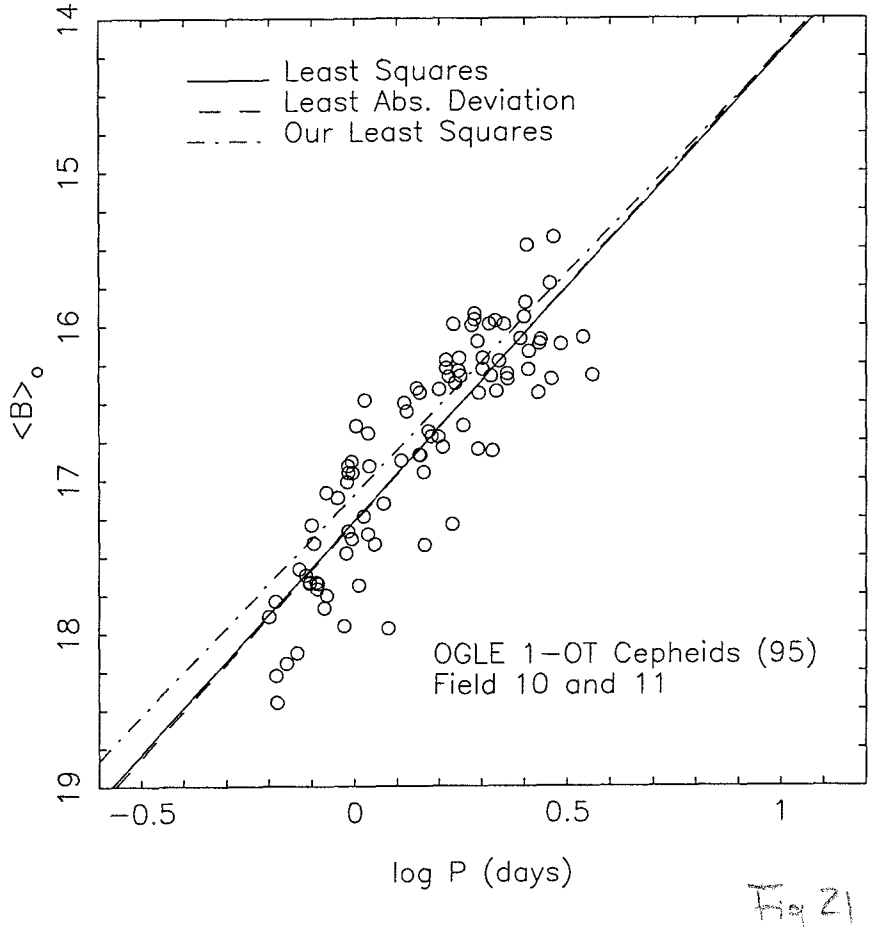
Least Squares
Least Abs. Deviation
Our Least Squares
OGLE 1−OT Cepheids (95)
Field 10 and 11
<B>o
log P (days)
14
15
16
17
18
19
−0.5
0
0.5
1

Fig 21

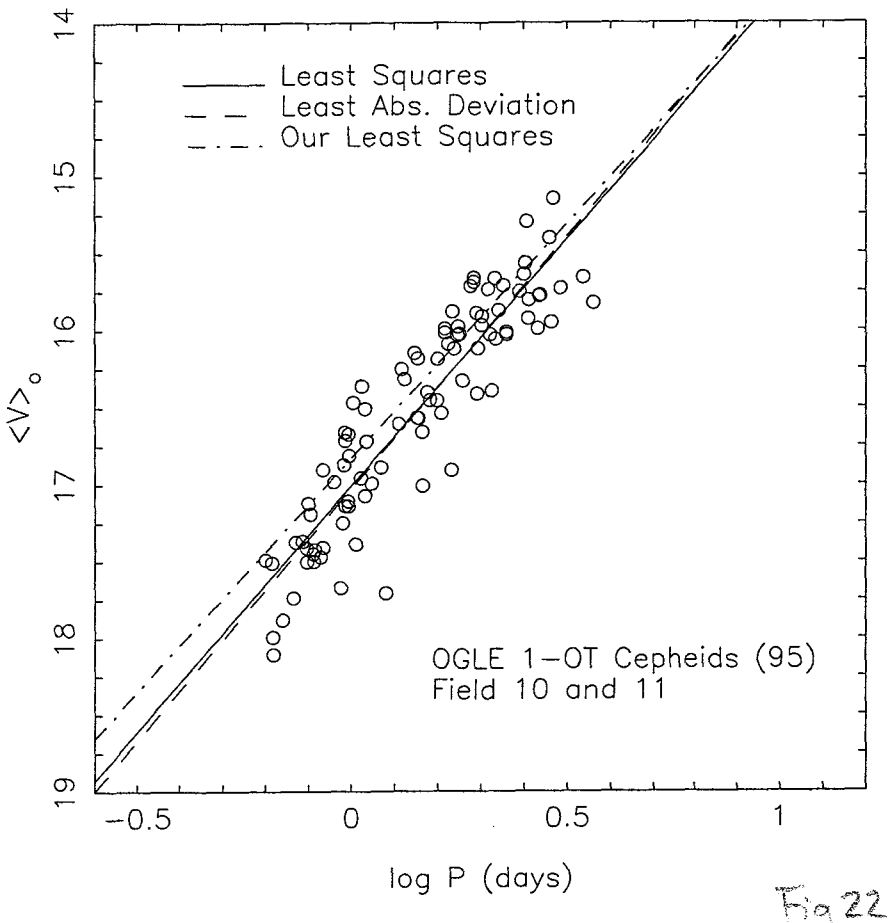
Least Squares
Least Abs. Deviation
Our Least Squares
OGLE 1–OT Cepheids (95)
Field 10 and 11
<V>o
log P (days)
14
15
16
17
18
19
−0.5
0
0.5
1

Fig 22